UNIVERSIDADE FEDERAL DE PELOTAS
Programa de Pós-Graduação em Ciência e Engenharia de Materiais

Tese

Espumas sustentáveis de poliuretano incorporadas com diferentes cargas: adsorção de Cr(III) e SARS-CoV-2 em soluções aquosas

Thays França Afonso

Pelotas, 2023

Thays França Afonso

Espumas sustentáveis de poliuretano incorporadas com diferentes cargas: adsorção de Cr(III) e SARS-CoV-2 em soluções aquosas

Tese apresentada ao Programa de Pós-Graduação em Ciência e Engenharia de Materiais da Universidade Federal de Pelotas, como requisito parcial a obtenção do título de Doutor em Ciência e Engenharia de Materiais.

Orientador: Prof. Dr. Robson Andreazza

Co-Orientador: Prof. Dr. Rafael de Avila Delucis

Pelotas, 2023

Universidade Federal de Pelotas / Sistema de Bibliotecas
Catalogação da Publicação

A257e Afonso, Thays França

Espumas sustentáveis de poliuretano incorporadas com diferentes cargas: adsorção de Cr(III) e SARS-CoV-2 em soluções aquosas / Thays França Afonso; Robson Andreazza, orientador; Rafael de Avila Delucis, coorientador. — Pelotas, 2023.
112 f. : il.

Tese (Doutorado) — Programa de Pós-Graduação em Ciência e Engenharia de Materiais, Centro de Desenvolvimento Tecnológico, Universidade Federal de Pelotas, 2023.

1. Bioespumas. 2. Biocarvão. 3. Biocarvão ativado. 4. Caroço de pêssego. 5. Metais pesados. I. Andreazza, Robson, orient. II. Delucis, Rafael de Avila, coorient. III. Título.

CDD 620.11063

Elaborada por Simone Godinho Maisonave CRB: 10/1733

Thays França Afonso

Espumas sustentáveis de poliuretano incorporadas com diferentes cargas: adsorção de Cr(III) e SARS-CoV-2 em soluções aquosas

Tese aprovada, como requisito parcial, para obtenção do grau de Doutor em Ciência e Engenharia de Materiais, Programa de Pós-Graduação em Ciência e Engenharia de Materiais, Universidade Federal de Pelotas.

Data da defesa: 14 de dezembro de 2023

Banca examinadora:

_____

Prof. Dr. Robson Andreazza
Doutor em Ciência do Solo pela Universidade Federal do Rio Grande do Sul, UFRGS, Brasil.

_____

Prof. Dr. Rafael de Avila Delucis
Doutor em Engenharia de Minas, Metalúrgica e de Materiais pela Universidade Federal do Rio Grande do Sul, UFRGS, Brasil.

_____

Prof. Dr. Fernando Machado Machado
Doutor em Engenharia de Minas, Metalúrgica e de Materiais pela Universidade Federal do Rio Grande do Sul, UFRGS, Brasil.

_____

Dr.ª Mery Luiza Garcia Vieira
Doutora em Engenharia e Ciência de Alimentos pela Universidade Federal de Rio Grande, FURG, Brasil.

_____

Prof. Dr. Tito Roberto Sant'Anna Cadaval Junior
Doutor em Química Tecnológica e Ambiental pela Universidade Federal de Rio Grande, FURG, Brasil.

Agradecimentos

Agradeço primeiramente a Deus, por colocar pessoas especiais na minha trajetória, me incentivando a concluir esta pesquisa.

À minha mãe, meu esposo por sempre estarem ao meu lado me apoiando e em especial a minha filha Sophia que nasceu durante doutorado.

Aos meus orientadores pela dedicação, estímulo e esforço proporcionado e colegas Laboratório de Química Ambiental da UFPel, pelo apoio e bom ambiente de trabalho proporcionado durante a realização dessa pesquisa.

Ao Laboratório de Metrologia da Química da UFPel, através do Professor Dr. Anderson Ribeiro e doutoranda Daisa Bonemann pelo auxílio nos ensaios de Espectroscopia de absorção atômica.

Ao Laboratório de Bioquímica e Biologia Molecular de Microrganismos da UFPel, através do Professor Dr. Rodrigo Vaucher, pelo auxílio nas análises de SARS-CoV-2.

Ao Laboratório de Ciência da Madeira da UFPel, através do Professor Dr. Darci Gatto pelo auxílio nas análises de TGA.

Ao Centro de Desenvolvimento e Controle de Biomateriais (CDC-Bio), da faculdade de Odontologia da UFPel, pelo auxílio nas análises de FT-IR.

À Escola de Química e Alimentos da FURG, através do Professor Dr. Tito Cadaval Jr pelo auxílio nas análises de MEV e DRX.

Ao Programa de Pós-Graduação em Engenharia de Processos e Tecnologias, da Universidade de Caxias do Sul, através do Professor Marcelo Godinho pelo auxílio nas análises de BET/BJH.

Às agências de fomento, Coordenação de Aperfeiçoamento de Pessoal de Nível Superior – Brasil (CAPES) – Código de Financiamento 001, do Conselho Nacional de Desenvolvimento Científico e Tecnológico (CNPq) e Fundação de Amparo à Pesquisa do Estado do Rio Grande do Sul (FAPERGS), pelo apoio na realização deste trabalho.

Resumo

AFONSO, Thays França. **Espumas sustentáveis de poliuretano incorporadas com diferentes cargas: adsorção de Cr(III) e SARS-CoV-2 em soluções aquosas**. Orientador: Robson Andreazza. 2023. 112f. Tese (Doutorado em Ciência e Engenharia de Materiais) – Programa de Pós-Graduação em Ciência e Engenharia de Materiais, CDTEC, Universidade Federal de Pelotas, Pelotas, Brasil, 2023.

Devido à contaminação dos recursos hídricos pelo lançamento de águas residuais industriais, municipais, agrícolas, e hospitalares, contendo metais pesados e microrganismos patogênicos, surge a necessidade de processos de tratamento de baixo custo, eficientes e ecológicos na remoção desses contaminantes. Nesse sentido, a adsorção é uma alternativa, por ser considerada eficaz na remoção de uma diversidade de poluentes em meio aquoso. Desse modo, o presente estudo teve a finalidade de sintetizar e caracterizar espumas de poliuretano (PU) com adição de cargas para aplicação na adsorção de Cr(III) e SARS-CoV-2, em meio aquoso sintético. Para tal, as espumas foram impregnadas com carvão ativado comercial (CAC) e biomassa vegetal (obtida a partir de caroços de pêssego) tanto *in natura* quanto ativada (biocarvão ativado). Os resultados mostraram altos percentuais de remoção de SARS-CoV-2, acima de 98%, para todas as espumas e, a presença das cargas (*in natura* e biocarvão ativado) nelas potencializou a capacidade de adsorção de Cr(III). Os modelos isotérmicos de Sips e cinético de Elovich apresentaram o melhor ajuste na adsorção de Cr(III), enquanto os estudos termodinâmicos indicaram adsorção espontânea, processo endotérmico e reação favorável na adsorção de Cr(III) para as espumas com adição de cargas. Além disso, a elevação do pH (4 - 6,5) aumentou a capacidade de adsorção de Cr(III) pelas espumas, atingindo níveis máximos remoção de 42,6% e 62,2% em pH 6,5, concentração de adsorvente 0,6 g L^{-1}, para as espumas contendo o caroços de pêssego *in natura* e o biocarvão ativado. Além disso, adição das cargas nas espumas de poliuretano reduziu a densidade aparente delas e aumentou a sua capacidade de absorção de água. Em suma, este estudo fornece informações relevantes sobre o uso potencial de espumas de poliuretano funcionalizadas como adsorvente de base vegetal para a remoção de SARS-CoV-2 e Cr(III) da água. O presente trabalho abre espaço para o desenvolvimento de novas pesquisas que analisem a capacidade de remoção de outros agentes contaminantes pelas espumas de poliuretano, mencionadas anteriormente, além de incentivar o uso de resíduos agroindustriais, assegurando a sustentabilidade ambiental.

Palavras chaves: Bioespumas. Biocarvão. Biocarvão Ativado. Metais Pesados. Caroço de Pêssego.

Abstract

AFONSO, Thays França. **Sustainable polyurethane foams incorporated with different fillers: adsorption of Cr(III) and SARS-CoV-2 in aqueous solutions**. Advisor: Robson Andreazza. 2023. 112f. Thesis (PhD in Materials Science and Engineering) – Science and Engineering of Materials Postgraduate Program, CDTEC, Federal University of Pelotas, Pelotas, Brazil, Brazil, 2023.

Due to the contamination of water resources by the discharge of industrial, municipal, agricultural, and hospital wastewater containing heavy metals and pathogenic microorganisms, it is indispensable, to implement cost-effective, efficacious, and environmentally-friendly treatment procedures to eliminate these contaminants. In this sense, adsorption is an alternative, as it is considered to be effective in removing a variety of pollutants from aqueous media. The aim of this study was to synthesize and characterize polyurethane (PU) foams with added vegetable fillers for the adsorption of Cr(III) and SARS-CoV-2 in synthetic aqueous. To accomplish this objective, the foams were impregnated with commercial activated carbon (CAC) and vegetable biomass (derived from peach stone and its activated biochar). The results showed high percentages of SARS-CoV-2 removal, above 98%, for all the foams, and the presence of the fillers (peach stone and its activated biochar) in them enhanced the Cr(III) adsorption capacity. The Sips isotherm and Elovich kinetic models showed the best fit for Cr(III) adsorption, while the thermodynamic studies revealed that the adsorption process was endothermic, spontaneous, and favorable for Cr(III) adsorption for the foams with fillers. In addition, increasing the pH (4 – 6.5) increased the Cr(III) adsorption capacity of the foams, reaching maximum removal levels of 42.6% and 62.2% at pH 6.5, mass concentration 0.6 g L^{-1}, for the foams containing the peach stone and its activated biochar. Moreover, the incorporation of fillers into polyurethane foams resulted in a reduction of their apparent density and an enhancement of their water absorption capacity. In short, this study provides relevant information on the potential use of functionalized polyurethane foams as a plant-based adsorbent for the removal of SARS-CoV-2 and Cr(III) from water. This work opens up space for the development of new research analyzing the removal capacity of other contaminants by the polyurethane foams mentioned above, as well as encouraging the use of agro-industrial waste, ensuring environmental sustainability.

Keywords: Bio-foams. Biochar. Activated Biochar. Heavy Metals. Peach Stone.

Lista de Figuras

Lista de Tabelas

Sumário

1 Introdução

A poluição da água é um problema crescente e impacta o meio ambiente, a vida humana bem como, os vegetais e animais. A poluição por ser gerada por atividades antropogênicas ou naturais sendo uma séria ameaça à saúde pública em todo o mundo. Ter acesso a água limpa e segura são essenciais para sustentar a vida e prevenir doenças que podem ser transmitidas via ambientes hídricos contaminados. Tal ambiente é fonte importante de água potável, agrícola e água industrial (Babuji *et al.*, 2023). Assim, a sua descontaminação é de extrema importância.

A contaminação ambiental dos recursos hídricos ocorre devido à descarga descontrolada de águas residuárias industriais (indústrias têxtis, cosméticos, fundição, celulose, síntese de corantes e farmacêuticas), municipais (esgotos domésticos), hospitalares e agrícolas não tratadas (Anand *et al.*, 2022; Babuji *et al.*, 2023; Li *et al.*, 2022).

Os contaminantes podem ser produtos químicos (corantes, detergentes, pesticidas, agrotóxicos, inseticidas, fertilizantes, fármacos, hormônios, fragrâncias ente outros), metais pesados e microrganismos patogênicos, como vírus e bactérias. Diferentemente dos poluentes orgânicos que em sua maioria são suscetíveis à degradação biológica, os íons metálicos não se degradam (Guerrero-Latorre *et al.*, 2020; Panhwar *et al.*, 2024; Zamhuri *et al.*, 2022).

O cromo (Cr) é classificado como metal pesado e considerado altamente tóxico. Na saúde humana ele têm efeitos adversos, incluindo câncer de próstata, danos ao fígado, enfraquecimento dos ossos, insuficiência renal, alterações no sistema nervoso central e no sistema reprodutivo (Hong *et al.*, 2020). Além disso, são um risco potencial a vida e ao meio ambiente, além do seu potencial de bioacumulação (ocorrem dentro de um organismo) e biomagnificação (ocorre entre os diferentes níveis da cadeia alimentar) (Ali; Khan; Ilahi, 2019). Em vista dos efeitos nocivos associados aos metais pesados, agências regulamentadoras têm definido padrões internacionais rigorosos para lançamentos de efluentes, limitando assim, seus níveis nos recursos hídricos (Anastopoulos *et al.*, 2019).

Comumente, os contaminantes (metais pesados tóxicos e/ou patógenos) podem ser removidos de águas residuárias através de diferentes processos como, ozonização, oxidação, eletrólise, enzimas, microrganismo, filtração por membrana, coagulação, floculação, osmose reversa, adsorção entre outros (Malik *et al.*, 2023; Panhwar *et al.*, 2024).

Porém, alguns processos apresentam limitações, como exemplo, a remoção incompleta de alguns contaminantes como os íons metálicos; falta de seletividade entre os íons; custos operacionais elevados (Das *et al.*, 2023; Warren-Vega *et al.*, 2023; Zaimee; Sarjadi; Rahman, 2021). Com isso, cada vez mais, processos eficientes e de baixo custo são requisitados para tratamento de águas residuárias.

Uma alternativa é a adsorção, considerada um processo de baixo custo operacional e eficaz na remoção de uma diversidade de poluentes em meio aquoso. A adsorção envolve a aplicação de adsorventes podendo ser utilizada para a remoção de contaminantes em tratamentos de efluentes secundários ou terciários (Chi, 2019; Lima *et al.*, 2021).

Existe uma gama de materiais que podem ser utilizados como adsorventes, na remoção de diferentes poluentes (metais, vírus e bactérias), tais como, os resíduos florestais e agrícolas (cascas de arroz, amêndoas, restos de madeira, frutas e vegetais, caroços de pêssego, polpa de beterraba, entre outros) (Alsulaili; Elsayed; Refaie, 2023; Das *et al.*, 2023; Shaikhiev; Kraysman; Sverguzova, 2023).

Visando aplicações ambientais e a sustentabilidade têm-se incorporado diversos materiais, entre eles, resíduos agroindustriais, como cargas, em espumas de poliuretano (PU) na faixa de 1 a 10% em massa. As cargas podem modificar e potencializar as propriedades, mecânicas, físico-químicas (permeabilidade, elasticidade, resistência química, hidrofobicidade) e térmicas no PU, bem como otimizar a adsorção e absorção de substâncias orgânicas e inorgânicas (Abdullah; Mohd Rus; Abdullah, 2019; Acosta *et al.*, 2022; da Rosa Schio *et al.*, 2019; de Avila Delucis *et al.*, 2018; Hejna *et al.*, 2023; Oribayo *et al.*, 2017).

Nesse cenário, espumas de poliuretano (PU), podem ser consideradas como materiais adsorventes na remoção de substâncias como óleo (Mohammadpour; Mir Mohamad Sadeghi, 2020), corantes (da Rosa Schio *et al.*, 2019; Ren *et al.*, 2021a),

compostos orgânicos e emergentes (Singh; Vaish, 2019), metais pesados (Prasad, P. Supriya *et al.*, 2022) e vírus (Schoeler *et al.*, 2022).

As PU podem ser aplicadas na retenção de moléculas livres com alta polarizabilidade, por exemplo: compostos aromáticos, metálicos e ânions grandes, em função da presença de grupos polares e apolares em sua estrutura, devido à natureza química das membranas das PU, vários mecanismos de adsorção de complexos metálicos aniônicos podem ocorrer como: troca de ligante, adição de ligante, troca iônica, extração por solvente e cátion-quelação (Baldez; Robaina; Cassella, 2008; Santos *et al.*, 2017).

Nesse contexto, embora as PU sejam capazes de reter diferentes classes de substâncias, há uma carência na literatura de pesquisas aplicando biomassa do caroço de pêssego como cargas em espumas de poliuretano. Assim, o presente estudo avaliou tal biomassa (*in natura* e na forma de carvão ativado) incorporada em PU como agentes adsorventes na adsorção de Cr(III) e SARS-CoV-2 em meio aquoso.

2 Objetivos Gerais

O presente estudo objetivou o desenvolvimento e caracterização de bioespumas de poliuretano com adição de diferentes cargas para potencial aplicação em processos de adsorção de Cr(III) e SARS-CoV-2 em meio aquoso sintético.

2.1 Objetivos específicos

- ✓ Verificar a viabilidade técnica da incorporação de 5% de cargas provenientes do caroço de pêssego *in natura*, biocarvão ativado do carroço de pêssego e carvão ativado comercial em espumas poliuretano;
- ✓ Avaliar os efeitos decorrentes da ativação química do biocarvão nos processos de adsorção SARS-CoV-2 e Cr(III);
- ✓ Caracterizar as cargas por análise morfológica, área superficial específica, porosidade, densidade aparente, pH, teor de cinzas e umidade;
- ✓ Caracterizar a bioespuma de poliuretano e as bioespumas compostas com as cargas do caroço de pêssego *in natura*, biocarvão ativado do carroço de pêssego e carvão ativado comercial por análise morfológica - microscopia eletrônica de varredura (MEV), termogravimétrica (TA), espectroscopia no infravermelho por transformada de Fourier (FT-IR), difratometria de raios X (DRX), densidade aparente, potencial zeta e grau intumescimento;
- ✓ Aplicar as bioespumas de poliuretano e as bioespumas compostas na adsorção de SARS-CoV-2;
  - ➢ Determinar a carga viral removida de SARS-CoV-2;
  - ➢ Comparar o percentual de remoção de SARS-CoV-2 entre as bioespumas;
- ✓ Aplicar as bioespumas de poliuretano e as bioespumas compostas em operações descontínuas (batelada):
  - ➢ Estudar os efeitos do pH, da massa de adsorvente na adsorção de Cr(III);

- Determinar a cinética de adsorção em diferentes concentrações de Cr(III) e equilíbrio experimentais e ajustar a modelos da literatura;
- Estimar os parâmetros cinéticos, isotérmicos e termodinâmicos de adsorção de Cr(III);

✓ Avaliar o potencial adsortivo de SARS-CoV-2 e Cr(III) pelas bioespumas de poliuretano e as bioespumas compostas;

3 Revisão Bibliográfica

3.1 Tratamento de águas residuárias

A contaminação da água é uma questão ambiental que prejudica e impacta negativamente a vida ao redor do mundo. Existem diversas fontes de contaminação dos recursos hídricos, como atividades de mineração, fertilizantes e pesticidas, resíduos radioativos, efluentes urbanos e industriais, entre outros (CRINI; LICHTFOUSE, 2019). Estas atividades liberam compostos como mercúrio, arsênio, cromo, chumbo e cádmio não só em corpos hídricos, mas também no solo e ar (Joseph *et al.*, 2019).

Fontes de águas contaminadas colocam em risco a saúde dos seres vivos devido à exposição a compostos químicos tóxicos, microrganismos patogênicos e metais pesados, por isso, à necessidade da sua descontaminação (Mishra *et al.*, 2019).

Nessa perspectiva o tratamento de águas residuárias é um fator primordial. E para isso várias tecnologias podem ser aplicadas (Tabela 1) na sua descontaminação, tais como os tratamentos primário, secundário e terciário, comumente utilizados ao redor do mundo (Awad; Gar Alalm; El-Etriby, 2019). Porém, esses tratamentos tem limitações quanto a remoção completa de metais e microrganismos patogênicos.

Tabela 1 – Processos de tratamento de água residuária.

Tipo de Tratamento	Tecnologia	Tipo de Composto removido
Primário	Coagulação	I, O, B
	Floculação	I, O, B
	Precipitação química	I, O
	Microfiltração	I, O
Secundário	Processo aeróbio ou anaeróbio	O
Terciário	Oxidação	I, O
	Destilação	I, O
	Precipitação eletroquímica	I, O
	Fotocatálise	I, O
	Cristalização	I, O
	Troca iônica	I, O
	Adsorção	I, O
	Processos por membrana	I, O

Em que: I = Inorgânico; O = Orgânico; B = Biológico.
Fonte: Adaptado (Bolisetty; Peydayesh; Mezzenga, 2019).

No tratamento de águas residuárias os custos de processo podem ser bem elevados, isso por que, a tecnologia a ser aplicada é específica para a remoção de um determinado composto e, por sua vez, para melhor efetividade no processo de tratamento, necessita-se de combinações de tecnologias para retirar do meio tal(is) composto(s) – orgânicos, biológicos e inorgânicos (metais pesados) (Bolisetty; Peydayesh; Mezzenga, 2019; Joseph *et al.*, 2019).

No tratamento convencional de águas residuárias, a etapa de pré-tratamento por processo de precipitação química é o mais comum para a remoção de metais, embora, outras tecnologias como a coagulação, floculação, microfiltração, filtração química também sejam utilizadas, mas com menor eficiência, quando comparadas com os tratamentos terciários (Azimi *et al.*, 2017).

No processo de precipitação química, ajusta-se para básico o pH da água e, através da reação dos agentes químicos com o metal, forma-se uma partícula insolúvel que precipita sendo removida por sedimentação simples (Rajasulochana; Preethy, 2016). Porém, os níveis residuais de metais na água continuam elevados, ou seja, esse processo não atende as concentrações finais exigidas pela legislação ambiental e ainda necessita de tratamento adicional ao final do processo (Crini; Lichtfouse, 2019).

O mesmo ocorre com os demais processos convencionais, além de, apresentarem como desvantagem a geração de lodo (no processo de coagulação/floculação), elevado consumo de produtos químicos e íons metálicos residuais na água pós-tratada. Dessas tecnologias para remoção de íons metálicos em meio aquoso, a microfiltração, que consiste na aplicação de tecnologias de filtragem por membranas de materiais cerâmicos e/ou poliméricos, com tamanho de poros entre 100-1000 nm, tem como vantagem o uso direto nos tratamentos terciários (ex. filtração por membrana, troca iônica e adsorção), embora não remova completamente os íons metálicos na água (Sekulić *et al.*, 2017, 2019).

Dos tratamentos terciários (Tabela 1), enfatiza-se a tecnologia de adsorção, que por sua vez, utiliza uma variedade de materiais (sorventes sílica-cabono, polímeros e nanossorventes) desde que esses apresentem mecanismos de adsorção

entre os íons metálicos e o adsorbato. O processo de adsorção é confiável, de fácil operação e remove uma gama de poluentes (Lima *et al.*, 2021).

Embora haja a possibilidade de recuperação dos adsorventes e íons metálicos no processo de tratamento, a recuperação dos adsorventes (carvão ativado) se torna um entrave para aplicação de determinados adsorventes em escala industrial devido à grande perda de adsorbato no processo (Das *et al.*, 2017; Kuyucak; Volesky, 1988).

Diversos estudos demonstram que algumas tecnologias envolvendo adsorção para remoção de compostos tóxicos na água têm alta eficiência (99%), mas isso ocorre em um ambiente controlado – condições idealizadas de pH, temperatura, fluxo de agitação, concentração do contaminante, entre outras variáveis operacionais (Chi, 2019; Lima *et al.*, 2021).

Em condições reais – efluentes ou água contaminada – a eficiência na remoção do contaminante cai consideravelmente em consequência da ocorrência simultânea de outros compostos no meio, a exemplo íons metálicos (Pb^{2+}, Cu^{2+}, Ni^{2+}, Cd^{2+}, Cr^{6+}) que competem pelo mesmo sítio ativo no adsorbato (Chen *et al.*, 2022) no tratamento de água com carvões ativados, por exemplo.

Os metais pesados são poluentes tóxicos gerados em processos industriais, e causam graves problemas ambientais e de saúde pública. Como eles são expressivamente tóxicos o limite máximo permitido nas águas pelas agências reguladoras pode variar (Tabela 2). Nessa perspectiva, há uma busca intensa por materiais de baixo custo, alta eficiência no processo de adsorção de íons metálicos e viabilidade técnica em nível de escala industrial. Portanto, devido à sua alta toxicidade, deve ser reduzido a níveis aceitáveis antes de ser lançado no meio ambiente (Gao *et al.*, 2021).

Tabela 2 – Informações ambientais e epidemiológicas sobre metais tóxicos.

Metal	**Fonte**	**Efeito na saúde humana**	**Nível máximo de contaminante**		
			WHO*	**CONAMA****	**USEPA*****
Mercúrio (Hg)	Industriais de eletrônicos; queima de combustíveis fósseis.	Dano ao sistema nervoso central e aos rins	0,006 mg L^{-1}	0,0002 mg L^{-1}	0,002 mg L^{-1}
Arsênio (As)	Industriais de eletrônicos; ocorrência natural.	Dano à pele e ao sistema circulatório	0,01 mg L^{-1}	0,01 mg L^{-1}	0,01 mg L^{-1}

Cromo (Cr)	Ocorre naturamente; indústria de curtume, galvanização e outras.	Vômito, diarreia, dermatites alérgica, náusea,	0,05mg L^{-1}	0,05 mg L^{-1}	0,1 mg L^{-1}
Chumbo (Pb)	Tintas; baterias; munições; ligas metálicas; indústrias de galvanização.	Danos aos rins; redução no desenvolvimento neural; náuseas; dor abdominal.	0,01 mg L^{-1}	0,01 mg L^{-1}	0,015 mg L^{-1}
Cádmio (Cd)	Indústrias de galvanização, de produtos químicos, de eletroeletrônicos e de fundição; Queima de combustíveis fósseis; Pilhas e baterias.	Danos aos rins; carcinogênico; alterações no sistema imunológico e sanguíneo;	0,003 mg L^{-1}	0,001 mg L^{-1}	0,005 mg L^{-1}

*Valores estabelecidos pela Organização Mundial da Saúde (WHO, 2017a; 2017b); ** Valores estabelecidos pela resolução CONAMA 357 para água doce classes 1 (BRASIL, 2005); *** Valores estabelecidos pela Agência de Proteção Ambiental dos Estados Unidos (USEPA, 2023).

3.1.1 Cromo

O cromo (Cr), deriva da palavra grega *Croma*, é o é o vigésimo quarto elemento mais comum e ocorre naturalmente na crosta terrestre (Kanwar *et al.*, 2020). As principais fontes antrópicas de liberação de Cr(III) e Cr(VI) no meio ambiente são oriundas da fabricação industrial de aço, couro e têxteis. Além dessas, o Cr(VI), resulta de processos de industrias de impressão, tingimento, eletropintura, fabricação química e metalurgia (Anna L. Rowbotham, 2000; Bachmann *et al.*, 2022; Ukhurebor *et al.*, 2021).

O Cr possui diferentes estados de oxidação (Figura 1), mas o Cr trivalente (III) e o Cr hexavalente (VI) são as formas mais estáveis encontradas na natureza. Uma das propriedades mais críticas do Cr(VI) é a sua alta solubilidade em água, fácil redução e mobilidade em comparação com o Cr(III). Isso resulta em um número relativamente maior de espécies biodisponíveis e persistentes no meio ambiente (Ukhurebor *et al.*, 2021).

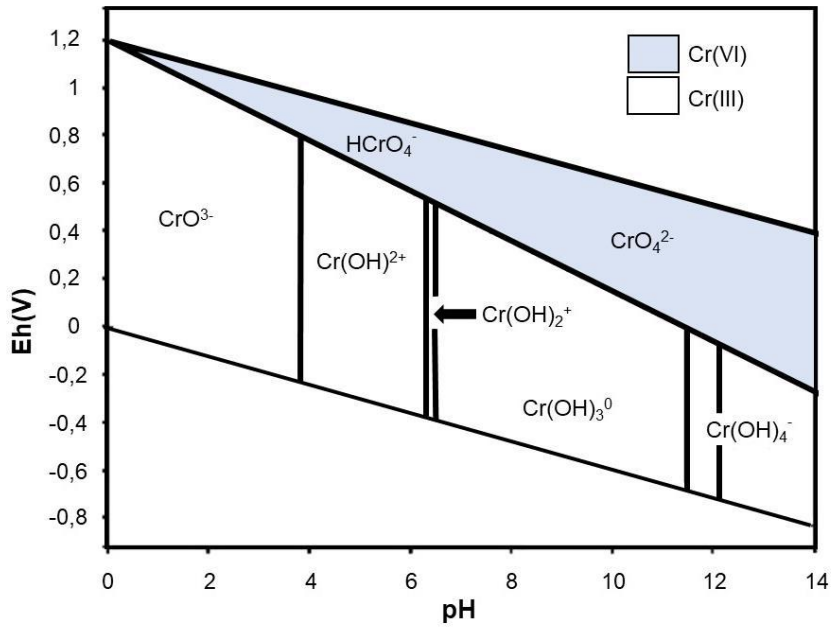

Figura 1 - Diagrama de Eh-pH do cromo em solução aquosa (25 °C e 1 atm).
Fonte:(Maronezi *et al.*, 2019).

Além disso, Cr(VI) pode ser reduzido a Cr(III) sob condições ácidas. O Cr(VI) é cancerígeno, mutagênico e altamente nocivo para os organismos vivos, já o Cr(III), embora tenha sido proposto como um elemento essencial, por mais de 60 anos, atualmente novos estudos mostram que o cromo só pode ser considerado farmacologicamente ativo e não um elemento essencial (Vincent, 2017).

Em doses excessivas o tanto o Cr(III) quanto o Cr(VI), resulta em efeitos adversos à saúde, como dermatites alérgica de contato, erupções cutâneas e outros (Georgaki *et al.*, 2023). Os íons Cr(III) também podem causar mais perturbações estruturais na membrana eritrocitária humana do que Cr(VI) (Dash; Jena; Rath, 2022; Suwalsky *et al.*, 2008).

A contaminação das águas pelo Cr pode ocorrer devido ao lançamento dos efluentes industriais não tratados nos corpos hídricos. Essa disposição inadequada dos efluentes e resíduos industriais causa graves problemas ambientais. Consequentemente, implica em riscos à saúde para os organismos vivos (animais e plantas), bem como para o meio ambiente (Ukhurebor *et al.*, 2021).

No entanto, diversos processos (precipitação química, osmose reversa, redução biológica, troca iônica e adsorção) estão atualmente em uso para tratar,

purificar e remediar Cr(VI e III) de efluentes industriais. Esses processos envolvem principalmente a imobilização ou redução do Cr(VI) nocivo para o Cr(III) menos nocivo (Bandara; Peña-Bahamonde; Rodrigues, 2020; Ukhurebor *et al.*, 2021).

Atualmente, os limites de descarga e a mitigação de perigos para Cr(VI) e Cr(III) quase não têm normas regulamentadoras comuns estabelecidos em todos os países do mundo. O tratamento da água é totalmente voluntário pelos países. Porém, é comum a utilização de carvão ativado em processos de adsorção para tratamento da água. Ele é muito eficaz na remoção da contaminação de Cr e microrganismos patogênicos presentes nos recursos hídricos (Bandara; Peña-Bahamonde; Rodrigues, 2020; Dash; Jena; Rath, 2022; Solis-Ceballos *et al.*, 2023).

Nesse contexto, embora o Cr (III) seja menos tóxico que o Cr (VI) (Shin *et al.*, 2023), a possibilidade de oxidação do estado (III) para o (VI) num ambiente aquático multiplica a sua periculosidade ocasionando uma maior preocupação ambiental (Dash; Jena; Rath, 2022). Assim, é necessário remover ambas espécies de íons Cr das águas residuais.

3.2 SARS-CoV-2

O COVID-19 é uma doença altamente infecciosa considerada uma síndrome respiratória aguda grave causada pelo coronavírus 2 (SARS-CoV-2) (Zhu *et al.*, 2020). A principal via de transmissão da doença é através da exposição humana a gotículas sprays ou aerossóis. O coronavírus (CoVs) é caracterizado como um vírus de RNA de fita simples e sentido positivo, não segmentado, têm quatro proteínas estruturais, denominadas proteínas S, envelope (E), membrana (M) e nucleocapsídeo (N) (Chan *et al.*, 2020; Ronchi *et al.*, 2020). Esse vírus causou pandemia de COVID-19 e afetou gravemente o sistema global, o meio ambiente, a economia e a saúde pública.

Diversos estudos vêm sendo realizados para identificar as principais vias de transmissão do vírus e sua estabilidade em diferentes meios. No entanto, existe a possibilidade de este vírus ser transmitido para humanos e animais pela via fecal-oral (Choi *et al.*, 2023; Kim *et al.*, 2020). Embora a transmissão do SARS-CoV-2 por aerossol esteja bem descrita, a transmissão pela água através dos excrementos humanos (matéria fecal e urina) é menos compreendida. Os excrementos humanos

(urina, escarro, sangue, fezes) de indivíduos infectados com doença COVID-19 chegam ao meio aquático ao serem liberados via águas residuais (Figura 2).

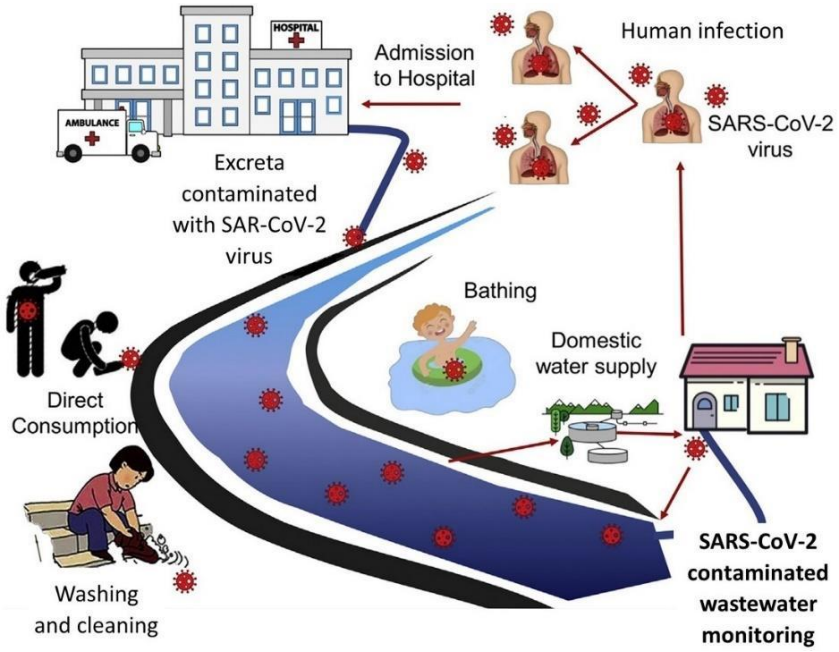

Figura 2 - Os caminhos do SARS-CoV-2 no sistema aquático.
Fonte: (Bhattacharya *et al.*, 2023).

Estudos mostram a presença de partículas virais do SARS-CoV-2 sobrevivendo em amostras de águas residuais municipal, hospitalares, aeronaves, navios de cruzeiro comerciais, bem como, rios (Foladori *et al.*, 2020; Guerrero-Latorre *et al.*, 2020; Medema *et al.*, 2020; Saththasivam *et al.*, 2021). Portanto, podem ser virulentos quando presentes nas águas superficiais ou nas águas residuais não tratadas (Li *et al.*, 2022).

O novo coronavírus pode sobreviver nas águas residuais e nas águas superficiais por muitos dias dependendo das condições ambientais da água, como a temperatura. O aumento da temperatura reduz a sobrevivência do vírus na água (Ahmed *et al.*, 2020; Fuschi *et al.*, 2021). No entanto, o potencial de transmissão do SARS-CoV-2 sugerem a transmissão fecal do vírus através de águas residuais contaminadas com fezes de pacientes imunocomprometidos (Anand *et al.*, 2022; Dergham *et al.*, 2021).

Nesse contexto, o conhecimento mais amplo a respeito do vírus ainda é limitado e as perspectivas de soluções sustentáveis para remoção do vírus em meio aquoso ainda estão por serem exploradas.

3.3 Adsorção

Diversos processos biológicos, físicos e químicos ocorrem na interface entre duas fases, enquanto outros são desencadeados como resultado dessa interação. Os processos podem ser examinados em diferentes sistemas dependendo dos tipos de fases que interagem, que incluem: líquido-líquido, líquido-gás, sólido-gás e sólido-líquido. A discrepância na concentração de uma substância específica nesta interface em comparação com as fases circundantes é conhecida como adsorção. (Chakraborty *et al.*, 2022).

O processo de adsorção pode ser dividido em duas categorias principais: adsorção química e física. Na adsorção química, a ligação adsorbato -adsorvente é formada por forças relativamente mais fortes, podendo haver formação de ligações químicas (ligações covalentes ou iônicas) entre as valências livres do sólido e do adsorbato. Na adsorção física, as partículas de adsorbato se fixam à superfície do adsorvente por meio de forças de van der Waals e ligações de hidrogênio (Alaqarbeh, 2021).

A adsorção física (fisissorção) ocorre quando o substrato e o adsorvente se ligam por meio de forças relativamente fracas, sem quaisquer alterações na estrutura química de ambos. A adsorção Química (quimissorção) ocorre através da formação de ligações químicas entre o adsorvente e o substrato, onde há rearranjo da densidade eletrônica entre eles, formando uma ligação iônica ou covalente (Alaqarbeh, 2021; Chakraborty *et al.*, 2022; Dąbrowski, 2001).

Neste contexto, o modelo de adsorção adequado para um determinado sistema é realizado com base em critérios físicos experimentais, como os estudos termodinâmicos, estudos de isotermas de adsorção, cinética ou de equilíbrio. Ambos os modelos podem explicar o mecanismo de adsorção (físico ou químico).

3.3.1 Fatores que influenciam a adsorção

O processo de adsorção é influenciado pela temperatura, pH e potencial de carga zero (pH_{PCZ}), força iônica, quantidade de adsorvente, área superficial específica e porosidade, concentração inicial do soluto, tempo e velocidade de agitação (Xue *et al.*, 2023).

A temperatura da solução afeta o processo de adsorção para um determinado adsorbato, por meio da alteração do estado de equilíbrio da adsorção e através da diminuição da viscosidade da solução com o aumento da temperatura (Zhang *et al.*, 2020). Isso, devido ao aumento da taxa de difusão das moléculas do adsorbato em toda camada limite interna e externa e nos poros da partícula do adsorvente.

O pH é um dos fatores que mais influencia o grau de distribuição das espécies químicas (Khamis *et al.*, 2023). Por isso, variações no pH do meio determinam a especiação química dos metais em solução, por exemplo, em termos de complexação por ligantes orgânicos, inorgânicos, potencial redox, hidrólise e também afeta o estado de dissociação do local de ligação (Das *et al.*, 2023, 2017; Fiol *et al.*, 2006). Em outras palavras, dependendo do pH a espécie química pode estar em um estado mais tóxico, tornando-se um risco ambiental (Bandara; Peña-Bahamonde; Rodrigues, 2020; Solis-Ceballos *et al.*, 2023; Suwalsky *et al.*, 2008).

Além disso, o pH pode determinar a carga superficial do material através do pHpcz; indicando a presença de atração ou repulsão entre adsorbato e adsorvente (Chi, 2019; Gao *et al.*, 2021). O valor do pHpcz determina quando a carga líquida do adsorvente é nula (ponto de carga zero). Assim, pH > pHpcz, a carga superficial do material é negativa, favorecendo a adsorção de cátions, logo pH < pHpcz, a carga superficial do material é positiva, favorecendo a adsorção de ânions (Gao *et al.*, 2021; Vakili *et al.*, 2023).

A força iônica também influencia a adsorção do soluto na superfície do adsorvente (Liu *et al.*, 2021, 2022; Liu, 2020, 2009). Desse modo, em solução aquosa o soluto e a superfície do adsorvente (biomassa), em duas fases, entram em contato, devido à interação eletrostática, eles então são cercados por uma dupla camada elétrica, logo, com o aumento da força iônica há uma diminuição na adsorção do metal de interesse (Dönmez; Aksu, 2002).

Quanto à quantidade de adsorvente, um aumento em sua concentração geralmente aumenta a quantidade de soluto adsorvido, mas até certa concentração de adsorvente (Das, 2010). Em contrapartida, concentrações muito elevadas de adsorvente diminuem a quantidade de soluto por unidade de massa do adsorvente devido a interações complexas. Por exemplo, o soluto disponível torna-se insuficiente para cobrir totalmente os locais trocáveis disponíveis no adsorvente, acarretando na baixa capitação do soluto e adsorção específica (Tangaromsuk *et al.*, 2002).

Além disso, o aumento na quantidade de soluto adsorvido pode estar relacionado com o tamanho da partícula do adsorvente. Assim, a área superficial específica, quanto maior, fornece mais locais de adsorção, com isso, há um aumento na quantidade de material adsorvido (Gao *et al.*, 2021). No entanto, o tamanho das partículas do adsorvente, quanto maiores, menor a área superficial, logo, pode reduz os sítios de adsorção (Gao *et al.*, 2023).

A porosidade fornece uma descrição da microestrutura do material e essa estrutura pode ser classificada conforme o diâmetro médio dos poros em microporos (diâmetro médio < 20 Å), mesoporos (20 Å < diâmetro médio < 500 Å) e macroporos (diâmetro médio < 20 Å > 500 Å) (Chi, 2019; Gao *et al.*, 2021). Assim, o tamanho e distribuição dos poros influencia na capacidade de adsorção, quanto maior a porosidade e o tamanho do poro, melhor a eficiência no processo de adsorção (Karimi; Tavakkoli Yaraki; Karri, 2019).

No que se refere à concentração inicial do soluto, a quantidade de material adsorvido pode aumentar com o aumento da concentração de adsorbato, mas até certo ponto (Das, 2010; Sharma; Dalai; Vyas, 2017). Isso ocorre devido ao número de sítios de ligação disponíveis ser limitado a uma concentração especifica do adsorvente (Biswas *et al.*, 2020; Hu *et al.*, 2020).

A velocidade de agitação também influencia o processo de adsorção. O aumento na velocidade de agitação pode aumentar a eficiência de remoção e a capacidade de adsorção até certo ponto. Quando a velocidade ideal de agitação é alcançada, ela reduzir a resistência à difusão dos íons (do adsorbato) em direção à superfície do adsorvente, por exemplo, carvão ativado, devido à formação de uma suspensão uniforme do carvão ativado e do adsorbato. Em velocidades de agitação

superiores a ideal a capacidade adsorção é reduzida. Isso pode ser atribuído ao fenômeno de vórtice e à falta de acessibilidade adequada dos íons (adsorbato) ao adsorvente (Abbas; Trari, 2020; Vakili *et al.*, 2023). Logo, a velocidade ideal de agitação evita o fenômeno vulnerável de vórtice durante o processo de adsorção.

Já o tempo de contato entre o adsorvente e adsorbato, para que ocorra a adsorção, é alcançado à medida que se atinge o equilíbrio. Esse tempo varia de acordo com o material adsorvente e com todos os fatores descritos anteriormente (Qiao *et al.*, 2020; Zhang; Tian, 2020).

3.3.2 Materiais aplicados como adsorventes

Nos últimos anos, a valorização de resíduos naturais, agrícolas e industriais tem sido investigado como materiais alternativos a adsorventes comerciais. Tais resíduos, são considerados adsorventes de baixo custo e podem ser aplicados na remoção de metais pesados tóxicos e microrganismos, presentes em águas e efluentes (Abbas; Trari, 2020; Alsulaili; Elsayed; Refaie, 2023; Demarco *et al.*, 2023; Khamis *et al.*, 2023; Prasad, P Supriya *et al.*, 2022; Schoeler *et al.*, 2022; Zaimee; Sarjadi; Rahman, 2021; Zhu *et al.*, 2021).

Os resíduos agrícolas por apresentarem em sua composição uma gama de grupos funcionais e alto teor de carbono, podem ser utilizados para produzir carvão ativado de baixo custo (biocarvão ativado), otimizando seu potencial em adsorção (Alsulaili; Elsayed; Refaie, 2023; Tokay; Akpınar, 2021). Além disso, a utilização do biocarvão ativado é um substituto econômico e sustentável quando comparado com carvão ativado comercial considerado caro (Tokula *et al.*, 2023).

Alguns desses resíduos como a casca de coco verde (aplicado na remoção de Cu; casca de *Pinus elliotti* (aplicado na remoção de Cr, Pb; lignina aplicado na remoção de Cu e Pb e outros, são materiais adsorventes sustentáveis (Bachmann *et al.*, 2022; Bosch *et al.*, 2022; Chakraborty *et al.*, 2022; de Aguiar Linhares; Romeu Marcílio; Juarez Melo, 2016; Karri; Sahu; Meikap, 2020; Lima *et al.*, 2021; Vakili *et al.*, 2023).

Destaca-se o caroço de pêssego (*Prunus persica L.*). O pêssego, embora seja uma fruta nativa da China e do sul da Ásia, é bem popular na cultura brasileira. A

produção global de pêssego foi cerca de 24,665 milhões de toneladas entre a Europa, Ásia, América do Norte e África América do Sul (FAOSTAT, 2018), sendo a maior parte produzida na China (15,195 milhões de toneladas) (Martin-Martinez *et al.*, 2018; Shaikhiev; Kraysman; Sverguzova, 2023).

Considerando que a quantidade de resíduos do processamento do pêssego é de aproximadamente 20 % do peso da fruta *in natura* gera um volume global de resíduos, principalmente caroço, superior a 5 milhões de toneladas por ano. Considerando o volume de resíduo, como a alternativa sustentável, é empregar esse material para tratar água residuária, agregando a ele, valor.

O caroço de pêssego é um adsorvente potencial na remoção de poluentes aquáticos tais como, metais (Pb, Cr, Au, Cd, Cu), corantes, pesticidas, microrganismos patogênicos, entre outros compostos, seja *in natura* ou como carvão ativado (Duranoğlu; Trochimczuk; Beker, 2010; Mohammad; El-Sayed, 2021; Núñez-Decap; Wechsler-Pizarro; Vidal-Vega, 2021; Parlayıcı, 2019; Shaikhiev; Kraysman; Sverguzova, 2023; Torrellas *et al.*, 2015; Tsoncheva *et al.*, 2018; Uysal *et al.*, 2014).

O processo de adsorção utilizando o caroço de pêssego é governado por múltiplos mecanismos em função de diversos parâmetros, como mencionados no item 3.3.1, que influenciam esse processo, assim como a sua composição (lignocelulósica) (Martin-Martinez *et al.*, 2018; Núñez-Decap; Wechsler-Pizarro; Vidal-Vega, 2021).

O caroço de pêssego possui teor considerável de lignina. Isso, influencia no processo de degradação sob o efeito do aumento da temperatura. A lignina por ser altamente hidrofóbica e potencializa a resistência à umidade. Quanto maior a quantidade de lignina no material melhor a sua resistência mecânica. Isso ocorre porque a lignina preenche as paredes celulares entre hemicelulose e celulose, ligando-se à hemicelulose por pontes de hidrogênio, conferindo resistência mecânica às paredes celulares (Núñez-Decap; Wechsler-Pizarro; Vidal-Vega, 2021; Zoghlami; Paës, 2019).

3.4 Carvão ativado

O carvão ativado (CA) é um material carbonáceo que consiste em camadas de grafite hidrofóbicas com grupos funcionais hidrofílicos, estrutura porosa, elevada área

superficial, baixa acidez/reatividade básica e estabilidade térmica. Logo, é um material adsorvente eficaz na remoção de compostos orgânicas e inorgânicas, como metais pesados e microrganismo patógenos em meio aquoso (Mohammad; El-Sayed, 2021; Shaikhiev; Kraysman; Sverguzova, 2023). Portanto, CA é um adsorvente essencial devido à sua alta reatividade superficial, grande área superficial específica bem como o seu caráter sustentável. Ele pode ser produzido utilizando diferentes materiais precursores por métodos de ativação química, física ou a combinação dois métodos.

Na ativação química há dois estágios. No primeiro estágio, uma vez selecionado um ativador químico (NaOH, Na_2CO_3, KOH, K_2CO_3, $AlCl_3$, H_3PO_4 e H_2SO_4 e $ZnCl_2$) impregna-se o precursor por um determinado período de tempo até concluir a ativação. No segundo estágio, o precursor já ativado quimicamente é aquecido em atmosfera inerte. Ativadores químicos têm efeitos desidratantes e influenciam a decomposição no processo pirolítico, além de, inibir a formação de alcatrão de fechamento de poros (Akçakal; Şahin; Erdem, 2019; Heidarinejad *et al.*, 2020) e liberar novos sítios ativos no adsorvente. Em tal ativação, as macromoléculas são fragmentadas e os componentes voláteis formados deixam a estrutura pelo efeito catalítico dos ativadores, restando, o material carbonáceo (Yahya; Al-Qodah; Ngah, 2015).

Na ativação física, o precursor é pirolisado em atmosfera inerte, em seguida o material carbonizado obtido é ativado pelo vapor (água ou CO_2) contribuindo para o aumento da porosidade no precursor (Akçakal; Şahin; Erdem, 2019; Heidarinejad *et al.*, 2020).

As propriedades do carvão ativado são influenciadas pelo tipo de ativação (químico ou físico), o tempo de ativação, a temperatura de carbonização e as condições de impregnação.

O carvão ativado comercial é um produto caro, assim, de modo a baixar os custos, resíduos agrícolas como o caroço de pêssego, pode ser aplicado como material precursor sustentável na produção de carvão ativado. Os resíduos agrícolas são materiais lignocelulósicos com alto teor de carbono, e alta capacidade adsortiva devido à alta porosidade, alta estabilidade físico-química, alta resistência mecânica, alta capacidade de reatividade superficial e imensa área superficial (Yan *et al.*, 2018).

O carvão ativado do caroço de pêssego contém relativamente elevado teor de carbono e baixa produção de cinzas (Akçakal; Şahin; Erdem, 2019; Ebadollahzadeh; Zabihi, 2020), ou seja, adequado para produção de carvão ativado e aplicação na remoção de diversos compostos. Quando esse é submetido ao processo de ativação físico-química, utilizando $ZnCl_2$, há um aumento na área superficial do material com o aumento da temperatura de pirólise, além de um aumento no volume de poros (poros pequenos) e aumento na porosidade (Martin-Martinez *et al.*, 2018; Mohammad; El-Sayed, 2021; Shaikhiev; Kraysman; Sverguzova, 2023; Torrellas *et al.*, 2015).

3.5 Espumas de Poliuretano

As espumas de poliuretanos (PU) representam uma das maiores produções mundiais dentre os materiais poliméricos, totalizando 25,3 milhões de toneladas para o ano de 2019 (RAPRA, 2018).

Os Poliuretanos (PU) são materiais poliméricos formados pela reação de polimerização (poliadição) entre grupos OH (hidroxilas) de um poliol com os grupos NCO (isocianatos). O poliol representa um segmento macio do polímero e o isocianato apresenta a segmento rígido (Abdullah; Ramtani; Yagoubi, 2023; Gama; Ferreira; Barros-Timmons, 2018). Espumas poliméricas são materiais constituídos por uma fase gasosa e uma fase sólida. Elas podem ser rígidas ou flexíveis e podem ser sintetizadas a partir de uma ampla gama de polímeros (Kuranchie; Yaya; Bensah, 2021).

O comprimento da cadeia, do poliol reagindo com o isocianato, confere as propriedades mecânicas do poliuretano, como resistência, viscoelasticidade e dureza. O poliol estabelece o caráter e o grau de ramificação ou reticulação do polímero final. Assim, poliuretanos com longas cadeias de poliol, possuem estruturas mais flexíveis. Além disso, o aumento no grau de reticulação do polímero final implica em uma temperatura de transição vítrea mais alta, maior ductilidade e menor alongamento na ruptura (Abdullah; Ramtani; Yagoubi, 2023; Gama; Ferreira; Barros-Timmons, 2018).

Quanto a estrutura celular interna da espuma entende-se que a temperatura afeta comportamento mecânico. Espumas de poliuretano com estruturas de células abertas com baixo teor de células completamente fechadas são mais flexíveis e

facilmente se recuperam. Enquanto espuma rígida possui muitas células fechadas que se formam independentemente da parede (Abdullah; Ramtani; Yagoubi, 2023).

As PU possuem propriedades diversas aplicações como selantes, isolamentos térmico e acústico, almofadas, colchões domésticos, embalagens, mobiliário, automotiva, calçados, brinquedos, aeroespaciais, materiais de construção, dentre outras (Cabulis; Ivdre, 2023; Gama; Ferreira; Barros-Timmons, 2018). Logo**,** as PU podem ser sintetizadas por meio de pequenas modificações ajustando os conteúdos de isocianato, poliol, surfactante, catalisador, aditivos e agentes de expansão em sua formulação, a fim de, alcançar as propriedades desejadas para uma determinada aplicação (Cabulis; Ivdre, 2023; Kuranchie; Yaya; Bensah, 2021).

Na produção de PU, o uso de polióis derivados de fontes vegetais (ex. poliéteres), embora os derivados do petróleo (ex. poliésteres) sejam tecnicamente superiores. Também, existe uma série de opções em isocianatos, incluindo certos produtos comerciais, tais como: diisocianato de tolueno (TDI), diisocianato de metileno difenil (MDI), hexametilenodiisocianato (HMDI) e soforonodiisocianato (IPDI).

Em se tratando dos agentes de expansão, eles podem ser sopradores químicos (água, expande o polímero pelo CO_2 produzido) ou físicos (solventes com baixo ponto de eluição: hexano, pentano ou acetona; que expande o polímero por vaporização) (SINGH, 2002).

Outro reagente utilizado na síntese de PU, é o surfactante; copolímeros compostos por uma estrutura de enxertos de poliol (óxido de etileno - óxido de co-propileno) ou silicone. Eles têm por função diminuir a tensão superficial, promover a nucleação de bolhas, emulsificar reagentes incompatíveis da formulação, estabilizar as células, agir sobre o tamanho da célula e permeabilidade das espumas, bem como, determinar o conteúdo de células abertas e controlar a espessura das arestas da parede celular, de modo a impedir sua ruptura prematura, antes que ocorra o evento de abertura da célula durante a polimerização (Gama; Ferreira; Barros-Timmons, 2018).

Os catalisadores são utilizados para acelerar a reação de síntese dos PU, sendo o estanho ou aminas, os catalisadores mais comumente aplicados. Para que haja uma expansão adequada durante a reação, necessita-se do equilíbrio entre a

geração de gás (sopro) e a polimerização (gelificação) (Ahmadijokani *et al.*, 2023; Gama; Ferreira; Barros-Timmons, 2018).

Pesquisas recentes têm buscado o desenvolvimento de PU a partir de matérias-primas de origem renováveis e biológicas, visando a sustentabilidade, tendo em vista que grande parte das matérias-primas para isocianatos e polióis, utilizados nessa síntese, são derivadas do petróleo (Ren *et al.*, 2023; Silva; Oréfice, 2023) .

Neste contexto, há interesse na aplicação de polióis de base biológica e polióis verdes na síntese de PU. Nos últimos 20 anos é crescente o número de trabalhos focados no desenvolvimento de polióis de base biológica, a partir de fontes renováveis, tais como: subprodutos industriais, óleos vegetais e resíduos de biomassas (Almeida *et al.*, 2020; Gama; Ferreira; Barros-Timmons, 2018; Gama, 2017; Huang *et al.*, 2022; Parcheta; Głowińska; Datta, 2020; Zhou *et al.*, 2016).

Polpa de beterraba, cortiça, amido de milho, lignina, quitosana estão entre algumas das matérias-primas recentemente aplicadas como fontes de polióis de base renovável (biopolióis) na síntese de PU (Biswas; Pal, 2021; Selvasembian *et al.*, 2021). Outros estudos vêm utilizando óleos vegetais (óleo de mamona, palma, canola, tunga, soja e outros) como fonte de polióis por conferir a mistura com polióis petroquímico convencionais, uma vez que esses são biodegradáveis e ecológicos, solúveis em grande parte dos solventes industriais (Cabulis; Ivdre, 2023).

Destaca-se o óleo de mamona dentre os polióis, pois não compete com os suprimentos alimentícios e possui um elevado conteúdo natural de hidroxilas. Ele é um triglicerídeo do ácido ricinoléioco, extraído das sementes da planta *Ricinus communis* (Ren *et al.*, 2023). Possui um grupo hidroxila secundário (C_{12}); dezoito átomos de carbono; funcionalidade de 2,7 grupos OH / mol; uma ligação dupla (C_9 – C_{10}); número de hidroxila de cera de 160 mg de KOH/g^{-1} e pode ser utilizado em quase todas as aplicações relacionados aos PU (Gama, 2017).

É interessante ressaltar que o uso de biopolióis, como a glicerina loira, aplicados na síntese de PU rígidos, uma vez que reduz o custo de produção das espumas e minimiza o impacto ambiental, melhorando a sustentabilidade na indústria de PU (Cabulis; Ivdre, 2023; Ren *et al.*, 2023).

3.5.1 Sustentabilidade de PUF e sua aplicação na descontaminação ambiental

A maioria dos polióis utilizados na produção de PUF são derivados de produtos petrolíferos, mas devido ao crescente interesse no uso de materiais renováveis e a crescente preocupação com o impacto ambiental, sustentabilidade e a futura escassez de petróleo, levou ao desenvolvimento de PU utilizando materiais de origem vegetal, biológicos e renováveis (Gama; Ferreira; Barros-Timmons, 2018; Okoli; Ofomaja, 2019; Selvasembian *et al.*, 2021).

A razão para isso é a crescente demanda por materiais com menor impacto ambiental e que possam ser reciclados, reutilizados ou provenientes de fontes não contaminantes (Gama; Ferreira; Barros-Timmons, 2018; Parcheta; Głowińska; Datta, 2020; Ren *et al.*, 2021b; Tokula *et al.*, 2023). Os biopolióis e os resíduos agroindustriais, são renováveis, portanto, uma alternativa sustentável aos derivados à base de petróleo na síntese dos PUs.

Nesse contexto, visando o apelo ambiental, espumas de poliuretano podem ser aplicadas em técnicas de adsorção para tratamentos de águas contaminadas e efluentes (Selvasembian *et al.*, 2021). Elas são capazes de reter diferentes classes de substâncias devido à presença de grupos polares e não-polares em suas estruturas, além de, excelente resistência mecânica, térmica e química (Abdullah; Ramtani; Yagoubi, 2023; Gama; Ferreira; Barros-Timmons, 2018; Kuranchie; Yaya; Bensah, 2021).

Ainda que, poucos trabalhos venham aplicando as PU na remoção de contaminantes, são crescentes os estudos com essa abordagem (Selvasembian *et al.*, 2021). Alguns resultados interessantes recentemente publicados dão conta de: uma remoção de 99,4% do corante verde brilhante em soluções aquosas, usando uma PU incorporada com 4% de carvão (KONG *et al*., 2016); remoção de 98% do corante *Food Red* 17 (FR17) de soluções aquosas, em PU incorporada com cargas de quitosana (da Rosa Schio *et al.*, 2019); remoção de 96% de corante catiônico azul de metileno em 3 h de adsorção em meio aquoso (Baldez; Robaina; Cassella, 2008); remoção cerca de 90% de Cd em PU com cargas de bentonita e/ou óxido de cobre (Ossman; Abdelfattah, 2018).

Nota-se que boa parte dos trabalhos tratam de espumas que foram produzidas utilizando materiais adsorventes auxiliares, enquanto cargas. Assim, a PU atua sinergicamente com a carga, a fim de promover uma maior retenção de contaminante.

As cargas podem ser compostas de diversos materiais e, devido ao apelo ambiental, fontes de origem vegetal, como resíduos agroindustriais, têm sido reportadas como adsorventes potenciais na remoção de metais pesados em soluções aquosas, já que, a presença de grupos funcionais, carboxil, hidroxil, hidrossulfonil, amido, lignina, em sua estrutura porosa favorece a adsorção (Cabulis; Ivdre, 2023; Kuranchie; Yaya; Bensah, 2021).

A adição de cargas pode causar diferentes efeitos na reação entre o isocianato e poliol, incluindo: a taxa de polimerização que pode sofrer interferência em decorrência do material de enchimento selecionado, uma vez que, altera o comportamento reológico da mistura de reação e/ou no acoplamento dos grupos de superfície do material de enchimento (cargas) com o isocianato, água e/ou o poliol e outros, o que pode prejudicar a maioria das propriedades tecnológicas finais da PU (Bernal; Lopez-Manchado; Verdejo, 2011; Gama; Ferreira; Barros-Timmons, 2018; Gama, 2017).

Desse modo, modificar a composição das PU por meio do emprego de cargas, seja utilizando materiais já processados pelas agroindústrias, pode aumentar sua capacidade adsortiva, além de, minimiza o impacto ambiental e um coprocessamento do material, considerado resíduo, agregando a ele valor.

Nesse contexto, espumas de poliuretano carregadas são um material promissor na remoção de íons metálicos e microrganismos patogênicos presentes em águas residuárias. Essa remoção pode ser aplicada pelo método de adsorção devido ao seu baixo potencial nocivo ao meio ambiente, não geração de subprodutos, fácil aplicação, condições operacionais simples, ampla aplicabilidade, alta eficiência de remoção, baixo custo, além de, possibilidade de reutilização do material adsorvente (Alaqarbeh, 2021).

4 Artigo 1

O artigo intitulado “**Polyurethane foams incorporated with different fillers to remove SARS-CoV-2 from water**” é apresentado conforme publicado na Revista Journal of Water Process Engineering, ISSN: 2214-7144, fator de impacto 7, classificação A2 na área de Materiais

Journal of Water Process Engineering 54 (2023) 104000

Contents lists available at ScienceDirect

Journal of Water Process Engineering

journal homepage: www.elsevier.com/locate/jwpe

Polyurethane foams incorporated with different fillers to remove SARS-CoV-2 from water

Thays França Afonso [a], Carolina Faccio Demarco [a], Guilherme Pereira Schoeler [b], Janice Luehring Giongo [c], Rodrigo de Almeida Vaucher [c,*], Tito Roberto Sant'Anna Cadaval Jr [d], Simone Pieniz [b], Rafael de Avila Delucis [b], Robson Andreazza [a,b,**]

[a] *Science and Engineering of Materials Postgraduate Program, Federal University of Pelotas, R. Gomes Carneiro 01, CEP 96010-610, Pelotas, RS, Brazil*

[b] *Environmental Sciences Postgraduate Program, Federal University of Pelotas, R. Benjamin Constant 989, CEP 96010-020 Pelotas, RS, Brazil*

[c] *Graduate Program in Biochemistry and Bioprospecting, Research Laboratory in Biochemical and Molecular Biology of Microorganisms (LaPeBBiOM), Federal University of Pelotas, Av. Eliseu Maciel, Campus Universita´rio, s/n, Capa˜o do Lea˜o CEP 96160-000, RS, Brazil*

[d] *School of Chemistry and Food, Federal University of Rio Grande, Av. Ita´lia, Km 8, s/n, Carreiros, CEP 96203-000 Rio Grande, RS, Brazil*

ARTICLE INFO

Keywords:
Adsorption
Polyurethane foam
RT-q PCR
COVID-19
SARS-CoV-2

ABSTRACT

Recent studies on viral shedding of SARS-CoV-2 have been reporting that this virus is excreted by infected patients. Because of that, high viral loads have been founded in effluents and wastewater from certain locations, where in high numbers of COVID-19 cases were reported. The increase in SARS-CoV-2 virus dispersion in the environment may increase the risk of new infections, therefore removal or inactivation techniques should be encouraged to prevent the spread of this virus. This study evaluated polyurethane foams (PUF) filled with different particulate adsorbents for the removal of SARS-CoV-2 from water. For that, the PUF were characterized in terms of chemical composition, morphology, surface charge, crystallinity, thermal degradation, density and zeta potential. Afterward, the virus removal efficiency of the studied PUF was analyzed using ribonucleic acid (RNA) extraction and reverse transcription-quantitative polymerase chain reaction (RT-qPCR). In this evaluation, the PUF were incubated in an inactivated SARS-CoV-2 viral suspension for 24 h. The results showed high per- centages of SARS-CoV-2 removal above 98 % for the neat PU, as well as for the PUF filled with peach stone (PUPS), peach stone-based activated carbon (PUPSAC) and commercial activated carbon (PUCAC). These results indicate that the production of PUF-based adsorbents is a sustainable way for adding value to commercially discredited vegetable matrixes.

*Corresponding author. **Correspondence to: R. Andreazza, Science and Engineering of Materials Postgraduate Program, Federal University of Pelotas, R. Gomes Carneiro 01, CEP 96010- 610 Pelotas, RS, Brazil. *E-mail addresses:* rodvaucher@hotmail.com (R. de Almeida Vaucher), robsonandreazza@yahoo.com.br (R. Andreazza).
https://doi.org/10.1016/j.jwpe.2023.104000 Received 6 April 2023; Received in revised form 15 June 2023; Accepted 29 June 2023; Available online 5 July 2023. 2214-7144/

1. Introduction

COVID-19 is a severe respiratory syndrome that occurs in humans due to the SARS-CoV-2 virus due to direct or indirect person-to-person contact, especially through respiratory transmission [1]. Nevertheless, some studies already affirmed that human cells are prone to be contaminated due to contact with infected environments [2]. For instance, when someone touches his eyes, nose or mouth after touching surfaces or objects that have been contaminated by the virus.

The pandemic of COVID-19 brought huge economic and health negative impacts, which have been extensively discussed in some recently published studies [3]. However, some environmental impacts of this global epidemic were not yet fully clarified [4]. Several recent studies mentioned the detection of SARS-CoV-2 in water and sewage around the world [5]. Furthermore, the detection of infectious viruses in urine and feces suggests that these substances may be capable of transmitting infection [6,7]. Additionally, epidemiological studies have shown that SARS-CoV-2 may be transmitted via contaminated sewage [8,9]. This type of virus may survive for days diluted in wastewater [10] and, for this reason, according to Bandala et al. [11], the SARS-CoV-2 concentration in water increases as the infection rate around this water body increases.

Therefore, the virus may enter water systems through sewage dis- charged by isolation centers, hospitals, or households, where contaminated people are recovered [5]. Then, the discharge of untreated sewage into rivers, inland waterways, and seas represents an epidemiological risk and can lead to the spread of this disease, especially via fecal-oral transmission [12]. The contamination via sewage or untreated water (secondary transmission) is even more worrying in low-income countries, wherein health policies may be ineffective due to poor sanitation infrastructure [13,14].

Several technologies are currently applied for removing and/or inactivating viruses spread in water bodies. These strategies include membranes, ultra/nano/reverse osmosis, nanofiltration, ultraviolet light, photodynamic oxidation, wet-peroxide oxidation, electro-coagulation, electro-oxidation, CO_2 bubbles, photo-catalysis with graphene oxide or carbon dots, photo-catalysis with TiO_2, cold plasma, chemical disinfection with either chlorine or ozone and adsorption processes [11].

Among these technologies, the adsorption processes stand out because of the wide range of adsorbent materials that can be applied. Adsorption consists in

accumulating atoms or ions from a gaseous, a liquid, or a solid adsorbate onto the surface of a solid adsorbent [15]. This process is advantageous due to the low energy consumption, ease of operation, and high removal efficiency [16]. Also, there are low-cost adsorbents endowed with high ecological appeal since they can be obtained from plant-based resources or residues [17].

Nowadays, activated carbon is the main adsorbent used for separating gases, recovering solvents, and removal of pollutants from wastewater. Its adsorption capacity is dependent on some physical properties, such as specific surface area, pore size and distribution, as well as surface chemistry [18]. These properties also may vary depending on the precursor and activation conditions used to produce the activated carbon. Peach stones are among the most produced fruit residues in southern Brazil and, to mitigate this environmental liability, the valorization of this biomass through the production of activated charcoal seems to be a promising strategy based on previous studies [18,19].

In this context, green materials and polymers such as modified polyurethane foams have been used as adsorbents and absorbents for the treatment of contaminated water and wastewater [20]. In order to improve its absorptive properties, various materials can be incorporated into PUF. Studies have shown that it's possible to produce foams with superhydrophilic/superoleophobic properties and an excellent ability to remove different types of oil by absorption [21] making modifications to their structures. Such as acrylamide can be used to modify PUF [22], and PUF can be coated with polydopamine/polypyrrole/polyaniline (PDA/ PPy/PANI) and incorporated with Fe-SA (stearic acid) nanocomposites [23], and also magnetic polyurethane foam (PUF) modified with pre- treated cellulose decafluorobiphenyl (MCF) by adding Fe_3O_4 NPs [24].

Polyurethane is a well-known porous polymer for its mechanical characteristics, durability, flexibility, and elasticity [25]. PUF is a kind of cellular polymer that has particularly advantageous physical and chemical characteristics, such as abundant binding sites, with a high surface area, as well as excellent thermal and chemical stability [20,26,27].

However, PUFs are easy to be touched with bacteria and viruses when they are exposed to the applied environment. Furthermore, the bacteria might damage the surface of PUFs, and generate a film by adhering to the surface which influences the life-span of foams [28–31]. Consequently, the antibacterial treatment of PUFs is

important to improve and significantly increase the service life [28,32,33]. Mean- while, PUFs are also promising substrates to support bio-adsorbents since they are able to retain different classes of substances [25,34,35,36–39] in addition, is interesting its ability to be touched with bacteria and viruses when they are exposed to the environment.

Unfortunately, to the best of our knowledge, there is a lack of studies investigating PUF-based support for bioadsorbents applied to SARS-CoV-2 removal; although, this strategy was already conducted to adsorb other contaminants [37]. These studies addressed fillers and PUF-based sup- ports that acted synergistically, yielding high retention of contaminants in the PUF cellular structure. In this work, the influence of different fillers on PUF is investigated for SARS-CoV-2 removal from water.

2. Materials and methods

2.1. Fillers preparation

A commercial activated carbon (CAC) was supplied by Dinâmica Química Contemporânea and, according to this supplier, the CAC has the following characteristics: relative density of 1.8–2.1 g cm^{-3} at 25 °C and molecular weight of 12.01 g mol^{-1}. Peach stones (PS) (*Prunus persica L.*) were donated by Oderich Canned Food Industry, which is located in Pelotas/Brazil. This material was initially washed with distilled water to remove impurities and was then oven-dried (at 105 °C for 24 h), grounded (using a Wiley mill), and sieved using a 150 μm screen. This powdered peach stone was used as a filler for the PUF and also as a precursor for a peach stone-based activated carbon. To prepare the activated carbon, a high purity (>97 %) zinc chloride ($ZnCl_2$), acquired from Dinâmica Química Contemporânea, was used as a chemical activator. For performing the chemical activation, 30 g of $ZnCl_2$ was dis- solved in 200 mL of distilled water and then 30 g of the precursor was added under stirring at 200 rpm for 24 h. The final solution was oven - dried at 105 ºC and then pyrolyzed at 700 °C for 1 h. The pyrolyzed material (called “PSAC”) was treated with 3 M HCl to remove the remaining chemical activator, following the procedure described by Akçakal et al. [40].

2.2. Polyurethane foam preparation

PUFs were prepared with the insertion of the three aforementioned fillers by the free-rise pouring method, which was described by Delucis et al. [41]. For that, filler (5 wt%), castor oil, glycerin PA, chain extender, surfactant, and catalyst were mechanically stirred at 1000 rpm for 60 s. Then, p-MDI was added to the reaction mixture at an NCO/OH ratio of 1, which was then manually mixed for extra 20 s. This final mixture was poured into an open wooden mold and left to cure at room temperature for 24 h. The resulting expanded polymers were post-cured in an oven at 60 ◦C for 2 h. Table 1 displays the amount of each reagent used. Hereafter, neat PUF, PUF filled with peach stones, PUF filled with peach stones-based activated carbon, and PUF filled with commercial activated carbon are called as neat PU, PUPS, PUPSAC and PUCAC, respectively.

Table 1 - PUF formulation.

Components	Weight (g)
Castor oil[a]	50.42
Glycerin PA[b]	16.81
Polyethylene glycol (chain extender)[b]	7.47
Distilled water (blowing agent)	2.99
Tegostab B8404 (surfactant)[c]	1.87
Tegoamin DMEA (catalyst)[c]	0.75
Polymeric methyl diphenyl isocyanate (p-MDI)[d]	119.70
Fillers	5 wt%
Peach Stone (PS)	10.53
Peach Stone Activated Carbon (PSAC)	10.53
Commercial Activated Carbon[b] (CAC)	10.53

[a] Acquired from Alpha Química.
[b] Acquired from Dinaˆmica Química Contemporânea Ltda.
[c] Donated by Evonik Degusssa Brasil Ltda.
[d] Acquired from Polisystem Indústria e Comercio de Poliuretano.

2.3. Characterization

2.3.1. Morphology and structural characterization

The specific surface area, total pore volume, and pore size of the fillers were determined by the Brunauer-Emmett-Teller (BET) method. The pore size and distribution were estimated through the Barrett-Joyner-Halenda (BJH) method utilizing

a 1200e Quantachrome Instruments automated apparatus, under a dynamic Nitrogen gas environment.

The specimens were degassed before the measurement through a nitrogen flow at 100–300 °C (depending on the filler type) for 20 h. Fourier transform infrared spectroscopy (FTIR) using a Prestige Shimadzu equipment equipped with an attenuated total reflectance (ATR) accessory. Thus, 32 scans were carried out in the range between 4000 and 400 cm^{-1} and a resolution of 4 cm^{-1}.

Moisture, volatile matter, and residue contents were obtained using thermogravimetric (TG) analysis under a nitrogen atmosphere at a heating rate of 20 °C min^{-1} using a Q50 thermal gravimetric analyzer (TA instruments), according to the ASTM D7582 procedure. The X-ray diffraction (XRD) patterns were obtained using a diffractometer (Brunker D–8, Germany) equipped with a diffracted beam monochromator and Ni-filtered CuKα radiation (λ = 1.5406 Å). A voltage of 40 kV and an intensity of 40 mA were adjusted. The 2θ angle was scanned between 10° and 60°, and the counting time was 1.0 s at each angle step (0.02°).

Surface morphology was analyzed by scanning electron microscopy (SEM) using a JSM 6610LV Jeol equipment, adjusted for a working voltage of 15 kV and a magnification of 100×.

Point of zero charges (PZC) was obtained by adding 0.1 g of solid sample to 20 mL of a KNO_3 solution (0.01 M) into a 50 mL plastic flask, which was stirred at 50 rpm for 24 h in initial pH solutions that varied from 1 to 12. The pH values were measured using a pH meter and the PZC was obtained after plotting ΔpH (pH final – pH initial) against the initial pH. This methodology was adapted from that described by Farage et al. [42]. Apparent density was determined for five specimens per group, which had the dimensions of 50 × 50 × 25 mm^3. For that, a digital caliper and an analytical scale were used according to the ASTM D1622. The database of apparent density was analyzed by one-way analysis of variance (ANOVA) followed by Tukey tests.

2.3.2. SARS-CoV-2 inactivated

An inactivated SARS-CoV-2 virus was used as a positive control and comes from isolated clinical specimens in Vero-E6 cells (SARS.COV-2/ SP02/human2020/Br, GenBank accession number MT126808.1). This virus was kindly provided by Professor Dr. Edison Luiz Durigon. He is a Full Professor at the Department of

Microbiology, Institute of Biomedical Sciences, University of São Paulo (USP), Brazil [43].

2.3.3. Removal and connection of SARS-CoV-2 to materials

A total of 10 mg of each adsorbent (neat PU, PUCAC, PUPS or PUPSAC) was properly dried at 37 ◦C for 2 h. Afterward, the adsorbent was transferred to a microtube containing 1.5 mL of sterile RNAse-Free ultrapure water. Then, 150 µL of the inactivated SARS-COV-2 viral suspension (2.5×10^6 copies mL^{-1}) was added to the microtube, which was followed by incubation at 28 ◦C and pH 7 under shaking of 200 rpm for 24 h. Subsequently, supernatant and adsorbent were removed and placed into another microtube and the viral RNA was extracted. The virus adsorption was calculated and presented as described by Demarco et al. [44]. The viral load removed was calculated using the following Eq. (1):

$$Viral\ load\ removal = Viral\ loads_{upern}) - (Viral\ load_{mat}) \quad (1)$$

where *Viral load removal* is expressed in copies mL^{-1}, $Viral\ load_{supern}$ and $Viral\ load_{mat}$ refers to the viral load in supernatant and viral load in material (copies mL^{-1}), respectively.

2.3.4. RNA extraction

The RNA was extracted from both supernatant and studied adsorbent using a MagMax™ Core Nucleic Acid Purification kit (Thermo Fisher Scientific, Waltham, MA, USA). The extracted RNA was quantified by NanoDrop® (Thermo Fisher Scientific, Waltham, MA, USA). A concentration of approximately 10 ng of RNA was used to perform the RT-qPCR detection.

2.3.5. RT-qPCR

In the RT-qPCR assays for SARS-CoV-2 the primer and probe used in PCR reactions were performed according to the protocol indicated by Centers for Disease Control and Prevention [45]. Briefly, reaction mixtures (25 µL) of final volume were used, with the following volumes added to the 1× concentrated master mix: 5 µL of sample RNA, 12.5 µL of 2 × reaction buffer, 1 µL of Superscript™ III One-Step with Platinum™ Taq DNA Polymerase (Invitrogen, Darmstadt, Germany), 0.4 mM of each

dNTP, 0.4 µL of a 50 mM $MgSO_4$ solution (Invitrogen), 1 µg of non-acetylated bovine albumin (Roche), 10 µM of each primer (Table 2), and DEPC water. The reaction occurred in StepOne™ Real- Time PCR System (Thermo Fisher Scientific, Waltham, MA, USA). CDC N1 and N2 primers and probes used in this study are shown in Table 2. The qPCR condition for SARS-CoV-2 was as follows: 55 °C for 10 min for reverse transcription, 95 °C for 3 min, and 40 cycles of 95 °C for 15 s and 58 °C for 30 s. The database of removal percentage was analyzed by one-way analysis of variance (ANOVA) followed by Bonferroni's multiple comparison tests adjusted for a significance level of 5 %.

Table 2 - Oligonucleotide sequences of primers and probes used in this study.

Assay	Primer/probe	Sequence (5´-3´)[1]
N1	2019-nCoVN1-F	GACCCCAAAATCAGCGAAAT
N2	2019-nCoVN1-R	TCTGGTTACTGCCAGTTGAATCTG
N3	2019-nCoVN1-P	FAM–ACCCCGCATTACGTTTGGTGGACC–BBQ

[a] FAM, 6-carboxyfluorescein [45].

3. Results and discussion

3.1. Adsorbent characterization

3.1.1. BET-surface area

BET-surface area and total pore volume of the PS sharply increased in the activated carbon production (Table 3), which is typical for activated carbon and can be attributed to the formed spongy-like porous structure shown in Fig. 1 [40]. The PSAC overcame the CAC in terms of BET-surface area and average pore size, which indicates a high adsorption potential to the former activated carbon. According to Yang et al. [46], the porosity of one activated carbon is related to the conversion of hemicelluloses, cellulose and lignin from the precursor by a series of dehydrating and polymerization reactions.

Table 3 - Textural properties of the fillers.

Fillers	BET-surface area (m^2 g^{-1})	Total pore volume (cm^3 g^{-1})	Average pore size (nm)
PS[a]	0.562	0.004	141.780
PSAC[b]	579.199	0.297	10.256
CAC[c]	469.595	0.267	11.352

[a]PS (Peach Stone in natura) (A), [b]PSAC (Peach Stone Activated Carbon) (B), [c]CAC (Commercial Activated Carbon) (C).

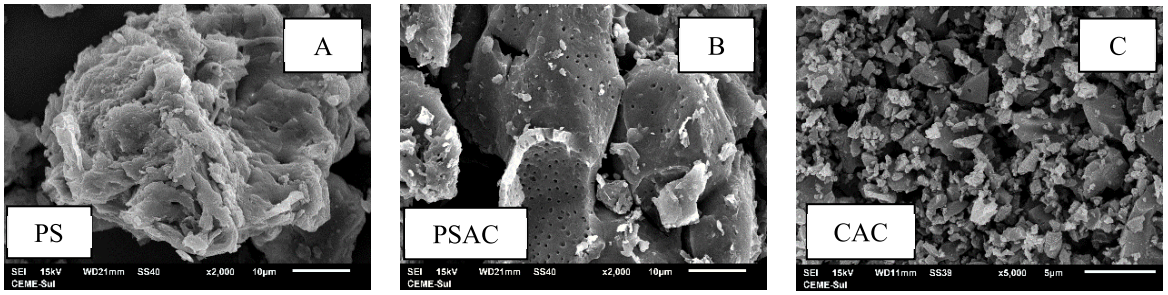

Fig. 1 – SEM images of the fillers. PS (Peach Stone in natura) (A), PSAC (Peach Stone Activated Carbon) (B), CAC (Commercial Activated Carbon) (C).

3.1.2. Fourier-transform infrared spectroscopy (FT-IR) and X-ray diffraction (XRD)

All PUF presented similarly shaped FTIR spectra, which means that they have similar chemical structures (Fig. 2a). In the case of PUF and its composites, the band at 3310 cm^{-1} and 3600 cm^{-1} was attributed to the stretching vibrations of N–H groups, whereas peaks at 2924 and 2858 cm^{-1} were ascribed to the asymmetric and symmetric C–H stretches, then represented the stretching vibrations of the methylene groups [38,46,48]. The broadband between 2300 and 2200 cm^{-1} was assigned to the stretching vibration of residual NCO groups. Another broadband between 1730 and 1600 cm^{-1} represented the C=O stretches of Biopol and urethane moieties, with the urethane C–N stretch observed at 1624 cm^{-1}, and the band corresponding to C–N stretching and N–H bending (1515 cm^{-1}). The characteristic tertiary amide C–N stretching and N–H deformation was observed at 1240 cm^{-1} [48,49]. In addition, the characteristic peak of the isocyanate functionality at 2266 cm^{-1} corresponds to unreacted N=C=O stretch. [46-48].

The XRD diffractogram of the PUF's and composites are shown in Fig. 2b. It is evident that PUF's samples have comparable XRD patterns, and this result confirms that they are made up of amorphous base polymer, by comparison with the ICDD reference database (#00-060- 1509) and JCPDS N◦ 41-1413 [32,50–55]. In fact, it was observed the presence of two broad diffraction haloes that peaked at around 20° and 41° 2θ, respectively, and that they were exactly related to the features of the phase amorphous patterns [51,52]. The broad base peaks of PUPSAC and PUCAC, at around 20° 2θ, decreases and they are assigned to the scattering from polyurethane (PU) chains with regular interplanar spacing [51–53].

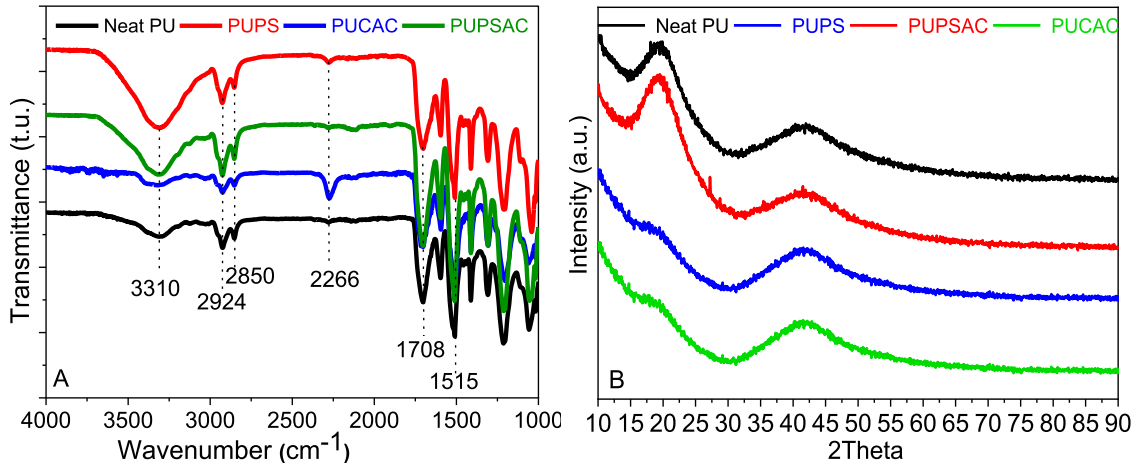

Fig. 2 - FTIR spectra of the studied PUF (a) and X-ray diffractograms of the PUF (b); Neat PU (Neat Polyurethane), PUPS (Polyurethane Peach Stone), PUPSAC (Polyurethane Peach Stone Activated Carbon), PUCAC (Polyurethane Commercial Activated Carbon).

3.1.3 Thermogravimetric profile of PUF

Fig. 3 shows the TG curves of the PUF. In addition, as shown in Table 4, some relevant data based on these curves were summarized. The mass loss until 200 °C is attributed to the evaporation of the moisture and the release of volatile compounds from the PUF cellular structure [46]. The PUPS presented the highest mass loss peak at this first region found in the DTG curve, which is attributed to some of its low molecular weight compounds, such as extractives, pentosans, and hexosans. These compounds were probably thermally decomposed when the PSAC was prepared, which explains why this prominent peak did not appear for the PUCAC and PUPSAC. This also explains the smallest T5% displayed by the PUPS, indicating that this 5% of mass loss is mostly attributed to the inserted filler.

The PUPSAC presented a sharply smaller T5% than the PUCAC, which indicates that the CAC is more thermally stable than the PSAC produced here, which is probably related to differences in both morphology and chemical composition of these two adsorbents [56]. The T5% values in the 170–270 °C temperature range showed by the studied PUF are related to the breaking of urethane linkages. On the other hand, the T50% values presented by the PUF are related to the degradation of urea groups [57]. In this sense, compared to the neat PU, the PUPSAC, and PUCAC presented higher T50% values, which indicates that these activated carbons conferred increases in thermal stability in all temperatures above 300 °C.

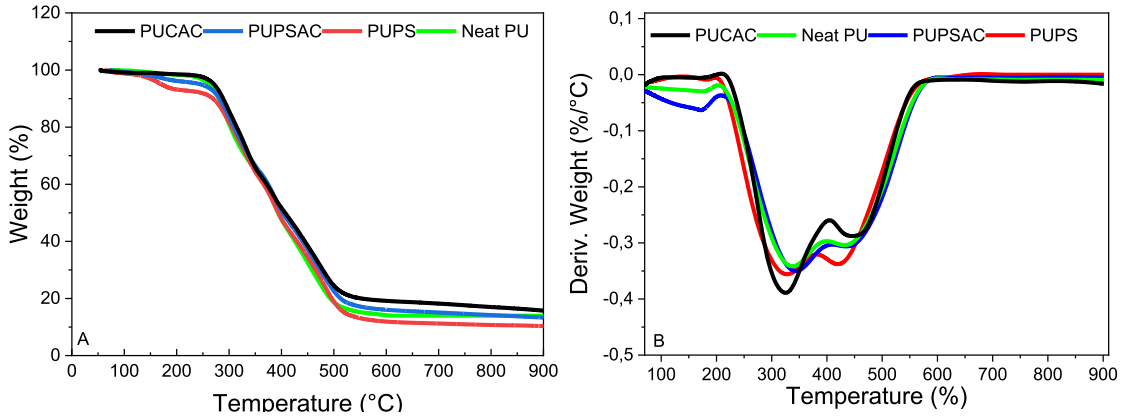

Fig. 3 - TG (A) and DTG (B) curves of the PUF (Neat PU (Neat Polyurethane), PUPS (Polyurethane Peach Stone), PUPSAC (Polyurethane Peach Stone Activated Carbon), PUCAC (Polyurethane Commercial Activated Carbon).

Table 4 – Main thermal events of the PUF evaluated by TG.

Sample	$T_{5\%}$ (°C)	$T_{50\%}$ (°C)	Residue at 600 ºC (wt%)
Neat PU[a]	262	394	14
PUPS[b]	171	394	12
PUPSAC[c]	246	403	16
PUCAC[d]	271	407	16

[a]Neat PU (Neat Polyurethane). [b]PUPS (Polyurethane Peach Stone). [c]PUPSAC (Polyurethane Peach Stone Activated Carbon). [d]PUCAC (Polyurethane Commercial Activated Carbon).

3.1.4 Scanning electron microscopy (SEM), density and point of zero charge (PZC)

Fig. 4 shows the SEM images of PUF. The neat PU presented rounded cells with a diameter mean of about 500 µm, which can be considered normal based on similar studies on PU [41]. The morphology in PUF is mostly related to rheological characteristics, such as viscosity, reactivity, presence of additives, and so on [41]. Compared to the neat PU, the filled PUF presented elliptically shaped cells, which indicates a cell orientation in relation to the rise direction. Elliptical polymer cells in filled PUF are a normal characteristic, which can be attributed to the steric hindrance mechanism imparted by the filler presence, in which the formation of urethane groups is hindered since isocyanate and hydroxyl groups are physically separated from each other by the filler particles [41].

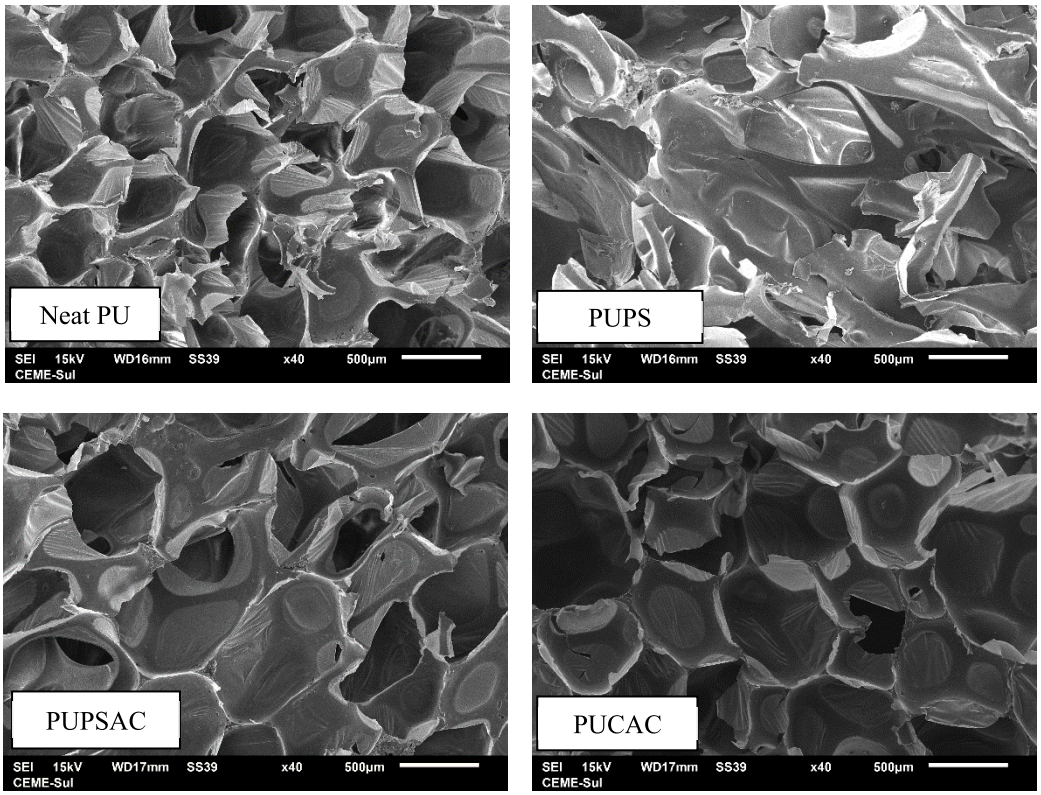

Fig. 4 – SEM of the studied PUF. (Neat PU (Neat Polyurethane), PUPS (Polyurethane Peach Stone), PUPSAC (Polyurethane Peach Stone Activated Carbon), PUCAC (Polyurethane Commercial Activated Carbon).

The PUPS presented a clearly uneven cell morphology, which is probably related to the hydrophilic nature of the PS since the PUF reinforced with the activated carbons presented homogenously distributed cell bubbles. According to Acosta et al. [59], the insertion of hydrophilic fillers in PUF may yield the formation of brittle, small, and thin cells, which are easily disrupted, releasing the encapsulated CO_2. In addition, the adsorbed moisture from hydrophilic fillers can be desorbed during the exothermic polymerization reaction of the PU, reacting then with NCO groups from the p-MDI. This may lead to the formation of polyurea groups, decreasing the overall PUF performance [57].

Based on their apparent densities above 40 kg m^{-3}, all the studied PUF can be considered rigid foams (ASTM E1730). The PUPS showed the highest apparent density (Fig. 5a), which is probably related to the aforementioned filler-PUF reactions. According to Delucis et al. [41], hygroscopic fillers present high host compatibility in isocyanate-based systems, which leads to increases in foam expansibility and cell anisotropy. In addition, the increase in apparent density compared to the neat PU

indicates a good polymer formation in the PUPS since the cells formed due to a filler insertion do not always lead to increases in apparent density [41].

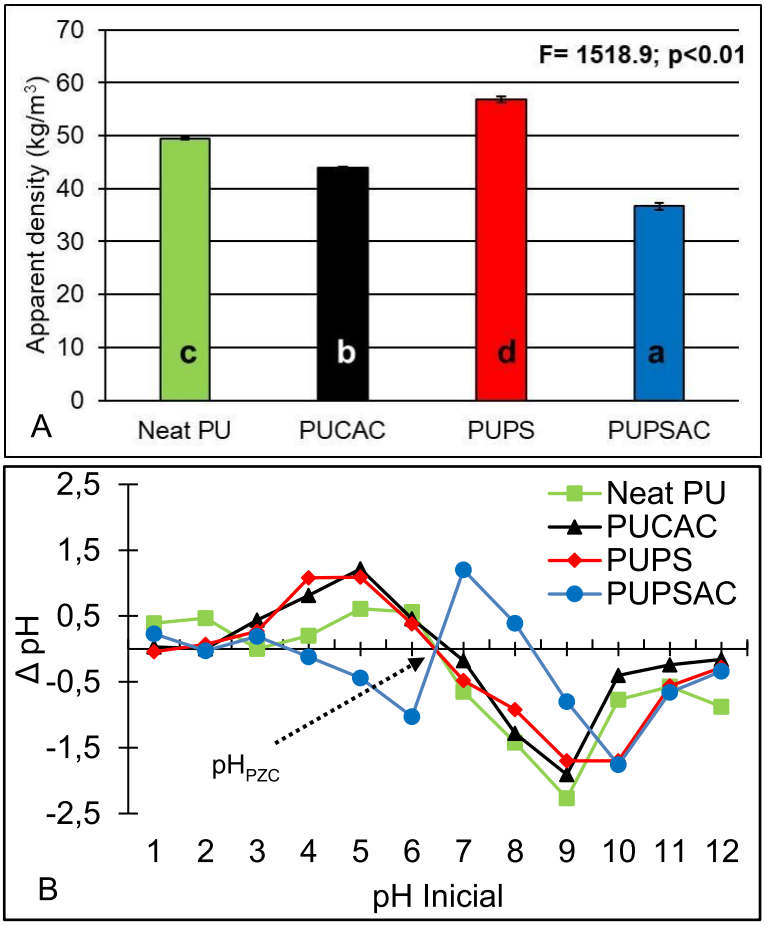

Fig. 5 – Apparent density of the PUF (A) and Point of zero charge of the studied PUF (B); (Neat PU (Neat Polyurethane), PUPS (Polyurethane Peach Stone), PUPSAC (Polyurethane Peach Stone Activated Carbon), PUCAC (Polyurethane Commercial Activated Carbon).

The inert fillers inserted in the PUCAC and PUPSAC lead to decreases in apparent density if compared to the neat PU. In fact, chemically incompatible fillers may lead to contrary mechanisms if compared to compatible ones, which were discussed above. Therefore, decreases in foam expansibility and apparent density associated with low host compatibility and weak filler-matrix bonding are expected for the insertion of CAC and PSAC as fillers in PUF. For Zhou et al. [60], a PU-based reaction mixture incorporated with one chemically incompatible filler may have high viscosity, which leads to restricted expansibility and, sometimes, the formation of egg-like cells.

According to Delucis et al. [41], incompatible fillers have opposite polarities if compared to the polymer matrix, which leads to a weak interface permeated by micro-

pores capable of encapsulating blowing gas. According to Schoeler [61], studies on colloidal flocculation apply PZC for measuring at which pH the net charge of an absorbent's surface is equal to zero. Fig. 5b shows the PZC pattern at variable pH values, which indicates that the surfaces of all PUF are positively charged after a pH value of 6.5. Therefore, it is expected increased SARS-CoV-2 removal above this pH value. This result is in agreement with those reported by Zhang et al. [62], who studied PUF incorporated with polyethyleneimine-based particles. This probably occurred due to the protonation of amine groups onto the PUF surface [62].

3.1.5 SARS-CoV-2 removal

As shown in Table 5, a reference number of 2.5 × 106 viral copies per mL was considered for 15 cycles. This concentration was defined based on recently reported SARS-COV-2 concentrations found in several countries during the pandemic, as shown in Table 6. The C_T values are inverse to viral load content and represent an indirect method of detecting viral RNA copy numbers [76]. In this type of analysis, the cycle threshold (C_T) value in RT-qPCR analysis is the number of amplification cycles required for the gene to exceed the threshold level. Regarding the supernatant and cycle threshold material (C_T), the filled PUF (i.e. PUPS, PUPSAC and PUCAC) did not differ from the neat PU. This also indicates a good quality of the PSAC produced here since PUPSAC and PUCAC presented similar removal capacities and adsorption behaviors.

Table 5 - Cycle threshold (C_T), viral load (copies mL^{-1}) and removal properties obtained after 24h of incubation.

	Neat PU[a]	PUPS[b]	PUPSAC[c]	PUCAC[d]
Control C_T	14.85±0.96			
Viral load in control (copies mL^{-1})	$2.5\times10^6\pm0.11\times10^6$			
Supernatant C_T	20.74±1.58a**	22.49±0,31a	24.91±0,71a	23.13±0,83a
Viral load in supernatant (copies mL^{-1})	4.76×10^4	1.47×10^4	0.27×10^4	0.92×10^4
Material C_T	31.93±2.83a	28.97±2.79a	30.78±1.27a	30.33±1.11a
Viral load in material (copies mL^{-1})	0.0020×10^4	0.0016×10^4	0.0047×10^4	0.0063×10^4
Viral load removed (copies mL^{-1})	4.76×10^4	1.46×10^4	0.26×10^4	0.90×10^4
Viral load removed (copies mLg^{-1})	4.76×10^6	1.46×10^6	0.26×10^6	0.91×10^6

[a]Neat PU (Neat Polyurethane). [b]PUPS (Polyurethane Peach Stone). [c]PUPSAC (Polyurethane Peach Stone Activated Carbon). [d]PUCAC (Polyurethane Commercial Activated Carbon). ** Bonferroni's multiple comparison tests adjusted for a significance level of 5%.

Table 6 - Concentration of SARS-CoV-2 in wastewater of various countries

Concentration (copies mL^{-1})	Country	Water type	Reference
5.00×10^{-5} to 1.87×10^{2}	China	Untreated wastewater	[63]
2.60×10^{-3} to 2.20	Netherland	sewage	[64]
9.50×10^{-3} to 3.70×10^{2}	Brasil	River water; wastewater	[65]
5.60×10^{-2} to 3.50×10^{-1}	India	Wastewater	[66]
1.20	Australia	Untreated wastewater; Primary sludge	[67,68]
10^{1} to 4.60×10^{5}	USA	Untreated wastewater; Primary sludge;	[69-71]
10^{2} to10^{3}	Spain	Untreated wastewater	[72]
2.70×10^{2} to 3.19×10^{3}	Ecuador	River water	[73]
1.00 to10^{3}	Turkey	Untreated wastewater	[74]
$>10^{3}$	France	Untreated wastewater	[75]

The percent removal of SARS-CoV-2 was 99.9 % by neat PU, 98.1 % by PUPSAC, 98.3 % by PUPS, and 98.2 % by PUCAC (Fig. 6). Superior results when compared to the percent removal of SARS-CoV-2 in water in PUF with fillers of dregs (91.55 %) [61] and the control group of free SARS-CoV-2 (Fig. 6). Therefore, the foams present considered outstanding performances in all cases. There were no statistically significant differences between the means evaluated for the different PUFs.

These results can be explained by the aforementioned characteristics, including surface area, presence of functional chemical groups (namely COO, COOH, NH_2 and NH_3^+), PZC and so on. Compared to the studied listed in Table 6, the results shown in Fig. 6 can be considered superior in most cases. Therefore, amino acids from SARS-CoV-2 probably interacted with the adsorbent's surfaces through hydrogen bonds, which favored the adsorption due to the electrostatic attraction between the virus and these groups.

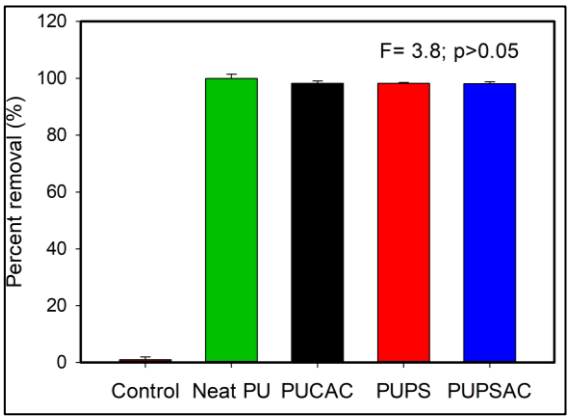

Fig. 6 - Percentage SARS-CoV-2 removal (%) of the studied PUF ((Neat PU (Neat Polyurethane), PUPS (Polyurethane Peach Stone), PUPSAC (Polyurethane Peach Stone Activated Carbon), PUCAC (Polyurethane Commercial Activated Carbon), and Control, represents free SARS-CoV-2 viral particles in water without the foams studied.

These are a few of the conditions that make the adsorption process feasible, as it is accomplished by electrostatic interactions between the virus/adsorbent surfaces in the presence of opposite charges between the surfaces [77]. Another issue is the morphology of the SARS-CoV-2 virus. The presence of the Spike (S) glycoprotein (outer part) that protrudes from the lipid membrane drives the adsorption of SARS-CoV-2. The glycoprotein, of hydrophobic nature, has a negative charge when the pH is above its isoelectric point, pH 5.9 [78]. This favored the adsorption of the foams, as they presented (pH_{PZC}) higher than that of the glycoprotein, regardless of the fillers incorporated in the foams.

Due to the above characteristics, any of the adsorbents (foams) can be considered promising in the removal of viral load (SARS-CoV-2), aqueous media, and applied mainly in low-income countries with inefficient wastewater treatment systems.

In the context of the Pandemic COVID-19, there is still little information regarding viral load concentrations (SARS-CoV-2) in natural water in wastewater in developing countries and with poor levels of environmental sanitation over time. In most Latin American countries, for example, only 30 % of wastewater is treated before it is discharged into water bodies [79], meaning that poor sanitation systems lead to a potential risk to public health.

Wastewater can be considered as one of the high-risk routes for transmission of the new coronavirus [80]. An example is the health facilities in the Palestinian West Bank, which only treated 2 % of their wastewater. Therefore, healthcare facilities are considered one of the high-risk sources of SARS-CoV-2 RNA in their wastewater, especially at COVID-19 peaks [81].

An ineffective sanitation system, is also a potential risk for contamination of the water system due to the presence of human excreta [82]. Studies show the presence of SARS-CoV-2 in the stool of patients even when respiratory tests were negative [83]. Viruses in human feces can extend from eleven to thirty-five days [71]. This indicates that although patients with COVID-19 are treated, their feces still contain the SARS-CoV-2 virus, leading to an increased viral load in water systems. This may be further intensified during peak periods of the pandemic.

In this context, studies have investigated the influence of parameters such as pH, sunlight exposure temperature, UV content, retention time, and appropriate disinfectant on the inactivation of SARS-CoV-2 in the environment. However, there are

few studies evaluating the infectivity of SARS-CoV-2 in water. Thus, there are still questions about SARS-CoV- 2 that are not well clarified in the literature.

In relation to the parameters, pH and temperature are highlighted because they can influence the adsorption process. Regarding pH, the literature shows that at extreme pHs (2–3 and 11–12) the infectivity of the virus (similar family of coronavirus) is lost in just one day, while pHs 3–10, has no significant effect on the virus survival [84,85]. If we take this parameter into consideration, we realize the effectiveness in the removal of SARS-CoV-2 by the bioadsorbents (Fig. 6), since in addition to performing our study at pH 7 we also used pH > pH_{zcp}.

Regarding temperature, it is understood that it has a direct effect on the inactivation of viruses from the coronaviridae family (SARS-CoV-1, HCoV-229E, MERS, etc.), because the lipid layer present in this family breaks down with increasing temperature [86].

This effect is also seen for SARS-CoV-2 in aqueous media. It is strongly sensitive to temperature increase, so at low temperatures (4 °C) the virus remains completely stable after 14 days, at room temperature (20–25 °C) 7 days and at warm temperature (33–37 °C) 1–2 days [84,85].

However, depending on the conditions of the water matrix, the number of days that the virus can remain viable can be diverse on a case-by-case basis, considering the most diverse climates around the world. The number of studies on the viability of SARS-CoV-2 in relation to temperature in various water matrices is still limited [82].

Although, it is currently possible to completely remove the various micropollutants through conventional tertiary treatment methods [87,88]. It is still a significant challenge and problem to remove SARS-CoV-2 in the advanced decline of water treatment [89].

In current years, many advanced technologies for water treatment have been developed, and are shown to be effective when removing or inactivating SARS-CoV-2. Although, they are not as accessible to everyone, due to the costs. In this context, the potential of polyurethane foams loaded with different materials of plant origin, as new alternative adsorbents in the removal of SARS-CoV-2 in aqueous media, stands out.

4. Conclusions

The present study evaluated the incorporation of different fillers in polyurethane foams to remove the viral load of SARS-CoV-2. Firstly, the successful incorporation of different fillers into PUF's is highlighted.

Furthermore, the impregnation of the salt ($ZnCl_2$) was successful in the synthesis of activated carbon from peach pits. For, the salt did not interfere with the synthesis of the polymer (PUF) and did not imply a reduction in the virus adsorption process.

Finally, through this research, it was possible to identify four new adsorbents capable of reducing the viral load, SARS-CoV-2. These new adsorbents obtained a high capacity to remove the virus through the adsorption process. Excellent results, above 98 % of the virus removal in aqueous medium, regardless of the charges incorporated in the polymer.

However, it is important to elucidate that the infectivity of SARS-CoV-2 in the aqueous medium is not completely clarified by the literature, since its behavior may vary depending on the conditions of the water matrix. It is therefore extremely important to search for new adsorbent materials capable of reducing the viral load of the medium.

Therefore, the synthesized polyurethane foams, besides using vegetable residues as fillers, encouraging the use of sustainable materials, and contributing to the environment have been shown alternative materials in the removal of this virus.

Funding

This study was supported by the Coordination for the Improvement of Higher Education (CAPES; Finance code 001) and the National Council for Scientific and Technological Development (CNPq).

Declaration of competing interest

The authors declare that they have no known competing financial interests or personal relationships that could have appeared to influence the work reported in this paper.

Data availability

No data was used for the research described in the article.

References

[1] M. Kitajima, W. Ahmed, K. Bibby, A. Carducci, C.P. Gerba, K.A. Hamilton, E. Haramoto, J.B. Rose, SARS-CoV-2 in wastewater: state of the knowledge and research needs, Sci. Total Environ. 739 (2020), 139076, https://doi.org/10.1016/j.scitotenv.2020.139076.

[2] N. Zhang, Y. Gong, F. Meng, Y. Shi, J. Wang, P. Mao, X. Chuai, Y. Bi, P. Yang, F. Wang, Comparative study on virus shedding patterns in nasopharyngeal and fecal specimens of COVID-19 patients, Sci. China Life Sci. 64 (3) (2021) 486–488, https://doi.org/10.1007/s11427-020-1783-9.

[3] C.M. Pulido, B. Villarejo-Carballido, G. Redondo-Sama, A. Gómez, COVID-19 infodemic: more retweets for science-based information on coronavirus than for false information, Int. Sociol. 35 (4) (2020) 377–392, https://doi.org/10.1177/0268580920914755.

[4] M.A. Zambrano-Monserrate, M.A. Ruano, L. Sanchez-Alcalde, Indirect effects of COVID-19 on the environment, Sci. Total Environ. 728 (2020), 138813, https://doi.org/10.1016/j.scitotenv.2020.138813.

[5] B. Adelodun, F.O. Ajibade, J.O. Ighalo, G. Odey, R.G. Ibrahim, K.Y. Kareem, H. O. Bakare, A.O. Tiamiyu, T.F. Ajibade, T.S. Abdulkadir, K.A. Adeniran, K.S. Choi, Assessment of socioeconomic inequality based on virus-contaminated water usage in developing countries: a review, Environ. Res. 192 (2021), 110309, https://doi.org/10.1016/j.envres.2020.110309.

[6] J. Sun, A. Zhu, H. Li, K. Zheng, Z. Zhuang, Z. Chen, Y. Shi, Z. Zhang, S. Chen, X. Liu, J. Dai, X. Li, S. Huang, X. Huang, L. Luo, L. Wen, J. Zhuo, Y. Li, Y. Wang, Y. Li, Isolation of infectious SARS-CoV-2 from urine of a COVID-19 patient, Emerg. Microbes Infect. 9 (1) (2020) 991–993, https://doi.org/10.1080/22221751.2020.1760144.

[7] W. Wang, Y. Xu, R. Gao, R. Lu, K. Han, G. Wu, W. Tan, Detection of SARS-CoV-2 in different types of clinical specimens, JAMA 323 (18) (2020) 1843–1844, https://doi.org/10.1001/jama.2020.3786.

[8] M. Kang, J. Wei, J. Yuan, J. Guo, Y. Zhang, J. Hang, Y. Qu, H. Qian, Y. Zhuang, X. Chen, X. Peng, T. Shi, J. Wang, J. Wu, T. Song, J. He, Y. Li, N. Zhong, Probable evidence of fecal aerosol transmission of SARS-CoV-2 in a high-rise building, Ann. Intern. Med. 173 (12) (2020) 974–980, https://doi.org/10.7326/M20-0928.

[9] J. Yuan, Z. Chen, C. Gong, H. Liu, B. Li, K. Li, X. Chen, C. Xu, Q. Jing, G. Liu, P. Qin, Y. Liu, Y. Zhong, L. Huang, B.-P. Zhu, Z. Yang, Sewage as a possible transmission vehicle during a coronavirus disease 2019 outbreak in a densely populated community: Guangzhou, China, April 2020, Clin. Infect. Dis. 73 (7) (2021) e1795–e1802, https://doi.org/10.1093/cid/ciaa1494.

[10] P.M. Gundy, C.P. Gerba, I.L. Pepper, Survival of coronaviruses in water and wastewater, Food Environ. Virol. 1 (1) (2008) 10, https://doi.org/10.1007/ s12560-008-9001-6.

[11] E.R. Bandala, B.R. Kruger, I. Cesarino, A.L. Leao, B. Wijesiri, A. Goonetilleke, Impacts of COVID-19 pandemic on the wastewater pathway into surface water: a review, Sci. Total Environ. 774 (2021), 145586, https://doi.org/10.1016/j. scitotenv.2021.145586.

[12] P. Foladori, F. Cutrupi, N. Segata, S. Manara, F. Pinto, F. Malpei, L. Bruni, G. la Rosa, SARS-CoV-2 from faeces to wastewater treatment: what do we know? A review, Sci. Total Environ. 743 (2020), 140444, https://doi.org/10.1016/j. scitotenv.2020.140444.

[13] D. Liu, J.R. Thompson, A. Carducci, X. Bi, Potential secondary transmission of SARS-CoV-2 via wastewater, Sci. Total Environ. 749 (2020), 142358, https://doi. org/10.1016/j.scitotenv.2020.142358.

[14] C. Yeo, S. Kaushal, D. Yeo, Enteric involvement of coronaviruses: is faecal-oral transmission of SARS-CoV-2 possible? Lancet Gastroenterol. Hepatol. 5 (4) (2020) 335–337, https://doi.org/10.1016/S2468-1253(20)30048-0.

[15] R. Chakraborty, A. Asthana, A.K. Singh, B. Jain, A.B.H. Susan, Adsorption of heavy metal ions by various low-cost adsorbents: a review, Int. J. Environ. Anal. Chem. 102 (2) (2022) 342–379, https://doi.org/10.1080/03067319.2020.1722811.

[16] S. Tamjidi, H. Esmaeili, B. Kamyab Moghadas, Application of magnetic adsorbents for removal of heavy metals from wastewater: a review study, Mater. Res. Express 6 (10) (2019), 102004, https://doi.org/10.1088/2053-1591/ab3ffb.

[17] R. Foroutan, A. Oujifard, F. Papari, H. Esmaeili, Calcined Umbonium vestiarium snail shell as an efficient adsorbent for treatment of wastewater containing Co (II), 3 Biotech 9 (3) (2019) 78, https://doi.org/10.1007/s13205-019-1575-1.

[18] T. Uysal, G. Duman, Y. Onal, I. Yasa, J. Yanik, Production of activated carbon and fungicidal oil from peach stone by two-stage process, J. Anal. Appl. Pyrolysis 108 (2014) 47–55, https://doi.org/10.1016/j.jaap.2014.05.017.

[19] T. Tsoncheva, A. Mileva, B. Tsyntsarski, D. Paneva, I. Spassova, D. Kovacheva, N. Velinov, D. Karashanova, B. Georgieva, N. Petrov, Activated carbon from Bulgarian peach stones as a support of catalysts for methanol decomposition, Biomass Bioenergy 109 (2018) 135–146, https://doi.org/10.1016/j.biombioe.2017.12.022.

[20] T.A. Saleh, Protocols for synthesis of nanomaterials, polymers, and green materials as adsorbents for water treatment technologies, Environ. Technol. Innov. 24 (2021), 101821, https://doi.org/10.1016/j.eti.2021.101821.

[21] M. Satria, T.A. Saleh, Facile approach of eco-friendly superhydrophilic/underwater superoleophobic zinc-functionalized polyurethane foams for continuous oil-water separation, J. Mol. Liq. 367 (2022), 120341, https://doi.org/10.1016/j.molliq.2022.120341.

[22] A.A. Alazab, T.A. Saleh, Underwater superoleophobic cellulose/acrylamide-modified magnetic polyurethane foam for efficient oil/water separation, Mater. Chem. Phys. 302 (2023), 127609, https://doi.org/10.1016/j.matchemphys.2023.127609.

[23] M. Satria, T.A. Saleh, Synthesis of superhydrophobic/superoleophilic stearic acid and polymer-modified magnetic polyurethane for oil-water separation: effect of polymeric nature, J. Colloid Interface Sci. 629 (2023) 522–534, https://doi.org/10.1016/j.jcis.2022.08.180.

[24] A.A. Alazab, T.A. Saleh, Magnetic hydrophobic cellulose-modified polyurethane filter for efficient oil-water separation in a complex water environment, J. Water Process Eng. 50 (2022), 103125, https://doi.org/10.1016/j.jwpe.2022.103125.

[25] P.S. Prasad, T. Gomathi, P.N. Sudha, M. Deepa, K. Rambabu, F. Banat, Biosilica/silk fibroin/polyurethane biocomposite for toxic heavy metals removal from aqueous streams, Environ. Technol. Innov. 28 (2022), 102741, https://doi.org/10.1016/j.eti.2022.102741.

[26] M. Khodakarami, M. Bagheri, Recent advances in synthesis and application of polymer nanocomposites for water and wastewater treatment, J. Clean. Prod. 296 (2021), 126404, https://doi.org/10.1016/j.jclepro.2021.126404.

[27] T.A. Saleh, A. Sarı, M. Tuzen, Carbon nanotubes grafted with poly(trimesoyl, m-phenylenediamine) for enhanced removal of phenol, J. Environ. Manag. 252 (2019), 109660, https://doi.org/10.1016/j.jenvman.2019.109660.

[28] P. Li, X.-C. Jiang, W.-M. Song, L.-Y. Zhang, Y.-J. Xu, Y. Liu, P. Zhu, Green organic-inorganic coatings for flexible polyurethane foams: evaluation of the effects on flame retardancy, antibacterial activity, and ideal mechanical properties, J. Clean. Prod. 411 (2023), 137265, https://doi.org/10.1016/j.jclepro.2023.137265.

[29] L.-Y. Qu, J.-L. Liu, Y.-Y. Liu, G.-Q. Zhang, Y.-J. Xu, P. Zhu, Y.-Z. Wang, Anchoring silver nanoparticles using catechol-derived resins: an efficient and versatile approach for producing durable antimicrobial fabrics, Prog. Organic Coat. 176 (2023), 107397, https://doi.org/10.1016/j.porgcoat.2022.107397.

[30] F. Siedenbiedel, J.C. Tiller, Antimicrobial polymers in solution and on surfaces: overview and functional principles, Polymers 4 (1) (2012) 46–71, https://doi.org/ 10.3390/polym4010046.

[31] Y. Wang, X. Yang, L. Xiao, W. Li, X. Huo, C. Wang, M. Li, T. Sun, Altered anterior insula-superior frontal gyrus functional connectivity is correlated with cognitive impairment following total sleep deprivation, Biochem. Biophys. Res. Commun. 624 (2022) 47–52, https://doi.org/10.1016/j.bbrc.2022.07.078.

[32] P. Król, Ł. Uram, B. Król, K. Pielichowska, M. Sochacka-Piętal, M. Walczak, Synthesis and property of polyurethane elastomer for biomedical applications based on nonaromatic isocyanates, polyesters, and ethylene glycol, Colloid Polym. Sci. 298 (8) (2020) 1077–1093, https://doi.org/10.1007/s00396-020-04667-8.

[33] B. Lin, A.C.Y. Yuen, S. Oliver, J. Liu, B. Yu, W. Yang, S. Wu, G.H. Yeoh, C.H. Wang, Dual functionalisation of polyurethane foam for unprecedented flame retardancy and antibacterial properties using layer-by-layer assembly of MXene chitosan with antibacterial metal particles, Compos. Part B 244 (2022), 110147, https://doi.org/ 10.1016/j.compositesb.2022.110147.

[34] E.E. Baldez, N.F. Robaina, R.J. Cassella, Employment of polyurethane foam for the adsorption of methylene blue in aqueous medium, J. Hazard. Mater. 159 (2) (2008) 580–586, https://doi.org/10.1016/j.jhazmat.2008.02.055.

[35] J. Chen, J. Wu, Y. Zhong, X. Ma, W. Lv, H. Zhao, J. Zhu, N. Yan, Multifunctional superhydrophilic/underwater superoleophobic lignin-based polyurethane foam for highly efficient oil-water separation and water purification, Sep. Purif. Technol. 311 (2023), 123284, https://doi.org/10.1016/j.seppur.2023.123284.

[36] L. Ren, Z. Tang, J. Du, L. Chen, T. Qiang, Recyclable polyurethane foam loaded with carboxymethyl chitosan for adsorption of methylene blue, J Hazard Mater. 417 (2021), 12613, https://doi.org/https://doi.org/10.1016/j.jhazmat.2021.126130.

[37] L. Ren, X. Gao, X. Zhang, T. Qiang, Stable and recyclable polyporous polyurethane foam highly loaded with UIO-66-NH2 nanoparticles for removal of Cr(VI) in wastewater, Polymer 255 (2022), 125117, https://doi.org/10.1016/j. polymer.2022.125117.

[38] P.A.P. Silva, R.L. Oréfice, Bio-sorbent from castor oil polyurethane foam containing cellulose-halloysite nanocomposite for removal of manganese, nickel and cobalt ions from water, J. Hazard. Mater. 454 (2023), 131433, https://doi.org/10.1016/j. jhazmat.2023.131433.

[39] M. Udayakumar, B. El Mrabate, T. Koós, K. Szemmelveisz, F. Kristály, M. Leskó, Á. Filep, R. Géber, M. Schabikowski, P. Baumli, J. Lakatos, P. Tóth, Z. Németh, Synthesis of activated carbon foams with high specific surface area using polyurethane elastomer templates for effective removal of methylene blue, Arab. J. Chem. 14 (7) (2021), 103214, https://doi.org/10.1016/j.arabjc.2021.103214.

[40] Ö. Akçakal, M. Sahin, M. Erdem, Synthesis and characterization of high-quality activated carbons from hard-shelled agricultural wastes mixture by zinc chloride activation, Chem. Eng. Commun. 206 (7) (2019) 888–897, https://doi.org/ 10.1080/00986445.2018.1534231.

[41] R. de A. Delucis, W.L.E. Magalhães, C.L. Petzhold, S.C. Amico, Thermal and combustion features of rigid polyurethane biofoams filled with four forest-based wastes, Polym. Compos. 39 (S3) (2018) E1770–E1777, https://doi.org/10.1002/ pc.24784.

[42] R.M.P. Farage, M.J. Quina, L. Gando-Ferreira, C.M. Silva, J.J.L.L. de Souza, C.M.M. E. Torres, Kraft pulp mill dregs and grits as permeable reactive barrier for removal of copper and sulfate in acid mine drainage, Sci. Rep. 10 (1) (2020) 4083, https:// doi.org/10.1038/s41598-020-60780-2.

[43] E.G. Dorlass, C.O. Monteiro, A.O. Viana, C.P. Soares, R.R.G. Machado, L. M. Thomazelli, D.B. Araujo, F.B. Leal, E.D. Candido, B.L. Telezynski, C.A. Valério, V.N. Chalup, R. Mello, F.J. Almeida, A.S. Aguiar, A.C.M. Barrientos, C. Sucupira, M. De Paulis, M.A.P. Sáfadi, D.B.L. Oliveira, Lower cost alternatives for molecular diagnosis of COVID-19: conventional RT-PCR and SYBR green-based RT-qPCR, Braz. J. Microbiol. 51 (3) (2020) 1117–1123, https://doi.org/10.1007/s42770- 020-00347-5.

[44] C.F. Demarco, T.F. Afonso, G.P. Schoeler, V. dos S. Barboza, L. dos S. Rocha, S. Pieniz, J.L. Giongo, R. de A. Vaucher, A.V. Igansi, T.R.S. Cadaval, R. Andreazza,

New low-cost biofilters for SARS-CoV-2 using *Hymenachne grumosa* as a precursor, J. Clean. Prod. 331 (2022), 130000, https://doi.org/10.1016/j.jclepro.2021.130000.

[45] CDC, CDC 2019-novel coronavirus (2019-nCoV) real-time RT-PCR diagnostic panel: instructions for use. https://www.cdc.gov/coronavirus/2019-ncov/downloads/rt-pcr-panel-for-detection-instructions.pdf, 2020.

[46] R. Yang, M. Li, X. Zhang, J. Li, Preparation of a catalyst-free and water-blown rigid polyurethane foam from malic-co-citric acid-based polyols, Ind. Crop. Prod. 169 (2021), 113648, https://doi.org/10.1016/j.indcrop.2021.113648.

[47] J. Wang, Z. Dong, J. Chen, S. Chen, Preparation of UV Debonding Acrylate Adhesives by a Postgrafting Reaction, Materials. 16 (2023) 5911, https://doi.org/10.3390/ma16175911.

[48] M.L.B. Almeida, E. Ayres, M. Libânio, D. de Souza Gamarano, C.C. Ribeiro, R. L. Oréfice, Bio-based polyurethane foams with enriched surfaces of petroleum catalyst residues as adsorbents of organic pollutants in aqueous solutions, J. Polym. Environ. 28 (9) (2020) 2511–2522, https://doi.org/10.1007/s10924-020-01794-9.

[49] M.L.B. Almeida, E. Ayres, F.C.C. Moura, R.L. Oréfice, Polyurethane foams containing residues of petroleum industry catalysts as recoverable pH-sensitive sorbents for aqueous pesticides, J. Hazard. Mater. 346 (2018) 285–295, https://doi.org/10.1016/j.jhazmat.2017.12.033.

[50] T. Autthawong, O. Namsar, A. Yu, T. Sarakonsri, Cost-effective production of SiO2/ C and Si/C composites derived from rice husk for advanced lithium-ion battery anodes, J. Mater. Sci. Mater. Electron. 31 (12) (2020) 9126–9132, https://doi.org/10.1007/s10854-020-03442-3.

[51] V. Daniele, L. Macera, G. Taglieri, A. Di Giambattista, G. Spagnoli, A. Massaria, M. Messori, E. Quagliarini, G. Chiappini, V. Campanella, S. Mummolo, E. Marchetti, G. Marzo, V. Quinzi, Thermoplastic disks used for commercial orthodontic aligners: complete physicochemical and mechanical characterization, Materials 13 (10) (2020) 2386, https://doi.org/10.3390/ma13102386.

[52] ICDD, PDF-4+ 2013 (Database), 2013.

[53] P.Y. Jia, X.M. Liu, G.Z. Li, M. Yu, J. Fang, J. Lin, Sol–gel synthesis and characterization of SiO_2@$CaWO_4$,SiO_2@$CaWO_4$:Eu^{3+}/Tb^{3+} core–shell structured spherical particles, Nanotechnology 17 (3) (2006) 734, https://doi.org/10.1088/0957-4484/17/3/020.

[54] A.P. Sasidharan, V. Meera, V.P. Raphael, Investigations on characteristics of polyurethane foam impregnated with nanochitosan and nanosilver/silver oxide and its effectiveness in phosphate removal, Environ. Sci. Pollut. Res. 28 (10) (2021) 12980–12992, https://doi.org/10.1007/s11356-020-11257-2.

[55] V. Suba, G. Rathika, E. Ranjith Kumar, M. Saravanabhavan, V.N. Badavath, K. S. Thangamani, Enhanced adsorption and antimicrobial activity of fabricated Apocynaceae leaf waste activated carbon by cobalt ferrite nanoparticles for textile effluent treatment, J. Inorg. Organomet. Polym. Mater. 29 (2) (2019) 550–563, https://doi.org/10.1007/s10904-018-1030-5.

[56] A.-N.A. El-Hendawy, A.J. Alexander, R.J. Andrews, G. Forrest, Effects of activation schemes on porous, surface and thermal properties of activated carbons prepared from cotton stalks, J. Anal. Appl. Pyrolysis 82 (2) (2008) 272–278, https://doi.org/ 10.1016/j.jaap.2008.04.006.

[57] A.P. Acosta, C.G. Otoni, A.L. Missio, S.C. Amico, R. de A. Delucis, Rigid polyurethane biofoams filled with chemically compatible fruit peels, Polymers 14 (21) (2022) 4526, https://doi.org/10.3390/polym14214526.

[59] A. Acosta, A.B. Aramburu, R. Beltrame, D.A. Gatto, S. Amico, J. Labidi, R. de A. Delucis, Wood flour modified by poly (furfuryl alcohol) as a filler in rigid polyurethane foams: effect on water uptake, Polymers 14 (24) (2022) 5510, https://doi.org/10.3390/polym14245510.

[60] X. Zhou, J. Sethi, S. Geng, L. Berglund, N. Frisk, Y. Aitomäki, M.M. Sain, K. Oksman, Dispersion and reinforcing effect of carrot nanofibers on biopolyurethane foams, Mater. Des. 110 (2016) 526–531, https://doi.org/ 10.1016/j.matdes.2016.08.033.

[61] G.P. Schoeler, T.F. Afonso, C.F. Demarco, V. dos Santos Barboza, T.R. Sant'anna Cadaval, A.V. Igansi, M.A. Gelesky, J.L. Giongo, R. de Almeida Vaucher, R. de Avila Delucis, R. Andreazza, Correction to: SARS-CoV-2 removal with a polyurethane foam composite, Environ. Sci. Pollut. Res. 30 (8) (2022) 22033, https://doi.org/ 10.1007/s11356-022-24031-3.

[62] Z. Zhang, L. Zhu, Z. Zhang, L. Sun, Y. Shi, L. Xie, D. Xu, J. Jin, Z. Xue, X. Ma, Synthesis of polyethyleneimine modified polyurethane foam for removal of Pb(II) ion from aqueous solution, Desalin. Water Treat. 160 (2019) 288–296, https://doi. org/10.5004/dwt.2019.24376.

[63] D. Zhang, H. Ling, X. Huang, J. Li, W. Li, C. Yi, T. Zhang, Y. Jiang, Y. He, S. Deng, X. Zhang, X. Wang, Y. Liu, G. Li, J. Qu, Potential spreading risks and disinfection challenges of medical wastewater by the presence of Severe Acute Respiratory Syndrome Coronavirus 2 (SARS-CoV-2) viral RNA in septic tanks of Fangcang Hospital, Sci. Total Environ. 741 (2020), 140445, https://doi.org/10.1016/j. scitotenv.2020.140445.

[64] G. Medema, L. Heijnen, G. Elsinga, R. Italiaander, A. Brouwer, Presence of SARS-Coronavirus-2 RNA in sewage and correlation with reported COVID-19 prevalence in the early stage of the epidemic in the Netherlands, Environ. Sci. Technol. Lett. 7 (7) (2020) 511–516, https://doi.org/10.1021/acs.estlett.0c00357.

[65] M.S. Fonseca, B.A.S. Machado, C. de A. Rolo, K.V.S. Hodel, E. dos S. Almeida, J. B. de Andrade, Evaluation of SARS-CoV-2 concentrations in wastewater and river water samples, Case Studies Chem. Environ. Eng. 6 (2022), 100214, https://doi. org/10.1016/j.cscee.2022.100214.

[66] M. Kumar, A.K. Patel, A. Shah, J. Raval, N. Rajpara, M. Joshi, C.G. Joshi, First proof of the capability of wastewater surveillance for COVID-19 in India through detection of genetic material of SARS-CoV-2, Sci. Total Environ. 746 (2020), 141326, https://doi.org/10.1016/j.scitotenv.2020.141326.

[67] W. Ahmed, P.M. Bertsch, K. Bibby, E. Haramoto, J. Hewitt, F. Huygens, P. Gyawali, A. Korajkic, S. Riddell, S.P. Sherchan, S.L. Simpson, K. Sirikanchana, E. M. Symonds, R. Verhagen, S.S. Vasan, M. Kitajima, A. Bivins, Decay of SARS-CoV-2 and surrogate murine hepatitis virus RNA in untreated wastewater to inform application in wastewater-based epidemiology, Environ. Res. 191 (2020), 110092, https://doi.org/10.1016/j.envres.2020.110092.

[68] W. Ahmed, P.M. Bertsch, A. Bivins, K. Bibby, K. Farkas, A. Gathercole, E. Haramoto, P. Gyawali, A. Korajkic, B.R. McMinn, J.F. Mueller, S.L. Simpson, W. J.M. Smith, E.M. Symonds, K. Thomas, v, Verhagen, R., & Kitajima, M., Comparison of virus concentration methods for the RT-qPCR-based recovery of murine hepatitis virus, a surrogate for SARS-CoV-2 from untreated wastewater, Sci. Total Environ. 739 (2020), 139960, https://doi.org/10.1016/j. scitotenv.2020.139960.

[69] A. Nemudryi, A. Nemudraia, T. Wiegand, K. Surya, M. Buyukyoruk, C. Cicha, K. K. Vanderwood, R. Wilkinson, B. Wiedenheft, Temporal detection and phylogenetic assessment of SARS-CoV-2 in municipal wastewater, Cell Rep. Med. 1 (6) (2020), 100098, https://doi.org/10.1016/j.xcrm.2020.100098.

[70] J. Peccia, A. Zulli, D.E. Brackney, N.D. Grubaugh, E.H. Kaplan, A. Casanovas-Massana, A.I. Ko, A.A. Malik, D. Wang, M. Wang, J.L. Warren, D.M. Weinberger, S. B. Omer, SARS-CoV-2 RNA concentrations in primary municipal sewage sludge as a leading indicator of COVID-19 outbreak dynamics, MedRxiv (2020), https://doi.org/10.1101/2020.05.19.20105999, 2020.05.19.20105999.

[71] Y. Wu, C. Guo, L. Tang, Z. Hong, J. Zhou, X. Dong, H. Yin, Q. Xiao, Y. Tang, X. Qu, L. Kuang, X. Fang, N. Mishra, J. Lu, H. Shan, G. Jiang, X. Huang, Prolonged presence of SARS-CoV-2 viral RNA in faecal samples, Lancet Gastroenterol. Hepatol. 5 (5) (2020) 434–435, https://doi.org/10.1016/S2468-1253(20)30083-2.

[72] W. Randazzo, P. Truchado, E. Cuevas-Ferrando, P. Simón, A. Allende, G. Sánchez, SARS-CoV-2 RNA in wastewater anticipated COVID-19 occurrence in a low prevalence area, Water Res. 181 (2020), 115942, https://doi.org/10.1016/j.watres.2020.115942.

[73] L. Guerrero-Latorre, I. Ballesteros, I. Villacrés-Granda, M.G. Granda, B. Freire-Paspuel, B. Ríos-Touma, SARS-CoV-2 in river water: implications in low sanitation countries, Sci. Total Environ. 743 (2020), 140832, https://doi.org/10.1016/j.scitotenv.2020.140832.

[74] B.A. Kocamemi, H. Kurt, A. Sait, F. Sarac, A.M. Saatci, B. Pakdemirli, SARS-CoV-2 detection in Istanbul wastewater treatment plant sludges, MedRxiv (2020), https:// doi.org/10.1101/2020.05.12.20099358, 2020.05.12.20099358.

[75] S. Wurtzer, V. Marechal, J. Mouchel, Y. Maday, R. Teyssou, E. Richard, J. Almayrac, L. Moulin, Evaluation of lockdown effect on SARS-CoV-2 dynamics through viral genome quantification in waste water, Greater Paris, France, 5 March to 23 April 2020, Eurosurveillance 25 (50) (2020), https://doi.org/10.2807/1560-7917.ES.2020.25.50.2000776.

[76] S.N. Rao, D. Manissero, V.R. Steele, J. Pareja, A systematic review of the clinical utility of cycle threshold values in the context of COVID-19, Infect. Dis. Ther. 9 (3) (2020) 573–586, https://doi.org/10.1007/s40121-020-00324-3.

[77] E. Joonaki, A. Hassanpouryouzband, C.L. Heldt, O. Areo, Surface chemistry can unlock drivers of surface stability of SARS-CoV-2 in a variety of environmental conditions, Chem 6 (9) (2020) 2135–2146, https://doi.org/10.1016/j.chempr.2020.08.001.

[78] L.M. Pandey, Surface engineering of personal protective equipments (PPEs) to prevent the contagious infections of SARS-CoV-2, Surf. Eng. 36 (9) (2020) 901–907, https://doi.org/10.1080/02670844.2020.1801034.

[79] D.J. Rodriguez, H.A. Serrano, A. Delgado, D. Nolasco, G. Saltiel, From waste to resource, in: Water Papers, World Bank, 2020, https://doi.org/10.1596/33436.

[80] A. Bogler, A. Packman, A. Furman, A. Gross, A. Kushmaro, A. Ronen, C. Dagot, C. Hill, D. Vaizel-Ohayon, E. Morgenroth, E. Bertuzzo, G. Wells, H.R. Kiperwas, H. Horn, I. Negev, I. Zucker, I. Bar-Or, J. Moran-Gilad, J.L. Balcazar, E. Bar-Zeev, Rethinking wastewater risks and monitoring in light of the COVID-19 pandemic, Nat. Sustain. 3 (12) (2020) 981–990, https://doi.org/10.1038/s41893-020-00605- 2.

[81] F. Anayah, I.A. Al-Khatib, B. Hejaz, Assessment of water and sanitation systems at Palestinian healthcare facilities: pre- and post-COVID-19, Environ. Monit. Assess. 193 (1) (2021) 41, https://doi.org/10.1007/s10661-020-08791-4.

[82] S.M. Parsa, Reliability of thermal desalination (solar stills) for water/wastewater treatment in light of COVID-19 (novel coronavirus “SARS-CoV-2”) pandemic: what should consider? Desalination 512 (2021), 115106 https://doi.org/10.1016/j. desal.2021.115106.

[83] Y. Chen, L. Chen, Q. Deng, G. Zhang, K. Wu, L. Ni, Y. Yang, B. Liu, W. Wang, C. Wei, J. Yang, G. Ye, Z. Cheng, The presence of SARS-CoV-2 RNA in the feces of COVID-19 patients, J. Med. Virol. 92 (7) (2020) 833–840, https://doi.org/ 10.1002/jmv.25825.

[84] K.-H. Chan, S. Sridhar, R.R. Zhang, H. Chu, A.Y.-F. Fung, G. Chan, J.F.-W. Chan, K. K.-W. To, I.F.-N. Hung, V.C.-C. Cheng, K.-Y. Yuen, Factors affecting stability and infectivity of SARS-CoV-2, J. Hosp. Infect. 106 (2) (2020) 226–231, https://doi. org/10.1016/j.jhin.2020.07.009.

[85] A.W.H. Chin, J.T.S. Chu, M.R.A. Perera, K.P.Y. Hui, H.-L. Yen, M.C.W. Chan, M. Peiris, L.L.M. Poon, Stability of SARS-CoV-2 in different environmental conditions, Lancet Microbe 1 (1) (2020), e10, https://doi.org/10.1016/S2666- 5247(20)30003-3.

[86] M.B. Araújo, B. Naimi, Spread of SARS-CoV-2 coronavirus likely constrained by climate, MedRxiv (2020), https://doi.org/10.1101/2020.03.12.20034728, 2020.03.12.20034728.

[87] W. Qi, H. Singer, M. Berg, B. Müller, B. Pernet-Coudrier, H. Liu, J. Qu, Elimination of polar micropollutants and anthropogenic markers by wastewater treatment in

Beijing, China, Chemosphere 119 (2015) 1054–1061, https://doi.org/10.1016/j.chemosphere.2014.09.027.

[88] K. Van Gijn, Y.L. Chen, B. van Oudheusden, S. Gong, H.A. de Wilt, H.H. M. Rijnaarts, A.A.M. Langenhoff, Optimizing biological effluent organic matter removal for subsequent micropollutant removal, J. Environ. Chem. Eng. 9 (5) (2021), 106247, https://doi.org/10.1016/j.jece.2021.106247.

[89] A. Lesimple, S.Y. Jasim, D.J. Johnson, N. Hilal, The role of wastewater treatment plants as tools for SARS-CoV-2 early detection and removal, J. Water Process Eng. 38 (2020), 101544, https://doi.org/10.1016/j.jwpe.2020.101544.

5 Artigo 2

O artigo intitulado **“Green chemistry for Cr(III) removal from water solution”** é apresentado conforme submetido na Revista Colloids and Surfaces A: Physicochemical and Engineering Aspects, ISSN: 0927-7757, fator de impacto 5.2, classificação A2 na área de Materiais.

Green chemistry for Cr(III) removal from water solution

Thays França Afonso[a], Guilherme Pereira Schoeler[b], Carolina Faccio Demarco[a], Maurizio Silveira Quadro[b], Daisa Hakbart Bonemann[c], Anderson Schwingel Ribeiro[c], Benedict C Okeke[a,d], Simone Pieniz[b,d], , Fernando Machado[a], Rafael de Avila Delucis[a,b], Robson Andreazza[a,b]*

[a]Science and Engineering of Materials Postgraduate Program. Federal University of Pelotas. R. Gomes Carneiro 01, CEP 96010-610, Pelotas, RS, Brazil.

[b]Environmental Sciences Postgraduate Program. Federal University of Pelotas. R. Benjamin Constant 989, CEP 96010-020 Pelotas, RS, Brazil.

[c]Chemistry Postgraduate Program. Federal University of Pelotas. Av. Eliseu Maciel, Campus Universitário, s/n, Capão do Leão, CEP 96160-000, RS, Brazil

[d]Department of Biology and Environmental Science, Auburn University at Montgomery, AL 36117, USA

[e]Faculty of Nutrition, Federal University of Pelotas, Pelotas 96015-560, Rio Grande do Sul, Brazil;

*Corresponding author: e-mail: robsonandreazza@yahoo.com.br; Phone +55 53 3921 1432; Fax +55 53 3921 1432.

Abstract

The study examines the use of biowaste-based additions from peach stones to modify polyurethane foams (PUF) and remove trivalent chromium (Cr(III)) from the water. Powdered peach stone (PUPS) and peach stone-based activated carbon (PUPSAC) were used to create filled PUF. The modified PUF foams were then physically and chemically activated to determine their potential as an adsorbent for removing Cr(III) from aqueous solutions. In the foam's polymerization process, glycerol and castor oil were utilized instead of the conventional cross-linked polyols to decrease costs and toxicity. An optimal filler weight fraction was determined to be 5% and the functionalization of the biowaste-filled foam yielded improved Cr(III) adsorption. The study investigated the effects of different Cr(III) removal conditions (e.g. pH, initial Cr(III) concentration, mass concentration, and temperature) on percent removal. At pH 6.5, a mass concentration of 0.6 g L^{-1} displayed the highest Cr(III) removal capacity. The Sips isotherm model and Elovich kinetics model yielded the best fit for the adsorption of Cr(III) from modified PUF. The thermodynamic functions, including internal energy, free enthalpy, and entropy, indicate that the reactions are endothermic, feasible, and spontaneous. The experimental results regarding the uptake capacity of the PUF variants indicated that, once activated and carbonized, the activated carbon formed a sponge-like structure with pores of varying sizes and shapes. Furthermore, the adsorption capacity for Cr(III) increased as pH increased from 4 to 6.5. At pH 6.5, both foams, PUPSAC and PUPS, exhibited more favorable conditions for Cr(III) adsorption and achieved maximum levels of 98.3 mg g^{-1} and 68.2 mg g^{-1}, respectively, with a percentage removal of 62.2% and 42.6%. In conclusion, this study offers significant insights regarding the potential usage of functionalized PUF as an adsorbent for the removal of Cr(III) from water or wastewater.

Keywords: Polyurethane foam; Adsorption; Heavy metal; Advanced materials; Low-cost biosorbents; Agricultural waste.

1 Introduction

Every year, millions of people are impacted by water contaminated with chromium (Cr), which is an important environmental and public health issue due to its toxic effect on human beings and ecological systems (Bachmann et al., 2022; Kanwar et al., 2020). Cr may infiltrate groundwater due to industrial activities, such as refining ores, electroplating,and tanning leather (Zhang et al., 2023). Trivalent chromium Cr(III) and hexavalent chromium Cr(VI) are the two most common forms of Cr present in water. It is important to consider that catalytic reduction of Cr(VI) can lead to the generation of carbon dioxide (CO2), which is a by-product that has harmful impacts on the environment (Farooqi et al.,2021). Furthermore, extracting Cr(III), which is a reduced form of Cr(VI), using adsorbentscan be challenging, although the accumulation of Cr(III) may pose ecological risks (Solis-Ceballos et al., 2023). The toxicity of Cr is highly related to its valence state, therefore Cr(VI) is much more toxic than Cr(III) and Cr(0) (Islam et al., 2023; Prasad et al., 2021).

The United States Environmental Protection Agency (EPA) mandates that 0.05 mgL^{-1} is the maximum permitted concentration of total Cr in potable water, while industrial effluents must not contain an average of more than 1.71 mg L^{-1} per month. Even so, Cr concentrations in certain industrial effluents, particularly those from the tannery sector, canrange from 0.7 mg L^{-1} to 345 mg L^{-1} (EPA, 1990; Prasad et al., 2021).

Many methodologies have been used to remove Cr from water, including, electrochemical treatments, membrane filtration, microbial treatment, and adsorption (Islam et al., 2023). Adsorption is often considered an effective, affordable, and uncomplicated method for achieving this objective (Syeda and Yap, 2022). Also, the use of green materials for adsorption has many advantages over synthetic, since these former materials are renewable, low-cost, and ecologically friendly (Bekchanov et al., 2024).

Most of the common adsorbents for the removal of heavy metals include inorganic materials, such as minerals, zeolites, siliceous materials, metal oxides, carbonaceous, graphene, and clays (Zaimee et al., 2021). Composite materials based on mixtures of organic and inorganic materials, as well as wastes or byproducts from animals, agriculture, and industry, have been alternative materials (Karthik et al., 2023). Additionally, polymer-based materials, including synthetic and natural polymers, like polyurethane foam (PUF), have also been utilized (Li et al., 2023). Such materials exhibit a high degree of chemical stability and porosity, as well as a large surface area (Ashok Kumar et al., 2023; Jalalah et al., 2023; Li et al., 2023).

PUF is an excellent sorbent material composed of a cellular structure, remarkable chemical and thermal resistance, and the ability to chemically retain various types of substances due to the presence of polar and non-polar groups in their structures. These features allow them to be easily separated from aqueous solutions and make them have remarkable mass transfer properties and rapid adsorption rates (Zhang et al., 2019). For this reason, unmodified PUF has been widely used to separate a wide variety of inorganic and organic species from aqueous media. However, the low adsorption efficiency of PUF limited their practical application, which justifies their modification toward reaching improved adsorption efficiency. The most common techniques for achieving PUF-based adsorbents with high performance in water treatment applications include surface modification, nanostructure integration, chemical functionalization, cross-linking, pore control, composite formation, and the development of regeneration methods (Zhang et al., 2019).

When PUF are filled with vegetables, the overall cost may be negligible compared with ion-exchange resins or industrial activated carbons. Most of these bio-based materials contain functional groups associated with polysaccharides, proteins, or lignin as major constituents (Elgarahy et al., 2023). Chemically treating vegetal materials can lead to an increase in adsorption capacity due to the presence of functional groups such as hydroxyl (-OH), carboxyl (-COOH), and amine ($-NH_2$) groups. These groups can become more accessible and reactive upon chemical modification, enhancing the metal uptake to adsorb contaminants in water treatment applications (Aslam et al., 2023; Parlayıcı, 2019).

Materials, such as peach stones, hold significant promise in addressing environmental concerns associated with their generation while offering substantial potential for contaminant removal applications (Shah et al., 2023). The generation of peach stones, a biomass of the food industry, contributes to environmental challenges due to their disposal. However, these pits represent an abundant and cost-effective resource that can be harnessed for various applications.

Peach stones exhibit biocompatibility, renewability, and cost-effectiveness align with the principles of Green Analytical Chemistry (GAC), which encourages its use as a sustainable and eco-friendly resource (Shi et al., 2023).

Furthermore, one intriguing avenue involves the conversion of peach stones into activated carbon (Nayeem et al., 2023; Parlayıcı, 2019). This process yields an adsorbent material that possesses an enhanced capacity for contaminant removal. By subjecting peach stones to controlled activation processes, the resulting activated carbon can be tailored to efficiently adsorb a wide range of pollutants from water sources. This dual-purpose approach

not only addresses the environmental concern of peach pit disposal but also offers a sustainable and cost-effective means of producing effective adsorbents for water treatment.

The search for alternative new, cheap, eco-friendly, and efficient adsorbents to replace the commercially available ones is ongoing (Nayeem et al., 2023; Parlayıcı, 2019). Several studies suggest combining multiple materials to form a single adsorbent to enhance metal adsorption. Therefore, this study focuses on the removal of Cr from contaminated water by employing PUF with PS-based fillers.

2 Materials and Methods

2.1 Characterizations

Peach stones obtained from Oderich Canned Food Industry®, located in Pelotas, Brazil were air-dried and sieved through a 150 µm screen. Thirty grams of the precursor was impregnated with 30 g of $ZnCl_2$ (activating agent). The biomass and $ZnCl_2$ were mixed and dried in an oven at 105°C overnight. Subsequently, the product was carbonized at 700 °C for 60 minutes. The carbonized material, referred to as peach stone-based activated carbon 'PSAC,' was treated with 3M HCl to remove the remaining chemical activator and to complete the activation process, using the procedure described by (Akçakalet al., 2019).

Bulk densities of carbon-based materials were determined according to ASTM D2854-96, (2004). The bulk density, ash content, pH, moisture content, and particle size of PSAC were determined as 0.47 g mL^{-1}, 89%, 8.14, 7.26%, 0.125-0.150 mm, respectively. The specific surface area, total pore volume, and pore size of filler materials were conducted on a1200e Quantachrome Instruments automated devices Micromeritics volumetric analyzer at 77 K. The specific surface area was calculated using the BET (Brunauer, Emmett, and Teller) method (Brunauer et al., 1938), and the pore size was quantified by the BJH (Barret, Joyner, and Halenda) method (Barrett et al., 1951) (see Table 1).

Table 1 - Textural properties of the biomass.

Fillers	PS*	PSAC**
BET-surface area ($m^2\ g^{-1}$)	0.562	579.199
Total pore volume ($cm^3\ g^{-1}$)	0.0039	0.2970
Average pore size (nm)	141.781	10.256

*PS is peach stones; **PSAC is peach stone-based activated carbon.

The free-rise pouring method was used to prepare PUF by inserting the two fillers mentioned earlier, as described by Delucis et al. (2018). The quantity of each reagent used can

be found in Afonso et al. (2023). PU, PUPS, and PUPSAC are the labels for neat PU, PU filled with peach stones, and PU filled with peach stones-based activated carbon, respectively.

The PZC was determined following the protocol outlined by Farage et al. (2020) and was measured as 6.5 to all PUF. The Fourier Transform Infrared Spectroscopy (FT-IR) of the foam was recorded in the range 4000–400 cm^{-1} on a Prestige Shimadzu device equipped with an Attenuated Total Reflectance (ATR) attachment. The absence of a signal at 2266 cm^{-1} indicates complete consumption of the NCO groups from the p-MDI. This indicates successful bonding between the OH groups and NCO groups of the polyol to form urethane groups containing C=O (1730 cm^{-1}), C-O-C (1140–1180 cm^{-1}), C-N (1240 cm^{-1}), and N-H (3340 cm^{-1}) groups.

X-ray diffraction (XRD) patterns were obtained using a diffractometer (Brunker D-8, Germany) equipped with a diffracted beam monochromator and Ni-filtered CuKα radiation (λ = 1.5406 Å). A voltage of 40 kV and an intensity of 40 mA were set. The 2θ angle was scanned between 10° and 60°, and the counting time was 1.0 s at each angular step (0.02°). The XRD diffractogram of the neat PU suggests that it is a highly amorphous material, displaying wide amorphous halos at 20° and 41°, which can be attributed to the rigid segments of the PUF (Afonso et al., 2023; Jamsaz et al., 2021; Sasidharan et al., 2021; Wang et al., 2017). The incorporation of peach stone particles and peach stone activated carbon into the polyurethane structure did not significantly alter the material's amorphous structure.

Surface morphology was analyzed with SEM employing a JSM 6610LV Jeol instrument set to a working voltage of 15 kV and a magnification of 100×. After activation and carbonization, a sponge-like morphology was formed by activated carbon and pores of different sizes and different shapes. A high degree of porosity and a tendency towards less homogeneous and more deformed cell structures of the foams. The Feret diameter of the cells was not significantly affected by the presence of fillers, except for PUPS (Afonso et al., 2023).

2.2 Experiments

2.2.1 Adsorption

A number of the factors affecting the adsorption have been studied including initial concentration of Cr(III), pH, mass concentration, and temperature. Three adsorbents were used (Neat PU, PUPS, and PUPSAC).

Cr (III), which is chloride hexahydrate ($CrCl_3.6H_2O$) (Dynamic, PM: 266.45), was used to prepare Cr(III) stock solution of 1000mg L^{-1}. The adjustment of pH was achieved by adding NaOH or H_2SO_4 using a mPa-210 bench pH meter (MS Tecnopon Instrumentation).

The kinetic studies were established by the following conditions: initial Cr(III) concentration (50 mg L^{-1}); solution pH (4, 5, 6.5); mass concentration (0.3, 0.6, 1.2 g L^{-1}); and temperature (25 °C). The assays were performed under a fixed stirring of 200 rpm using a Jartest JTM 6036 (Milan). Aliquots (1 mL) were taken at 1, 5, 10, 15, 30, 60, 120, 180, 240, 300, 360, 420, 480, 540, 600 and 720 min. When studying the effect of one-factor in an experiment, the other factors remained unchanged for comparison.

The adsorption isotherm studies were used to determine the adsorption rate. The study was undertaken with concentration Cr(III) of 0 - 90 mg L^{-1}, solution pH of 6.5, and mass concentration of 1.2 g L^{-1}, at three different temperatures: room temperature 25, 35, and 45 °C. The batch experiments were carried out in 250ml Erlenmeyer flasks, shaken in an orbital shaker at 200 rpm. One milliliter sample were withdrawn from the solution diluted and were then analyzed by atomic absorption spectrometry in a PerkinElmer AAnalyst™ 200 device.

2.2.2 Determination of Cr(III) removal efficiency and modelling

The percentage removal of Cr(III) was calculated using Eq. (1):

$$\text{Removal}\ (\%) = \frac{C_0 - C_e}{C_0}\ x\ 100\% \quad (1)$$

where C_o and C_e are the initial and equilibrium concentration Cr(III) in mg L^{-1}.

The adsorption capacity (q_t) is the amount of Cr(III) taken up by the adsorbent (mg g−1), which was calculated by the Eq. (2):

$$q_t = \frac{(C_0 - C_t)}{m}\ x\ V \quad (2)$$

2.2.3 Kinetic modelling

The adsorptions kinetic parameters were obtained by applying the kinetic equations for the pseudo-first-order model (Eq. 3), the pseudo-second-order model (Eq. 4) and Elovich (Eq. 5) in the Statistic 7.0 software (Statsoft, 2004) by the non-linear method.

$$q_t = q_1(1 - \exp(-k_1\, t)) \quad (3)$$

$$q_t = t/((1/k_2 q_2^2) + (1/q_2)) \quad (4)$$

$$q_t = 1/a\ \ln(1 + abt) \quad (5)$$

where: q_t (adsorption capacity on time (mg g^{-1})); q_1 and q_2 (theorical values for the adsorption capacity (mg g^{-1})); k_1 (constant of pseudo-first-order model (min^{-1})); k_2 (constant of pseudo-second-order model (g mg^{-1} min^{-1})); a (initial adsorption rate (mg g^{-1} min^{-1})); b (Elovich constant (g mg^{-1})); t = time (min).

The kinetic curves for each model were estimated by non-linear regression as a quasi-Newton function. The fitting of the kinetic models to the experimental data was evaluated by employing the coefficients of determination (R^2) and the mean relative error (MRE).

To find models that have the best fit to the experimental data, the coefficient of determination (R^2) and, mean relative error (MRE) were used. MRE can be calculated by Eq. (6):

$$MRE = {}^{100}/_{n} \sum_{1}^{n} ({}^{q_{e,exp} - q_{e,cal}}/_{q_{e,exp}}) \quad (6)$$

where $q_{e,exp}$ and $q_{e,cal}$ are the quantities of Cr(III) adsorbed obtained from the experiment and calculation from the equation of the model, respectively. n is the number of observations of the experiment.

2.2.4 Isotherms studies

The equilibrium experimental data were described by seven models (with two and three-parameter): Langmuir (1916), Freundlich (1906), Redlich & Peterson (1959), Toth, (1971), Khan et al. (1997), Sips (Chen et al., 2022) and Dubinin & Radushkevich (1947) (D-R).

The Langmuir isotherm model assumption is that the surface of the adsorbent is uniform, and the adsorption sites are equivalent, all the molecules do not interact with each other, and adsorption occurs through the same mechanism (Olalekan A.P et al., 2013; Srivastava et al., 2015). The Langmuir model can be described by Eq. (7):

$$q_e = {}^{q_m K_L C_e}/_{1 + K_L C_e} \quad (7)$$

where q_m and K_L are the Langmuir constants regarding the biosorption in mg g^{-1} and the adsorption energy in L g^{-1}, respectively.

The Freundlich isotherm model can be described as Eq. (8):

$$q_e = K_F C_e^{1/n} \quad (8)$$

where K_F (mg g^{-1}(mg L^{-1})$^{-1/n}$) is the Freundlich constant in relation to the adsorption capacity in definition as the adsorption or distribution capacity and it presents the quantity of Cr(III) adsorption on the adsorbent per unit concentration at the equilibrium. 1/n is the heterogeneity factor.

The Redlich–Peterson isotherm model is widely applied as a middle way between two extremes, which are the Freundlich and Langmuir models. The Redlich and Peterson (1959) isotherm model can be described by Eq. (9):

$$q_e = K_R C_e \Big/ 1 + a_R C_e^{\beta} \quad (9)$$

where and q_e is equilibrium adsorbate collected over adsorbent (mg g^{-1}), C_e is equilibrium liquid-phase concentration of the adsorbent (mg L^{-1}), K_R, (L mg^{-1}), a_R (L mg^{-1}) are the Redlich–Peterson isotherm model constants, and β Redlich-Peterson exponent.

The Toth model is an empirical and widely used model and is used for the heterogeneous system. It can be used at the limit of concentration. The Toth (1971) isotherm model can be described using Eq. (10):

$$q_e = K_T C_e \Big/ (a_T + C_e)^{1/t} \quad (10)$$

where K_T (mg g^{-1}), a_T (L mg^{-1}) and t are the Toth isotherm model constants. When t equals to 1, the Toth model can be reduced to the Langmuir model equation.

The Khan model is generalized and can be described by Eq. (11):

$$q_e = b_K q_S C_e / (1 + b_K C_e)^{a_K} \quad (11)$$

where b_K (mg g^{-1}) is Khan isotherm model constant, a_K is Khan isotherm model exponent and q_S (mg g^{-1}) is the quantity of the Cr(III) adsorbed at the maximum.

Sips isotherm or the combined Langmuir-Freundlich isotherm (a three-parameter isotherm model) assumes monolayer adsorption in heterogeneous and homogenous systems

because it avoids the limitations of increased concentrations of the adsorbate associated with the Freundlich model, which is described by the following Eq. (12):

$$q_e = (q_m K_L C_e^{n_s})/(1 + K_L C_e^{n_s}) \quad (12)$$

where q_m indicates Langmuir-Freundlich maximum adsorption capacity (mg g^{-1}); the K_L is Sips isotherm model constant (L mg^{-1}); n_s is heterogenous parameter between 0 and 1, and C_e is the equilibrium concentration. Homogeneous adsorption occurs when $n_s = 1$, whereas heterogeneous adsorption occurs when $n_s < 1$.

The Dubinin-Radushkevich (D-R) isotherm is another model for the analysis of isotherms of a high degree of rectangularity. The D-R isotherm is more general than the Langmuir isotherm because it does not assume a homogeneous surface or constant adsorption potential. The form of D-R isotherm Eq. (13, 14 and 15) is as follows:

$$ln\ q_e = ln\ q_m\ - \beta\varepsilon^2 \quad (13)$$

$$E = 1/\sqrt{2\beta} \quad (14)$$

$$\varepsilon = RTln(1 + 1/C_e) \quad (15)$$

where β is a constant and gives the mean free energy E (kJ mol^{-1}) of adsorption per molecule of the adsorbate when it is transferred to the surface of the solid from infinity in the solution (mol^2 kJ^{-2}) and R is the universal gas constant, T is the temperature (K) and q_m is the Dubinin–Radushkevich isotherm constant (mg g^{-1}).

2.2.5 Adsorption thermodynamics

According to the laws of thermodynamics, the standard change in Gibbs free energy (ΔG°) is directly calculated from Eq. 16-19 (Lima et al., 2021, 2019).

$$\Delta G° = -RTLnK_e^0 \quad (16)$$

$$\Delta G° = \Delta H° - T\Delta S° \quad (17)$$

$$LnK_e^0 = ((\Delta S°/R - \Delta H°/R)\ 1/T) \quad (18)$$

Where R is the universal gas constant (8.314 J K^{-1} mol^{-1}); T is the absolute temperature in kelvin (K); and K_e^0 (dimensionless) is the equilibrium constant.

3 Results and discussion

3.1 Effect of pH

The World Health Organization (WHO) recommends that wastewater discharge have a pH between 6.0 and 9.0 (WHO, 2022). However, it is recommended that the pH of the water entering the treatment plant be controlled at a pH between 6.5 and 8.5 to prevent pipe corrosion and for effective disinfection (Jagemma et al., 2023). Therefore, the adsorption was carried out at a pH close to 6.5 to align with real operating conditions.

Fig. 1 shows that pH is a crucial factor affecting the adsorption behavior of the Cr(III) with the three types of foams being considered in this study. The adsorption capacity for Cr(III) increases with increasing pH, and reaches a maximum at pH 6.5. The condition set at pH = 6.5 was more favorable for the Cr(III) adsorption by both foams PUPSAC and PUPS, and had a maximum uptake of 98.3 and 68.2 mg g^{-1} and percentage removal of 62.2% and 42.6%, respectively. As the solution pH increased, the adsorption capacity of Cr(III) increased. Solis-Ceballos et al. (2023) using starch-graft-itaconic acid hydrogel and Bai et al. (2020) using graphene oxide/alginate hydrogel membrane for the adsorption of Cr(III) reported similar observations.

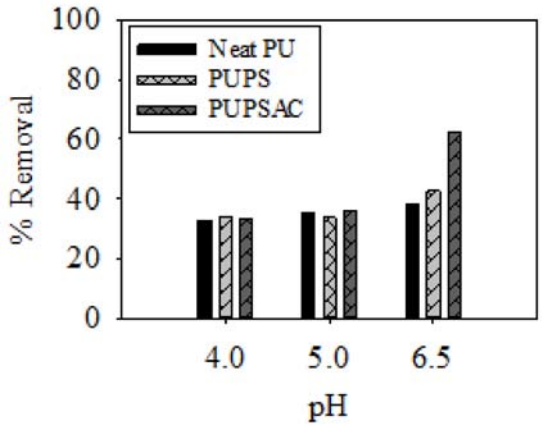

Fig. 1 - Effect of pH on the removal of Cr(III) from solution using PUF; initial concentration 50 mg L^{-1} (Cr III); mass concentration 0.3 g L^{-1}; 200 rpm and 25 ºC .

In the context of contaminant removal, peach stones possess a surface chemical composition comprising functional groups, such as nitrogen, oxygen, and sulfur. These groups include hydroxyl, carboxyl, amine, and sulfonic acid, all of which serve as potential binding

sites for heavy metal adsorption (Rocky et al., 2023). For example, under alkaline pH conditions, carboxyl (R−COOH) and hydroxyl (R-OH) groups readily donate their hydrogen atoms, transforming into negatively charged R−COO− and R−O− groups, respectively. These functional groups can effectively interact with positively charged metal ions, offering a sustainable and natural solution for water treatment (Badsha et al., 2021).

Interactions involving functional groups that contain oxygen are crucial for the adsorption of Cr(III). Carbonyl groups of this type have also been shown to form complexes with metals through oxygen-donating electron pairs (Zhang and Tian, 2020). This is because aqueous forms of Cr(III) exist as complex ions rather than isolated ions (Solis-Ceballos et al., 2023).

When the acidity is high, the hydroxyl and carboxyl groups of the adsorbent are protonated/positively charged. Many hydrogen ions in solution also compete with the Cr(III) ions for adsorption sites, resulting in low adsorption capacity for Cr(III) ions. As the pH increases, the carboxyl groups are converted to carboxylate anions, and the interactions between the metal ion and the foams is subsequently enhanced (Bai et al., 2020). Therefore, the adsorption capacity of foams for Cr(III) may be ascribed to their functional groups, as previously mentioned (Bandara et al., 2020; Olawale et al., 2022).

3.2 Effect of mass concentration

The effect of mass concentration on the adsorption of Cr(III) by foams was studied. As illustrated in Fig. 2, when the mass concentration increased, the removal increased in concentration 10-30 mg L^{-1} Cr(III).

For neat PU, PUPS, and PUPSAC, the maximum Cr(III) removal was 86%, 98%, and 99% respectively achieved when the mass concentration was 0.6 g L^{-1}. For Cr(III) ions, after the initial concentration increased from 10.0 mg L^{-1} to 50.0 mg L^{-1}, the adsorption capacity increased as the mass concentration increased from 0.3 g L^{-1} to 1.2 g L^{-1}. However, when the mass concentration increased from 0.6 g L^{-1} to 1.2 g L^{-1}, the adsorption capacity was reduced.

Therefore the initial concentration of heavy metal ions (Cr(III)) provides a strong driving force to overcome the mass transfer resistance between the solid phase and the aqueous phase of the adsorbate, resulting in an increase in the adsorption capacity with an increase in concentration of Cr(III) ions (Chen et al., 2010). Then, as the concentration of Cr(III) ions increases, the collision probability between metal ions and the adsorbent surface in the solution is higher, promoting adsorption (Nag et al., 2018). Thus, at low concentrations of Cr(III) ions,

the adsorption sites do not reach saturation, and the adsorption capacity increases rapidly as the concentration increases.

On the other hand, increasing the mass concentration from 0.6 g L^{-1} to 1.2 g L^{-1} at a fixed Cr(III) concentration and volume leads to the saturation of adsorption sites during the adsorption process (this behavior becomes more evident for initial Cr(III) concentrations of 50 mg L^{-1} , see Fig. 2(A) and (B)). A reduction in adsorbent capacity may result from adsorbent aggregation, which occurs as a consequence of a high mass concentration. This aggregation leads to a decrease in the total surface area of the adsorbent, as well as an increase in the diffusional path length (Lima et al., 2015a).

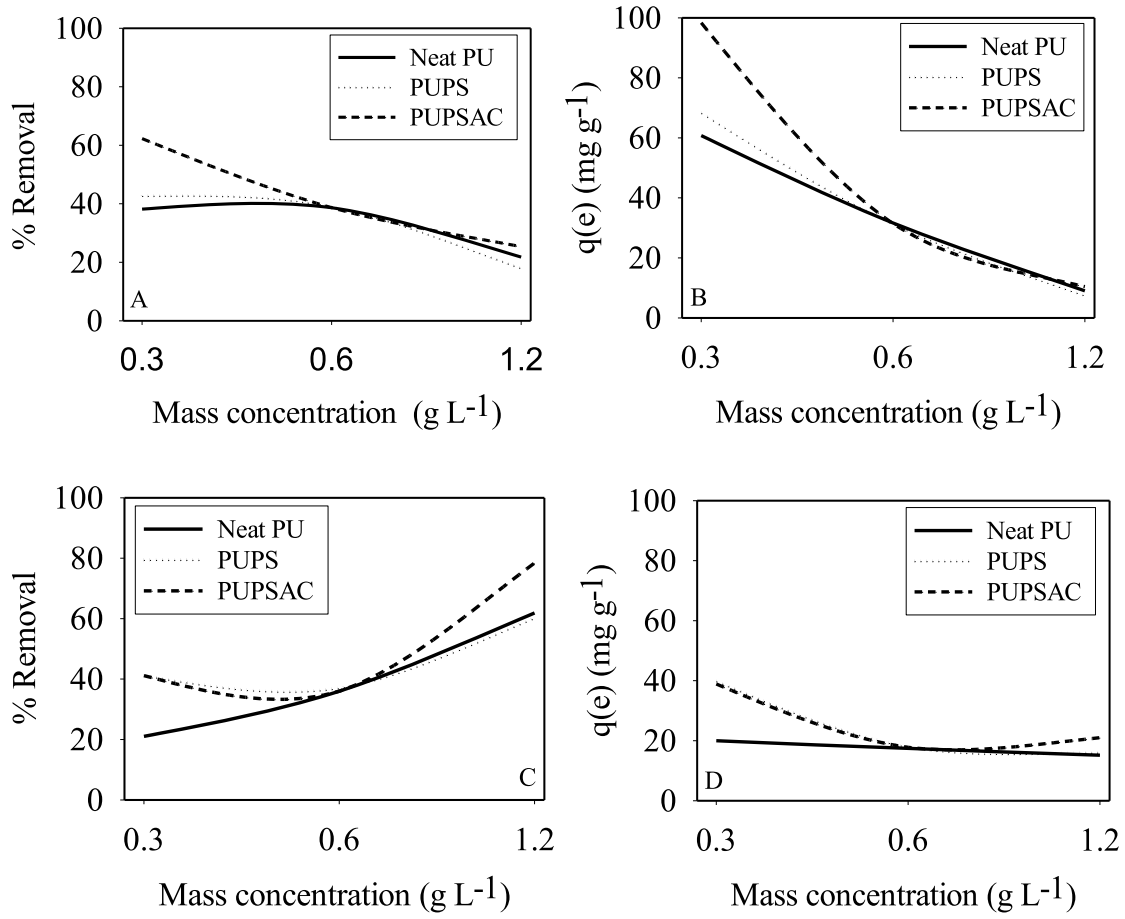

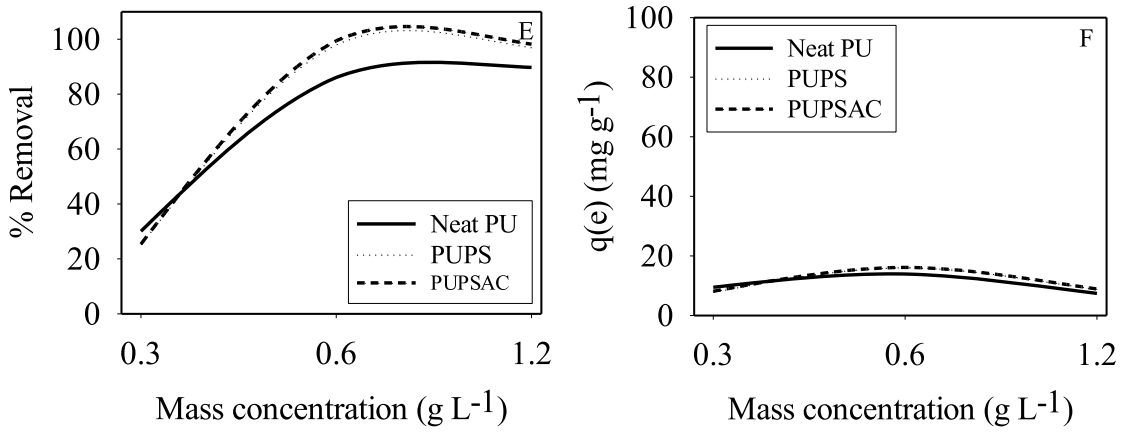

Fig. 2 - Effect of mass concentration on the removal of Cr(III) from solution using PUF; C_o = 50 mg L^{-1} (Cr III) (A and B); C_o = 30 mg L^{-1} (Cr III) (C and D); C_o = 10 mg L^{-1} (Cr III) (E and F); pH 6.5; 200 rpm and 25 ºC.

3.3 Effect of initial adsorbate concentrations

The effect of initial adsorbate concentration, in the range of 10-50 mg L^{-1}, on the adsorption of Cr(III) on foams was studied. The result showed that Cr(III) removal depends significantly on the initial Cr(III) concentration (Fig. 3). When the initial concentration of Cr(III) increased the remaining concentration of Cr(III) in the aqueous solution increased for all materials. This behavior is credited to the greater driving force resulting from a higher concentration gradient at elevated Cr(III) concentration levels (Lima et al., 2015a).

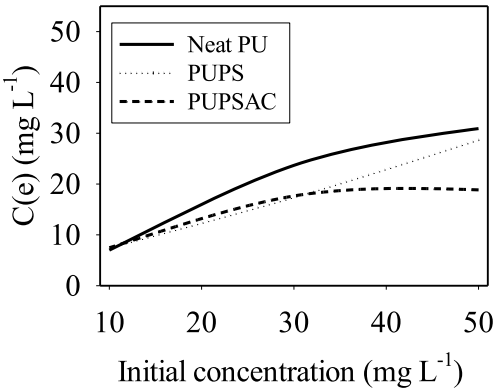

Fig. 3 - Effect of initial solution concentration on equilibrium concentration of Cr(III) from solution using PUF; 200 rpm; room temperature (25 ºC); mass concentration 0.3 g L^{-1}; pH 6.5.

3.4 Adsorption kinetics

The kinetics of adsorption of the Cr(III) was evaluated using nonlinear fit and theoretical models, including pseudo-first order, pseudo-second order, and Elovich (Table 2).

Table 2 - The adsorption kinetic model parameters for Cr(III) adsorption at experimental conditions: initial Cr(III) concentration: 50 mg L^{-1} ; pH 6.5; mass concentration of 0.3 to 1.2 g L^{-1}; 25 °C.

Model	Parameters	Neat PU*			PUPS**			PUPSAC***		
		Mass concentration (g)								
		0.3	0.6	1.2	0.3	0.6	1.2	0.3	0.6	1.2
Pseudo 1st order	q_t (mg g^{-1})	21.58	28.20	8.03	77.67	29.01	5.97	95.71	29.38	9.63
	k_1 (min^{-1})	0.12	0.07	0.14	0.003	0.08	0.09	0.01	0.08	0.06
	MRE(%)	2.87	6.46	1.25	11.96	6.02	0.72	9.59	7.38	1.18
	R^2	0.95	0.93	0.77	0.98	0.94	0.81	0.94	0.92	0.88
Pseudo 2nd order	q_t (mg g^{-1})	22.70	29.69	8.30	111.76	29.92	6.25	103.31	30.60	10.13
	k_2 (g mg^{-1} min^{-1})	0.01	0.004	0.03	0.00002	0.004	0.02	0.0002	0.004	0.01
	MRE(%)	2.23	2.37	0.84	10.60	2.95	0.52	6.28	2.53	0.73
	R^2	0.96	0.98	0.85	0.98	0.97	0.86	0.96	0.97	0.93
Elovich	a (mg g^{-1} min^{-1})	85.45	34.54	165.70	0.26	52.87	10.75	3.97	59.11	6.29
	b (g mg^{-1})	0.39	0.28	1.36	0.03	0.30	1.37	0.05	0.29	0.75
	MRE(%)	3.18	2.15	0.43	9.32	2.64	0.31	2.28	1.21	0.48
	R^2	0.94	0.98	0.92	0.99	0.98	0.92	0.99	0.99	0.95

* Neat PU (Neat Polyurethane), **PUPS (Polyurethane Peach Stone), *** PUPSAC (Polyurethane Peach Stone Activated Carbon)

Based on Table 2, it is possible to see that the experimental kinetic data were suitably fitted by the Elovich kinetic model, which displayed low MRE values and high R^2 values (close to 1), for all foam adsorbents. The pseudo-first and second-order kinetic models were not suitably fitted, and for this reason, these fittings were not presented in Figure 4.

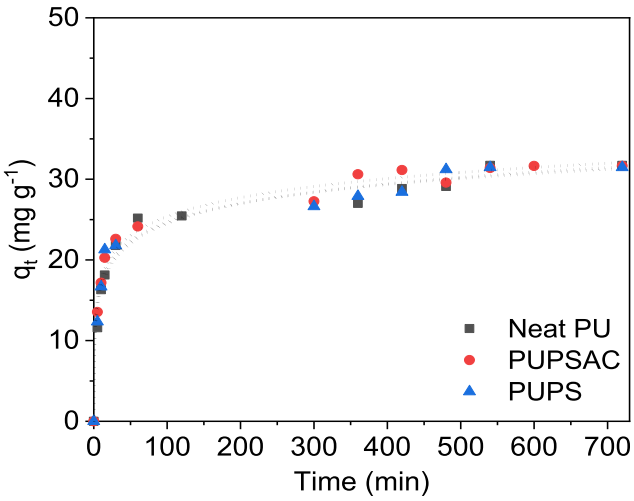

Fig. 4 – Kinetic adsorption curves for Cr(III) onto Neat PU, PUPS and PUPSAC. Experimental conditions: Co of 50 mg L^{-1}; 0.6 g L^{-1} of adsorbent, pH = 6.5, and temperature of 25 °C. The dot line is a plot representing the Elovich fitting**.**

The Elovich equation has been satisfactorily used for some chemisorption processes (Lima et al., 2015). The best fit of the experimental kinetic data by this model suggests that the adsorption systems tested here are probably governed by a chemisorption process, especially those that used PUPS and PUPSAC for removing Cr(III) from water solutions. This process includes electron exchange, ion exchange, the formation of chemical complexes, and electron sharing (Li et al., 2018). Although the Elovich kinetic model has nonuniform activation energy, it is often used to explain chemisorption and multiphase interactions and shows strong evidence for foam surface heterogeneity during adsorption (Çapan et al., 2023; Shahryari et al., 2022; Wang et al., 2023).

The times required to achieve the equilibrium were 360 min (PUPS) 480 (PUPS) min, and 540 min (Neat PU). Thus, the equilibrium time decreases with the activation of the peach stone.

3.5 Adsorption isotherms

The experimental isotherm data were analyzed using seven isotherm models: Langmuir, Freundlich, Toth, Redlich–Peterson (R-P), Khan, Sips, and Dubinin-Radushkevich. The adsorption isotherms of the foams are presented in Table 3.

Table 3 – The constants of each isotherm model, correlation coefficients (R^2), mean relative error (MRE) of PUF at experimental conditions: pH: 6.5; mass concentration 1.2 g L^{-1} of adsorbents

Model	Parameters	Temperature								
		25 °C			35 °C			45 °C		
		Neat PU*	PUPS**	PUPSAC***	Neat PU	PUPS	PUPSAC	Neat PU	PUPS	PUPSAC
Langmuir	K_L	0.01	0.02	0.01	0.01	0.01	0.003	0.02	0.003	0.001
	q_m	8.39	7.52	13.51	9.41	8.76	19.73	5.99	34.26	123.54
	R^2	0.97	0.89	0.97	0.97	0.99	0.99	0.90	0.98	0.99
	MRE (%)	6.31	24.73	14.34	3.26	2.92	1.17	16.03	7.35	2.89
Freundlich	1/n	0.73	0.60	0.70	0.09	0.02	0.04	0.27	0.06	0.06
	K_F	0.18	0.32	0.32	0.86	1.36	1.17	0.63	1.16	1.06
	R^2	0.93	0.86	0.94	0.97	0.99	0.99	0.88	0.99	0.99
	MRE (%)	11.42	26.23	27.69	5.22	1.24	0.86	28.17	5.55	2.98
Toth	a_T	16.99	1.48	26.59	24.74	0.01	0.02	15.81	0.02	0.02
	K_T	0.01	0.09	0.01	0.01	1.28E-4	2.28E-4	0.02	1.74E-4	3.10E-4
	t	2.20	0.59	1.99	5.32	1.19E-5	2.51E-5	2.31	1.72E-5	4.56
	R^2	0.98	0.89	0.98	0.99	0.97	0.99	0.92	0.98	0.99
	MRE (%)	4.74	26.00	10.97	1.73	9.03	3.94	20.00	12.40	3.61

Redlich–Peterson	K_R	0.08	0.23	0.12	0.06	0.08	0.09	0.10	0.11	0.08
	a_R	4.36E-5	0.248	9.56E-5	8.47E-11	59.37	5.50	6.43E-5	0.01	2672.09
	β	2.20	0.59	1.99	5.31	-1.45	-0.88	2.31	-67.73	-3.99
	R^2	0.98	0.89	0.98	0.99	0.99	0.99	0.93	0.98	0.99
	MRE (%)	4.74	26.00	10.97	1.73	0.55	0.78	20.00	12.37	1.75
Khan	q_S	11209.35	1.04	15997.65	2718.73	0.008	0.009	20855.41	0.008	0.008
	b_K	8.505E-6	0.196	9.33E-5	2.60E-5	8.29	9.04	5.99E-6	12.84	8.99
	a_K	950.47	0.46	813.74	244.48	1.00E-16	1.00E-16	2166.02	5.37E-18	1.00E-16
	R^2	0.97	0.88	0.977	0.97	0.97	0.99	0.92	0.98	0.99
	MRE (%)	5.87	26.07	13.09	3.69	9.03	3.94	22.90	12.40	3.61
Sips	q_m	4.29	12.82	7.428	3.29	10.58	39.24	3.40	14.66	10.15
	K_L	0.002	0.017	0.002	8.13E-4	3.69E-4	0.002	7.20E-6	0.001	7.57E-4
	n_s	1.89	0.77	1.80	2.18	1.82	1.44	4.26	1.60	1.27
	R^2	0.99	0.89	0.99	0.99	0.99	0.99	0.99	0.99	0.99
	MRE (%)	1.62	25.84	4.42	0.26	0.43	0.85	1.00	2.28	1.73
D-R	q_m	3.43	2.95	5.63	0.74	0.49	1.04	1.86	1.21	1.09
	β	3.67E-5	1.17E-5	4.17E-5	3.04E-7	8.41E-7	1.04E-7	1.67E-6	1.14E-6	1.49E-6
	E	116.79	206.92	109.56	1282.77	770.99	2192.76	547.91	661.13	577.96
	R^2	0.97	0.75	0.98	0.58	0.20	0.24	0.85	0.40	0.50
	MRE (%)	0.88	1.89	0.35	30.37	54.34	31.31	5.04	27.62	17.81

*Neat PU (Neat Polyurethane), **PUPS (Polyurethane Peach Stone), ***PUPSAC (Polyurethane Peach Stone Activated Carbon)

The correlation coefficients and MER presented in Table 3 and Fig. 5 indicate that the Sips model is more reasonable to fit the adsorption data under the studied concentration range. The Sips model consists of the combination of the Langmuir and Freundlich isotherm models. It shows the monolayer adsorption characteristic of Langmuir isotherm at high adsorbate concentration and reduces to Freundlich isotherm at low adsorbate concentration (Xia et al., 2021).

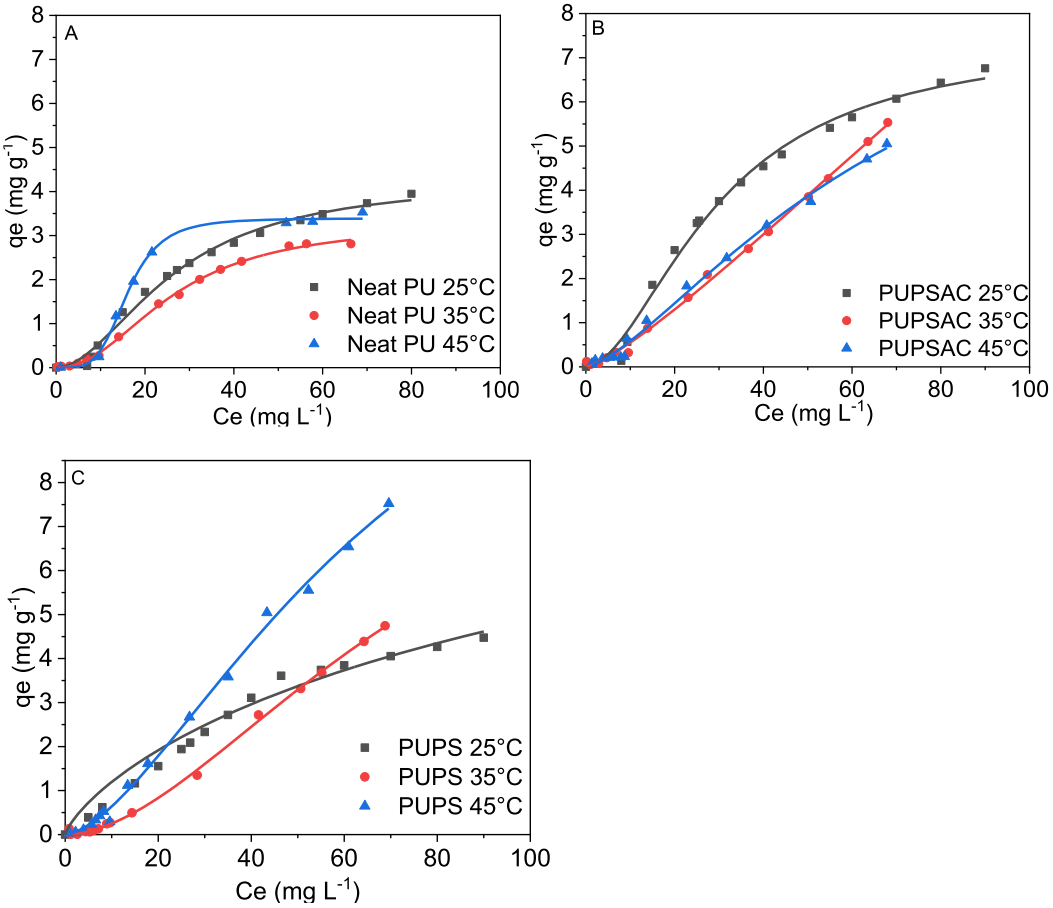

Fig. 5 – Adsorption isotherms of Cr(III) onto (A) Neat PU, (B) PUPSAC, and PUPS (between 25 and 45 °C). Mass concentration was 1.2 g L^{-1}; and pH of the solution was adjusted to pH 6.5. The continuous line is a plot of Sips model.

Observing the values of n_s in the sips model, it is noted that at temperatures above 25°C this parameter moves away from 1 for the adsorption by Neat PU, that is, the model moves away from the Langmuir model and approaches the model of Freundlich, who considers the surface to be heterogeneous. This may have occurred due to changes in the functional structure of the foam. However, for PUPS and PUPSAC, values of n_s approach 1 with increasing temperature, this could also have occurred due to changes in the functional or porous structure

of both the activated carbon foam and the peach stone foam. It is found that the adsorption of foams correlates much well with the Sips isotherm as compared to other isotherm models.

3.6 Thermodynamic parameters

Table 4 shows the estimated thermodynamic parameters; change in enthalpy (ΔH°), entropy (ΔS°), and change in free Gibbs energy (ΔG°) for the adsorption of Cr(III) onto foams. The negative (ΔH°) values for Neat PU indicated that the adsorption was exothermic in nature. Although, positive (ΔH°) values for PUPS and PUPSAC indicated that the adsorption was endothermic (Allahkarami et al., 2023). Additionally, by estimating the enthalpy of adsorption (ΔH°) between the adsorbates and Cr(III) ions, it is possible to determine whether the adsorption is chemisorption or physisorption (Lima et al., 2021). Physisorption typically exhibits a small ΔH° value (<20 kJ mol^{-1}) (de Azevedo et al., 2023). Since for adsorbents, the values of ΔH° > 20 kJ mol^{-1}, indicate that the interactions between Cr(III) and PUPS and PUPSAC are characterized by the magnitude of chemical processes. On the other hand, the interactions between Cr(III) and Neat PU are characterized by physical adsorption.

Table 4 - Thermodynamic parameters

Material	ΔH° ($kJmol^{-1}$)	ΔS° ($Jmol^{-1}K^{-1}$)	ΔG° ($kJmol^{-1}$)		
			25 °C	35°C	45°C
Neat PU	-12.71	-136.22	40.58	41.94	43.31
PUPS	31.19	118.40	-35.25	-36.44	-37.62
PUPSAC	54.84	176.20	-52.45	-54.22	-55.98

The positive standard entropy change (ΔS°) signified the increasing randomness at the solid–liquid interface, which might be explained through the concept of desorption of pre-adsorbed water surrounding the (PUPS and PUPSAC) interface in an aqueous suspension (Barshad, 1959; Rusmin et al., 2022). As the Cr(III) ions were adsorbed on the active sites, the pre-adsorbed water was displaced to accommodate Cr(III). Thus, the desorbed water molecules from the pre-adsorbed state to a free state increased the randomness in the system (Rusmin et al., 2022).

The ΔS° is positive, also indicating that the foams as fillers have great affinity for the adsorbent, and the degree of dispersion increases with an increase in temperature. This also explains the increasing randomness at the solution/adsorbent interface during the adsorption process (Bai et al., 2020).

The negative ΔG° values confirmed that the adsorption was spontaneous in nature and energetically favorable. On the other hand, the ΔG° became more negative at high temperatures onto PUPS and PUPSAC, which indicated that the adsorption was more spontaneous with temperature increase.

4 Conclusions

In this study, PUF showed adequate capacity for adsorbing Cr(III) in aqueous solution. The experimental equilibrium data satisfactorily fit the Sips model. The thermodynamic study indicated that the adsorption process of the Cr(III) is exothermic and the interactions between foams with fillers (peach stone and peach stone activated carbons) occurred spontaneously at the investigated temperatures. The results show that the addition of fillers in polyurethane foams favored the adsorption of Cr(III).

Thus, the present study has proved that PUF could be used as an efficient adsorbent for the removal of Cr(III) from aqueous solution. Moreover, the use of filled PUF as an adsorbent not only solves environmental pollution but also reduces the amount of agricultural by-products and decreases the overall cost of wastewater treatment.

References

Afonso, T.F., Demarco, C.F., Schoeler, G.P., Giongo, J.L., de Almeida Vaucher, R., Sant'Anna Cadaval, T.R., Pieniz, S., de Avila Delucis, R., Andreazza, R., 2023. Polyurethane foams incorporated with different fillers to remove SARS-CoV-2 from water. Journal of Water Process Engineering 54, 104000. https://doi.org/10.1016/j.jwpe.2023.104000

Akçakal, Ö., Şahin, M., Erdem, M., 2019. Synthesis and characterization of high-quality activated carbons from hard-shelled agricultural wastes mixture by zinc chloride activation. Chem Eng Commun 206, 888–897. https://doi.org/10.1080/00986445.2018.1534231

Allahkarami, E., Dehghan Monfared, A., Silva, L.F.O., Dotto, G.L., 2023. Toward a mechanistic understanding of adsorption behavior of phenol onto a novel activated carbon composite. Sci Rep 13, 167. https://doi.org/10.1038/s41598-023-27507-5

Ashok Kumar, S.S., Bashir, S., Pershaanaa, M., Kamarulazam, F., Saidi, N.M., Goh, Z.L., Ma, I.A.W., Kunjunee, V., Jamaluddin, A., Ramesh, K., Ramesh, S., Ramesh, S., Manikam, R., 2023. A review on the recent progress of the plant-based porous carbon materials as electrodes for high-performance supercapacitors. J Mater Sci 58, 6516–6555. https://doi.org/10.1007/s10853-023-08413-7

Aslam, Awais Ali, Hassan, S.U., Saeed, M.H., Kokab, O., Ali, Z., Nazir, M.S., Siddiqi, W., Aslam, Aamir Ali, 2023. Cellulose-based adsorbent materials for water remediation: Harnessing their potential in heavy metals and dyes removal. J Clean Prod 421, 138555. https://doi.org/10.1016/j.jclepro.2023.138555

ASTM D2854-96, 2004. Standard Test Method For Apparent Density Of Activated Carbon. ASTM Committee on Standards, Philadelphia.

Bachmann, S.A.L., Dávila, I.V.J., Calvete, T., Féris, L.A., 2022. Adsorption of Cr (VI) on lignocellulosic wastes adsorbents: an overview and further perspective. International Journal of Environmental Science and Technology 19, 12727–12748. https://doi.org/10.1007/s13762-022-03928-z

Bai, C., Wang, L., Zhu, Z., 2020. Adsorption of Cr(III) and Pb(II) by graphene oxide/alginate hydrogel membrane: Characterization, adsorption kinetics, isotherm and thermodynamics studies. Int J Biol Macromol 147, 898–910. https://doi.org/10.1016/j.ijbiomac.2019.09.249

Bandara, P.C., Peña-Bahamonde, J., Rodrigues, D.F., 2020. Redox mechanisms of conversion of Cr(VI) to Cr(III) by graphene oxide-polymer composite. Sci Rep 10, 9237. https://doi.org/10.1038/s41598-020-65534-8

Barrett, E.P., Joyner, L.G., Halenda, P.P., 1951. The Determination of Pore Volume and Area Distributions in Porous Substances. I. Computations from Nitrogen Isotherms. J Am Chem Soc 73, 373–380. https://doi.org/10.1021/ja01145a126

Barshad, I., 1959. Thermodynamics of Water Adsorption and Desorption on Montmorillonite. Clays Clay Miner 8, 84–101. https://doi.org/10.1346/CCMN.1959.0080110

Bekchanov, D., Mukhamediev, M., Yarmanov, S., Lieberzeit, P., Mujahid, A., 2024. Functionalizing natural polymers to develop green adsorbents for wastewater treatment applications. Carbohydr Polym 323, 121397. https://doi.org/10.1016/j.carbpol.2023.121397

Brunauer, S., Emmett, P.H., Teller, E., 1938. Adsorption of Gases in Multimolecular Layers. J Am Chem Soc 60, 309–319. https://doi.org/10.1021/ja01269a023

Çapan, R., Çapan, İ., Davis, F., 2023. A new approach for the adsorption kinetics using surface plasmon resonance results. Sens Actuators B Chem 134463. https://doi.org/10.1016/j.snb.2023.134463

Chen, J.H., Li, G.P., Liu, Q.L., Ni, J.C., Wu, W.B., Lin, J.M., 2010. Cr(III) ionic imprinted polyvinyl alcohol/sodium alginate (PVA/SA) porous composite membranes for selective adsorption of Cr(III) ions. Chemical Engineering Journal 165, 465–473. https://doi.org/10.1016/j.cej.2010.09.034

Chen, X., Hossain, M.F., Duan, C., Lu, J., Tsang, Y.F., Islam, M.S., Zhou, Y., 2022. Isotherm models for adsorption of heavy metals from water - A review. Chemosphere 307, 135545. https://doi.org/10.1016/j.chemosphere.2022.135545

de Azevedo, C.F., Rodrigues, D.L.C., Silveira, L.L., Lima, E.C., Osorio, A.G., Andreazza, R., de Pereira, C.M.P., Poletti, T., Machado Machado, F., 2023. Comprehensive adsorption and spectroscopic studies on the interaction of magnetic biochar from black wattle sawdust with beta-blocker metoprolol. Bioresour Technol 388, 129708. https://doi.org/10.1016/j.biortech.2023.129708

Delucis, R. de A., Magalhães, W.L.E., Petzhold, C.L., Amico, S.C., 2018. Thermal and combustion features of rigid polyurethane biofoams filled with four forest-based wastes. Polym Compos 39, E1770–E1777. https://doi.org/https://doi.org/10.1002/pc.24784

Dubinin, M.M., Radushkevich, L.V., 1947. Equation of the characteristic curve of activated charcoal. Proc. Acad. Sci. Phys. Chem, USSR.

Elgarahy, A.M., Eloffy, M.G., Guibal, E., Alghamdi, H.M., Elwakeel, K.Z., 2023. Use of biopolymers in wastewater treatment: A brief review of current trends and prospects. Chin J Chem Eng. https://doi.org/10.1016/j.cjche.2023.05.018

EPA, 1990. Environmental pollution alternatives. EPA/625/5-90/025, EPA/625/4-89/023. Cincinnati, US.

Farage, R.M.P., Quina, M.J., Gando-Ferreira, L., Silva, C.M., de Souza, J.J.L.L., Torres, C.M.M.E., 2020. Kraft pulp mill dregs and grits as permeable reactive barrier for removal of copper and sulfate in acid mine drainage. Sci Rep 10, 4083. https://doi.org/10.1038/s41598-020-60780-2

Farooqi, Z.H., Akram, M.W., Begum, R., Wu, W., Irfan, A., 2021. Inorganic nanoparticles for reduction of hexavalent chromium: Physicochemical aspects. J Hazard Mater 402, 123535. https://doi.org/10.1016/j.jhazmat.2020.123535

Freundlich, H.M.F., 1906. Over the Adsorption in Solution. J Phys Chem 57, 385–471.

Islam, Md.M., Mohana, A.A., Rahman, Md.A., Rahman, M., Naidu, R., Rahman, M.M., 2023. A Comprehensive Review of the Current Progress of Chromium Removal Methods from Aqueous Solution. Toxics 11, 252. https://doi.org/10.3390/toxics11030252

Jagemma, M., Worku, H., Gemeda, F.T., Gemeda, B.S., 2023. Variability in space effects of industrial wastewater on river physicochemical characteristics in a sample of towns of Oromia. International Journal of Environmental Science and Technology 20, 13299–13306. https://doi.org/10.1007/s13762-023-04874-0

Jalalah, M., Han, H., Mahadani, M., Nayak, A.K., Harraz, F.A., 2023. Novel interconnected hierarchical porous carbon derived from biomass for enhanced supercapacitor application. Journal of Electroanalytical Chemistry 935, 117355. https://doi.org/10.1016/j.jelechem.2023.117355

Jamsaz, A., Goharshadi, E.K., Barras, A., Ifires, M., Szunerits, S., Boukherroub, R., 2021. Magnetically driven superhydrophobic/superoleophilic graphene-based polyurethane sponge for highly efficient oil/water separation and demulsification. Sep Purif Technol 274, 118931. https://doi.org/10.1016/j.seppur.2021.118931

Kanwar, V.S., Sharma, A., Srivastav, A.L., Rani, L., 2020. Phytoremediation of toxic metals present in soil and water environment: a critical review. Environmental Science and Pollution Research 27, 44835–44860. https://doi.org/10.1007/s11356-020-10713-3

Karthik, V., Dhivya Dharshini, G., Senthil Kumar, P., Kiruthika, S., Rangasamy, G., Periyasamy, S., Senthil Rathi, B., 2023. Ferrite-Supported Nanocomposite Polymers for Emerging Organic and Inorganic Pollutants Removal from Wastewater: A Review. Ind Eng Chem Res. https://doi.org/10.1021/acs.iecr.3c01701

Khan, A.R., Ataullah, R., Al-Haddad, A., 1997. Equilibrium Adsorption Studies of Some Aromatic Pollutants from Dilute Aqueous Solutions on Activated Carbon at Different Temperatures. J Colloid Interface Sci 194, 154–165. https://doi.org/10.1006/jcis.1997.5041

Langmuir, I., 1916. THE CONSTITUTION AND FUNDAMENTAL PROPERTIES OF SOLIDS AND LIQUIDS. PART I. SOLIDS. J Am Chem Soc 38, 2221–2295. https://doi.org/10.1021/ja02268a002

Li, S., Huang, L., Wang, D., Zhou, S., Sun, X., Zhao, R., Wang, G., Yao, T., Zhao, K., Chen, R., 2023. A review of 3D superhydrophilic porous materials for oil/water separation. Sep Purif Technol 326, 124847. https://doi.org/10.1016/j.seppur.2023.124847

Li, Z., Wang, L., Meng, J., Liu, X., Xu, J., Wang, F., Brookes, P., 2018. Zeolite-supported nanoscale zero-valent iron: New findings on simultaneous adsorption of Cd(II), Pb(II), and As(III) in aqueous solution and soil. J Hazard Mater 344, 1–11. https://doi.org/10.1016/j.jhazmat.2017.09.036

Lima, É.C., Adebayo, M.A., Machado, F.M., 2015a. Experimental Adsorption. pp. 71–84. https://doi.org/10.1007/978-3-319-18875-1_4

Lima, É.C., Adebayo, M.A., Machado, F.M., 2015b. Kinetic and Equilibrium Models of Adsorption. pp. 33–69. https://doi.org/10.1007/978-3-319-18875-1_3

Lima, E.C., Hosseini-Bandegharaei, A., Moreno-Piraján, J.C., Anastopoulos, I., 2019. A critical review of the estimation of the thermodynamic parameters on adsorption equilibria. Wrong

use of equilibrium constant in the Van't Hoof equation for calculation of thermodynamic parameters of adsorption. J Mol Liq 273, 425–434. https://doi.org/10.1016/j.molliq.2018.10.048

Nag, S., Mondal, A., Roy, D.N., Bar, N., Das, S.K., 2018. Sustainable bioremediation of Cd(II) from aqueous solution using natural waste materials: Kinetics, equilibrium, thermodynamics, toxicity studies and GA-ANN hybrid modelling. Environ Technol Innov 11, 83–104. https://doi.org/10.1016/j.eti.2018.04.009

Nayeem, A., Ali, M.F., Shariffuddin, J.H., 2023. The recent development of inverse vulcanized polysulfide as an alternative adsorbent for heavy metal removal in wastewater. Environ Res 216, 114306. https://doi.org/10.1016/j.envres.2022.114306

Olalekan A.P, Dada A. O, Okewale A.O, 2013. Comparative Adsorption Isotherm Study of the Removal of Pb2+ and Zn2+ Onto Agricultural Waste. Res J Chem Environ Sci 1, 22–27.

Olawale, S.A., Bonilla-Petriciolet, A., Mendoza-Castillo, D.I., Okafor, C.C., Sellaoui, L., Badawi, M., 2022. Thermodynamics and Mechanism of the Adsorption of Heavy Metal Ions on Keratin Biomasses for Wastewater Detoxification. Adsorption Science & Technology 2022, 1–13. https://doi.org/10.1155/2022/7384924

Parlayıcı, Ş., 2019. Modified peach stone shell powder for the removal of Cr (VI) from aqueous solution: synthesis, kinetic, thermodynamic, and modeling study. Int J Phytoremediation 21, 590–599. https://doi.org/10.1080/15226514.2018.1540541

Prasad, S., Yadav, K.K., Kumar, S., Gupta, N., Cabral-Pinto, M.M.S., Rezania, S., Radwan, N., Alam, J., 2021. Chromium contamination and effect on environmental health and its remediation: A sustainable approaches. J Environ Manage 285, 112174. https://doi.org/10.1016/J.JENVMAN.2021.112174

Redlich, O., Peterson, D.L., 1959. A Useful Adsorption Isotherm. J Phys Chem 63, 1024–1024. https://doi.org/10.1021/j150576a611

Rusmin, R., Sarkar, B., Mukhopadhyay, R., Tsuzuki, T., Liu, Y., Naidu, R., 2022. Facile one pot preparation of magnetic chitosan-palygorskite nanocomposite for efficient removal of lead from water. J Colloid Interface Sci 608, 575–587. https://doi.org/https://doi.org/10.1016/j.jcis.2021.09.109

Sasidharan, A.P., Meera, V., Raphael, V.P., 2021. Investigations on characteristics of polyurethane foam impregnated with nanochitosan and nanosilver/silver oxide and its effectiveness in phosphate removal. Environmental Science and Pollution Research 28, 12980–12992. https://doi.org/10.1007/s11356-020-11257-2

Shah, S.W.A., Xu, Q., Ullah, M.W., Zahoor, Sethupathy, S., Morales, G.M., Sun, J., Zhu, D., 2023. Lignin-based additive materials: A review of current status, challenges, and future perspectives. Addit Manuf 74, 103711. https://doi.org/10.1016/j.addma.2023.103711

Shahryari, T., Singh, P., Raizada, P., Davidyants, A., Thangavelu, L., Sivamani, S., Naseri, A., Vahidipour, F., Ivanets, A., Hosseini-Bandegharaei, A., 2022. Adsorption properties of Danthron-impregnated carbon nanotubes and their usage for solid phase extraction of heavy metal ions. Colloids Surf A Physicochem Eng Asp 641, 128528. https://doi.org/10.1016/j.colsurfa.2022.128528

Shi, M., Zheng, X., Zhang, N., Guo, Y., Liu, M., Yin, L., 2023. Overview of sixteen green analytical chemistry metrics for evaluation of the greenness of analytical methods. TrAC Trends in Analytical Chemistry 166, 117211. https://doi.org/10.1016/j.trac.2023.117211

Solis-Ceballos, A., Roy, R., Golsztajn, A., Tavares, J.R., Dumont, M.-J., 2023. Selective adsorption of Cr(III) over Cr(VI) by starch-graft-itaconic acid hydrogels. Journal of Hazardous Materials Advances 10, 100255. https://doi.org/10.1016/j.hazadv.2023.100255

Srivastava, S., Agrawal, S.B., Mondal, M.K., 2015. Biosorption isotherms and kinetics on removal of Cr(VI) using native and chemically modified Lagerstroemia speciosa bark. Ecol Eng 85, 56–66. https://doi.org/10.1016/j.ecoleng.2015.10.011

Syeda, H.I., Yap, P.-S., 2022. A review on three-dimensional cellulose-based aerogels for the removal of heavy metals from water. Science of The Total Environment 807, 150606. https://doi.org/10.1016/j.scitotenv.2021.150606

Toth, J., 1971. State equations of the solid gas interface layer. Acta Chem. Acad. Hung 69, 311–317.

Wang, C., Ma, C., Mu, C., Lin, W., 2017. Tailor-made zwitterionic polyurethane coatings: microstructure, mechanical property and their antimicrobial performance. RSC Adv 7, 27522–27529. https://doi.org/10.1039/C7RA04379A

Wang, H., Wang, Shuai, Wang, Shixing, Fu, L., Zhang, L., 2023. The one-step synthesis of a novel metal–organic frameworks for efficient and selective removal of Cr(VI) and Pb(II) from wastewater: Kinetics, thermodynamics and adsorption mechanisms. J Colloid Interface Sci 640, 230–245. https://doi.org/10.1016/j.jcis.2023.02.108

WHO, 2022. Guidelines for drinking-water quality: Fourth edition incorporating the first and second addenda, Fourth. ed. Licence: CC BY-NC-SA 3.0 IGO.

Xia, J., Gao, Y., Yu, G., 2021. Tetracycline removal from aqueous solution using zirconium-based metal-organic frameworks (Zr-MOFs) with different pore size and topology:

Adsorption isotherm, kinetic and mechanism studies. J Colloid Interface Sci 590, 495–505. https://doi.org/10.1016/j.jcis.2021.01.046

Zaimee, M.Z.A., Sarjadi, M.S., Rahman, M.L., 2021. Heavy Metals Removal from Water by Efficient Adsorbents. Water (Basel) 13, 2659. https://doi.org/10.3390/w13192659

Zhang, R., Tian, Y., 2020. Characteristics of natural biopolymers and their derivative as sorbents for chromium adsorption: a review. Journal of Leather Science and Engineering 2, 24. https://doi.org/10.1186/s42825-020-00038-9

Zhang, T., Wang, P., Li, Y., Bao, Y., Lim, T.-T., Zhan, S., 2023. Advances in dual-functional photocatalysis for simultaneous reduction of hexavalent chromium and oxidation of organics in wastewater. Environmental Functional Materials. https://doi.org/10.1016/j.efmat.2023.05.001

Zhang, Zhenjiang, Zhu, L., Zhang, Zhongwei, Sun, L., Shi, Y., Xie, L., Xu, D., Jin, J., Xue, Z., Ma, X., 2019. Synthesis of polyethyleneimine modified polyurethane foam for removal of Pb(II) ion from aqueous solution. Desalination Water Treat 160, 288–296. https://doi.org/10.5004/dwt.2019.24376

6 Artigo 3

O artigo intitulado **“Water absorption of polyurethane foam reinforced with bio-fillers”** é apresentado conforme submetido na Revista Materials Letters, ISSN: 0167-577X, fator de impacto 3, classificação A2 na área de Materiais.

Water absorption of polyurethane foam reinforced with bio-fillers

Thays França Afonso[a], Rafael de Avila Delucis[a,b], Robson Andreazza[a,b]*.

[a]Science and Engineering of Materials Postgraduate Program. Federal University of Pelotas. R. Gomes Carneiro 01, CEP 96010-610, Pelotas, RS, Brazil.
[b]Environmental Sciences Postgraduate Program. Federal University of Pelotas. R. Benjamin Constant 989, CEP 96010-020 Pelotas, RS, Brazil.
*Corresponding author: e-mail: robsonandreazza@yahoo.com.br; Phone +55 53 3921 1432; Fax +55 53 3921 1432.

Abstract
Polyurethane foams (PUF) are widely used for a variety of applications. However, there has been limited research on polyurethane foam applications focusing on water absorption due to the hydrophobic nature of polyurethane foam. In this context, this study investigated the effect of biofiller on the cellular structure and water absorption properties of PUF. Although all foams absorbed water, the foams with peach stone fillers and the biochar activated foams achieved maximum water absorption much higher than neat PU and PUCAC. The percentage was practically quadrupled in PUPSAC and doubled in PUPS compared to neat PU. In conclusion, we have demonstrated a reliable approach to water uptake in PUF composites based on biomass as a porous substrate as a modifier of polyurethane foams. Therefore, this research aims to reinforce polyurethane foam with biofillers to increase its water uptake properties, which may allow it to be used in new applications such as the adsorption of heavy metals and pathogenic microorganisms.

Keywords: Polyurethane foam. Water absorbing properties. Biochar activated. Activated Carbon. Peach Stone.

1. Introduction

Polyurethane (PU) is a type of polymer foam that is widely used in commercial applications due to its properties, low density, good thermal conductivity, and mechanical properties [1].

The reaction between polyol and isocyanate, along with catalysts and additives, generates polyurethane foam (PUF) [2]. The resulting PUF is hydrophobic and boasts several benefits, including high strength-to-weight ratio, dimension stability, and low density [3].

PU is a versatile polymer because its properties can be easily modified by the addition of fillers (bio-fillers) or by changes in the chemical composition [4].

Therefore, biomass and biochar has been considered as reinforcement to enhance this area due to its favorable physical and chemical properties [5]. For instance, porous carbon derived from various cost-effective. Biomass carbon (biochar) has recently found successful applications in pollution control, chemical separation, energy storage, and supercapacitors due to its excellent properties, such as high strength, low density, high specific surface areas, and large pore volumes [6]. As a result, biomass is hydrophilic [7]. The addition of peach stone and biochar activated into PUF may effectively enhance water absorption.

Different levels of bio-fillers may impact PUF properties variously. Another approach to changing the water-absorption properties of PUF is to modify the biopoly that replaces it [8,9]. Ideally, adding more hydrophilic content to a composite will enhance its water-absorption capabilities. However, it should be noted that previous studies have yielded inconsistent results regarding the water-absorbing properties under various filler loading conditions [8].

This research examines the effects of utilizing peach stones and biochar/carbon activated as fillers on modified PUF's cellular structure and water-absorbing properties.

2. Materials and Methods

2.1 Synthesis of PUF

The PUF was synthesized by the free expansion method. Four foams were produced, neat PU (without added fillers), modified PU of 5% by weight with added fillers of peach stone activated biochar (PUSAC), commercial activated carbon (PUCAC) and peach stone (PUPS) [10]. Samples were prepared from a one-step mixing process and allowed the foam to rise freely and settle at room temperature.

2.2 Water absorption

The water absorption of the samples was determined according to ASTM D570-98. Briefly, 2 mm plates were cut, always in triplicate. The samples were completely immersed in distilled water at room temperature (25°C). The weight of each sample was then monitored every 30 minutes until a total immersion time of 300 minutes was

reached. The samples are weighed dry at the beginning and wet after soaking. The percentage of water absorption (*Wa*) is then calculated using Eq. (1).

$$Wa\ (\%) = \ (W_f - W_i)/W_i\ x\ 100) \quad (1)$$

Where W_i is initial weight and W_f is weight after absorbed water.

2.3. Foam Morphology and Density

Surface morphology was analyzed with SEM employing a JSM 6610LV Jeol instrument set to a working voltage of 15 kV and a magnification of 100×. The density test was conducted as per the standard ASTM D1622. The density is calculated by the formula shown in Eq. (2).

$$\rho = \ m/V \quad (2)$$

Where *m* is mass and *V* is volume of the sample.

3 Results

Figure 1 shows the water absorption capacity as a function of absorption time for Neat PU and PUs with added fillers. In the first 30 minutes of immersion in water, there was a rapid increase in the water absorption behavior of all foams. After this time, the water absorption by the foams increased with the time of exposure to water up to 240 minutes, after which occurrences were generally constant.

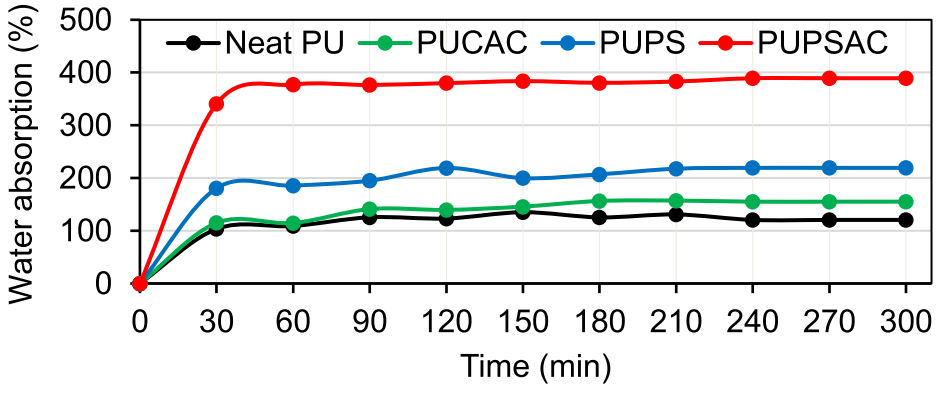

Fig. 1. Water absorption by PUFs. Neat Polyurethane, PUPS (Polyurethane Peach Stone), PUPSAC (Polyurethane Peach Stone Activated Carbon) and PUCAC (Polyurethane Commercial Activated Carbon).

Although all foams absorbed water, the foams with peach stone fillers and the peach stone activated trigger achieved maximum water absorption much higher than Neat

PU and PUCAC, the percentage practically quadrupled applied in PUPSAC and doubled to PUPS when compared to Neat PU.

The main factors justifying the increase in water absorption by the foams were the type of polyol (castor oil), the types of fillers, the size of the pores and the hydrophilic nature of the materials. Such polyol naturally favors solubility in water due to the presence of hydroxyl on carbon 12 of the lipophilic chain [11,12]. Furthermore, water diffusion is determined by the microstructure of the material and the affinity of the polymeric components for water [13]. Thus, the foam (Neat PU) showed greater resistance to water diffusion, in the water absorption process, when compared to foams that had fillers added.

Another factor that influenced the high percentages of water absorption in polyurethane foams with addition was the size of the particles. Particles with a large surface area ensure that more hydroxyls are available to interact with water molecules [8]. Therefore, the activation of peach stone biomass enhanced the water absorption process. Another factor that favored such water absorption refers to the chemical composition (lignocellulosic) of the fillers, which has a hydrophilic character [14]. Therefore, the percentage of water absorbed by the foams (PUPS and PUPSAC, PUCAC) increased. Such results can be considered favorable for the application of foams in adsorption processes.

The SEM images shown in Figure 1 indicate that all fillers are well dispersed into the PUF cell structure since no agglomerates are found. In addition, there are no noticeable signs of cell disruptions associated with the filler insertion, which indicates a good between matrix interaction and fillers.

However, the PUFs presented a clearly uneven cell morphology, which is probably related to the hydrophilic nature of the fillers [15]. The filler acts as a nucleating agent for the formation of pores, so a greater number of cells occur at the same time, reducing the availability of gas, affecting cell expansion and consequently favoring the formation of smaller pores [11].

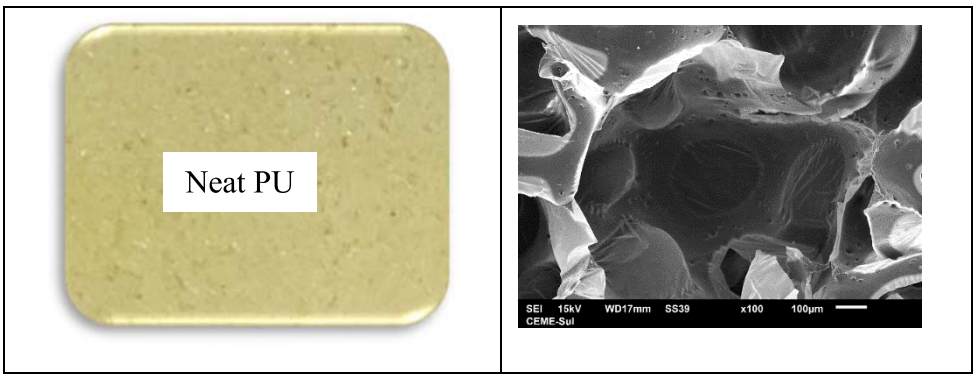

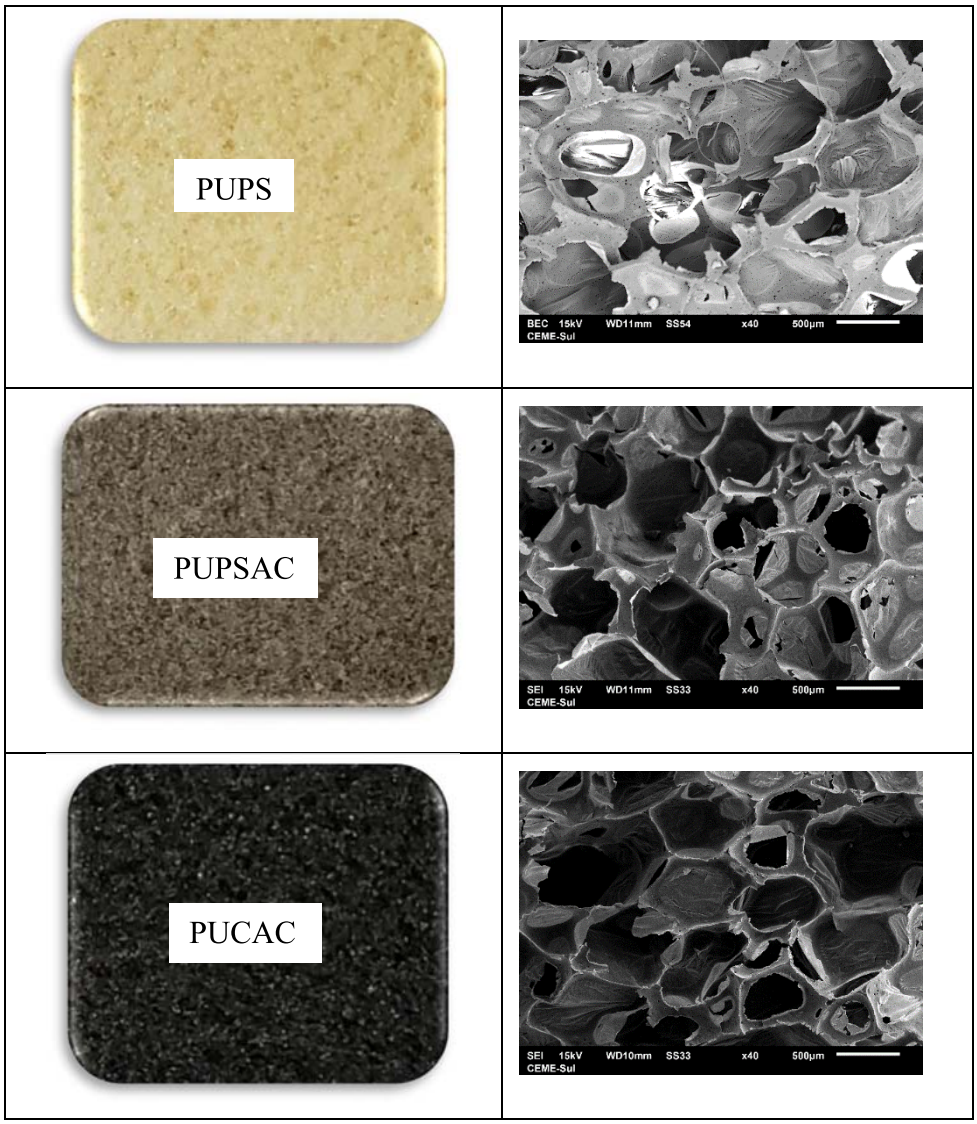

Fig. 2. SEM images of the studied PUFs. Neat Polyurethane, PUPS (Polyurethane Peach Stone), PUPSAC (Polyurethane Peach Stone Activated Carbon) and PUCAC (Polyurethane Commercial Activated Carbon).

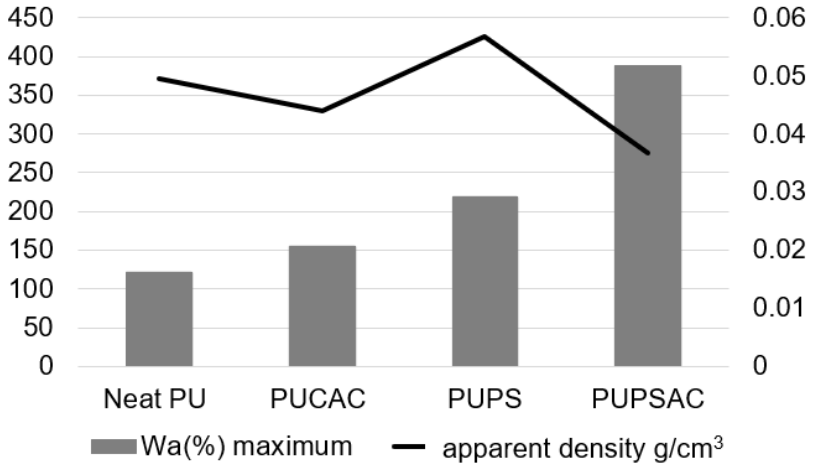

Fig. 3. Apparent density and maximum water absorption capacity of the PUFs

Apparent density plays an essential role in many industrial applications. It is an indirect measure of void content, and the greater the void content, the greater the gas content and the greater the insulation properties [15]. Furthermore, as shown in Figures 2 and 3, the volume of open pores directly reflected the water absorption capacity. As for apparent density, the addition of charges to the PUF prevents apparent density in all PUFs except PUPS when compared to Neat PU. The increase in PUPS apparent density represents the compatibility between the filler and the PUF matrix [15]. Furthermore, the increase in apparent density represents good polymer formation, however, as cells formed due to the insertion of a filler do not always lead to increases in apparent density [15].

4 Conclusions

In conclusion, it was demonstrated that a reliable approach to the uptake of water in PUF composite with bio-fillers. On this route, the bio-fillers were favorable for water uptake due to their hydrophilicity.

The water absorption properties of PUF increased by the introduction of bio-fillers due to the increased volume of empty pores in PUF. The addition of bio-filles in PUFs reduced the apparent density. However, for PUPS, the apparent density is shown to have a slight increase due to compatibility with the polymer matrix.

With the sustainable and environmental merits of the preparation procedure and the water uptake capacitated of PUF composites, it can be a potential candidate for practical application in adsorption.

References

[1] M. Ates, S. Karadag, A.A. Eker, B. Eker, Polyurethane foam materials and their industrial applications, Polym Int. 71 (2022) 1157–1163. https://doi.org/10.1002/pi.6441.

[2] F.M. de Souza, P.K. Kahol, R.K. Gupta, Introduction to Polyurethane Chemistry, in: 2021: pp. 1–24. https://doi.org/10.1021/bk-2021-1380.ch001.

[3] J. Joy, J. Abraham, J. Sunny, J. Mathew, S.C. George, Hydrophobic, super absorbing materials from reduced graphene oxide/MoS2 polyurethane foam as a promising sorbent for oil and organic solvents, Polym Test. 87 (2020) 106429. https://doi.org/10.1016/j.polymertesting.2020.106429.

[4] S. Gupta, S. Sharma, P. Sharma, A.K. Nadda, P. Raizada, P. Singh, CO2-philic adsorbents: an overview, in: CO2-Philic Polymers, Nanocomposites and Chemical Solvents, Elsevier, 2023: pp. 1–15. https://doi.org/10.1016/B978-0-323-85777-2.00016-0.

[5] M. Afraz, F. Muhammad, J. Nisar, A. Shah, S. Munir, G. Ali, A. Ahmad, Production of value-added products from biomass waste by pyrolysis: An updated review, Waste Management Bulletin. 1 (2024) 30–40. https://doi.org/10.1016/j.wmb.2023.08.004.

[6] A. Alsulaili, K. Elsayed, A. Refaie, Utilization of agriculture waste materials as sustainable adsorbents for heavy metal removal: A comprehensive review, Journal of Engineering Research. (2023). https://doi.org/10.1016/j.jer.2023.09.018.

[7] D. Peng, W. Li, X. Liang, L. Zheng, X. Guo, Enzymatic preparation of hydrophobic biomass with one-pot synthesis and the oil removal performance, Journal of Environmental Sciences. 124 (2023) 105–116. https://doi.org/10.1016/j.jes.2021.10.019.
[8] M.F. Anwar, L.J. Yu, Y.M. Lim, M.A. Tarawneh, E.N. Se Yong, N.Y.G. Lai, Water absorption properties of polyurethane foam reinforced with paper pulp, Mater Today Proc. (2023). https://doi.org/10.1016/j.matpr.2022.12.156.
[9] A.M. Radzi, S.M. Sapuan, M. Jawaid, M.R. Mansor, Water absorption, thickness swelling and thermal properties of roselle/sugar palm fibre reinforced thermoplastic polyurethane hybrid composites, Journal of Materials Research and Technology. 8 (2019) 3988–3994. https://doi.org/10.1016/j.jmrt.2019.07.007.
[10] T.F. Afonso, C.F. Demarco, G.P. Schoeler, J.L. Giongo, R. de Almeida Vaucher, T.R. Sant'Anna Cadaval, S. Pieniz, R. de Avila Delucis, R. Andreazza, Polyurethane foams incorporated with different fillers to remove SARS-CoV-2 from water, Journal of Water Process Engineering. 54 (2023) 104000. https://doi.org/10.1016/j.jwpe.2023.104000.
[11] B.P. de Oliveira, L.C.S. Balieiro, L.S. Maia, N.C. Zanini, E.J.O. Teixeira, M.O.T. da Conceição, S.F. Medeiros, D.R. Mulinari, Eco-friendly polyurethane foams based on castor polyol reinforced with açaí residues for building insulation, J Mater Cycles Waste Manag. 24 (2022) 553–568. https://doi.org/10.1007/s10163-021-01341-1.
[12] P.A.P. Silva, R.L. Oréfice, Bio-sorbent from castor oil polyurethane foam containing cellulose-halloysite nanocomposite for removal of manganese, nickel and cobalt ions from water, J Hazard Mater. 454 (2023) 131433. https://doi.org/10.1016/j.jhazmat.2023.131433.
[13] C. Yang, X. Xing, Z. Li, S. Zhang, A Comprehensive Review on Water Diffusion in Polymers Focusing on the Polymer–Metal Interface Combination, Polymers (Basel). 12 (2020) 138. https://doi.org/10.3390/polym12010138.
[14] A. Atiqah, M. Jawaid, M.R. Ishak, S.M. Sapuan, Moisture Absorption and Thickness Swelling Behaviour of Sugar Palm Fibre Reinforced Thermoplastic Polyurethane, Procedia Eng. 184 (2017) 581–586. https://doi.org/10.1016/j.proeng.2017.04.142.
[15] A. Acosta, A.B. Aramburu, R. Beltrame, D.A. Gatto, S. Amico, J. Labidi, R. de A. Delucis, Wood Flour Modified by Poly(furfuryl alcohol) as a Filler in Rigid Polyurethane Foams: Effect on Water Uptake, Polymers (Basel). 14 (2022) 5510. https://doi.org/10.3390/polym14245510.

7 Considerações finais

A contaminação dos recursos hídricos afeta qualidade da água, impactando o meio ambiente, a saúde humana, as plantas e animais. A presença de microrganismos patogênicos (vírus e bactérias) e metais pesados no ambiente aquático é de extrema preocupação devido à possibilidade de transmissibilidade do vírus (SARS-CoV-2) e intoxicação por metais tóxicos como o Cr, levando a efeitos adversos à saúde humana. Logo, a necessidade de remover tais contaminantes deve ser uma preocupação para a população e futuros trabalhos científicos.

Os resultados apresentados anteriormente mostraram a viabilidade técnica da incorporação das cargas de caroço de pêssego *in natura*, biocarvão ativado e carvão ativado comercial nas espumas poliuretano. Além disso, a utilização do cloreto de zinco não interferiu na viabilidade técnica da incorporação das referidas cargas no PU. PUs com as cargas incorporadas apresentaram estruturas semelhante ao PU sem a adição das cargas. Assim, a incorporação das cargas, especialmente as cargas de carvão ativado comercial e biocarvão, nas espumas, conferiram a elas um aumento na estabilidade térmica e redução na densidade aparente além de um aumento na capacidade de absorção de água quando comparadas com a espuma sem as cargas incorporadas.

Quanto a capacidade de adsorção, os resultados mostram o alto potencial de remoção do vírus (SARS-CoV-2) pelas novas espumas de poliuretano e, a adição das cargas (biocarvão ativado e caroço de pêssego *in natura*) nas referidas espumas potencializou a sua capacidade adsortiva na remoção de Cr(III). Por fim, a pesquisa evidenciou a capacidade promissora da utilização das novas espumas de poliuretano como novos adsorventes sustentáveis na descontaminação ambiental de cromo e SARS-CoV-2 em meio aquoso.

No entanto, não foram aplicadas espumas de poliuretano, funcionalizadas com biocarvão a base do caroço de pêssego, para remover metais pesados e microrganismos patogênicos no tratamento de águas residuais até o momento. Dado que esse material é ecologicamente viável, renovável e têm potencial para remediação ambiental, torna-se necessário uma maior exploração no campo da remoção tais contaminantes em efluentes reais.

A aplicação de vários materiais adsorventes de fontes renováveis (biocarvão, resíduos agroindustriais, biopolímeros, bioespumas) para remediação ambiental é

promissora num futuro próximo. Tais adsorventes, têm a capacidade de se tornarem mais atraentes para o mundo devido a versatilidade de compostos que são capazes de remover.

Por conseguinte, a capacidade das bioespumas ainda pode ser mais explorada para a remoção de outros contaminantes. Nesse sentido, o trabalho abre espaço para o desenvolvimento de novas pesquisas, utilizando as espumas de poliuretano apresentadas aqui, visando mitigar a contaminação dos recursos hídricos e assegurar a saúde pública mundial. Consequentemente, é importante para o avanço da ciência a continuidade de pesquisas utilizando adsorventes sustentáveis na descontaminação ambiental.

Referências

ABBAS, M.; TRARI, M. Removal of Methylene Blue in Aqueous Solution by Economic Adsorbent Derived from Apricot Stone Activated Carbon. **Fibers and Polymers**, [*s. l.*], v. 21, n. 4, p. 810–820, 2020.

ABDULLAH, N. M.; MOHD RUS, A. Z.; ABDULLAH, M. F. L. Functionalized Waterborne Polyurethane-Based Graphite-Reinforced Composites. **Advances in Materials Science and Engineering**, [*s. l.*], v. 2019, p. 1–13, 2019.

ABDULLAH, M.; RAMTANI, S.; YAGOUBI, N. Mechanical properties of polyurethane foam for potential application in the prevention and treatment of pressure ulcers. **Results in Engineering**, [*s. l.*], v. 19, p. 101237, 2023.

ACOSTA, A. P. *et al.* Rigid Polyurethane Biofoams Filled with Chemically Compatible Fruit Peels. **Polymers**, [*s. l.*], v. 14, n. 21, p. 4526, 2022.

AHMADIJOKANI, F. *et al.* Polyurethane-based membranes for CO_2 separation: A comprehensive review. **Progress in Energy and Combustion Science**, [*s. l.*], v. 97, p. 101095, 2023. Disponível em: https://www.sciencedirect.com/science/article/pii/S0360128523000254.

AHMED, W. *et al.* Decay of SARS-CoV-2 and surrogate murine hepatitis virus RNA in untreated wastewater to inform application in wastewater-based epidemiology. **Environmental Research**, [*s. l.*], v. 191, p. 110092, 2020.

AKÇAKAL, Ö.; ŞAHIN, M.; ERDEM, M. Synthesis and characterization of high-quality activated carbons from hard-shelled agricultural wastes mixture by zinc chloride activation. **Chemical Engineering Communications**, [*s. l.*], v. 206, n. 7, p. 888–897, 2019. Disponível em: https://doi.org/10.1080/00986445.2018.1534231.

ALAQARBEH, M. Adsorption Phenomena: Definition, Mechanisms, and Adsorption Types: Short Review. **RHAZES: Green and Applied Chemistry**, [*s. l.*], v. 13, p. 43–51, 2021.

ALI, H.; KHAN, E.; ILAHI, I. Environmental Chemistry and Ecotoxicology of Hazardous Heavy Metals: Environmental Persistence, Toxicity, and Bioaccumulation. **Journal of Chemistry**, [*s. l.*], v. 2019, p. 1–14, 2019.

ALMEIDA, M. L. B. *et al.* Bio-Based Polyurethane Foams with Enriched Surfaces of Petroleum Catalyst Residues as Adsorbents of Organic Pollutants in Aqueous Solutions. **Journal of Polymers and the Environment**, [*s. l.*], v. 28, n. 9, p. 2511–2522, 2020.

ALSULAILI, A.; ELSAYED, K.; REFAIE, A. Utilization of agriculture waste materials as sustainable adsorbents for heavy metal removal: A comprehensive review. **Journal of Engineering Research**, [*s. l.*], 2023.

ANAND, U. *et al.* SARS-CoV-2 and other pathogens in municipal wastewater, landfill leachate, and solid waste: A review about virus surveillance, infectivity, and inactivation. **Environmental Research**, [*s. l.*], v. 203, p. 111839, 2022.

ANASTOPOULOS, I. *et al.* Agricultural biomass/waste as adsorbents for toxic metal decontamination of aqueous solutions. **Journal of Molecular Liquids**, [*s. l.*], v. 295, p. 111684, 2019.

ANNA L. ROWBOTHAM, L. S. L. Chromium in the environment: an evaluation of exposure of the UK general population and possible adverse health effects. **Journal of Toxicology and Environmental Health, Part B**, [*s. l.*], v. 3, n. 3, p. 145–178, 2000.

AWAD, H.; GAR ALALM, M.; EL-ETRIBY, H. Kh. Environmental and cost life cycle assessment of different alternatives for improvement of wastewater treatment plants in developing countries. **Science of The Total Environment**, [*s. l.*], v. 660, p. 57–68, 2019.

AZIMI, A. *et al.* Removal of Heavy Metals from Industrial Wastewaters: A Review. **ChemBioEng Reviews**, [*s. l.*], v. 4, n. 1, p. 37–59, 2017.

BABUJI, P. *et al.* Human Health Risks due to Exposure to Water Pollution: A Review. **Water**, [*s. l.*], v. 15, n. 14, p. 2532, 2023.

BACHMANN, S. A. L. *et al.* Adsorption of Cr (VI) on lignocellulosic wastes adsorbents: an overview and further perspective. **International Journal of Environmental Science and Technology**, [*s. l.*], v. 19, n. 12, p. 12727–12748, 2022.

BALDEZ, E. E.; ROBAINA, N. F.; CASSELLA, R. J. Employment of polyurethane foam for the adsorption of Methylene Blue in aqueous medium. **Journal of Hazardous Materials**, [*s. l.*], v. 159, n. 2, p. 580–586, 2008. Disponível em: https://www.sciencedirect.com/science/article/pii/S030438940800294X.

BANDARA, P. C.; PEÑA-BAHAMONDE, J.; RODRIGUES, D. F. Redox mechanisms of conversion of Cr(VI) to Cr(III) by graphene oxide-polymer composite. **Scientific Reports**, [*s. l.*], v. 10, n. 1, p. 9237, 2020. Disponível em: https://www.nature.com/articles/s41598-020-65534-8.

BERNAL, M. M.; LOPEZ-MANCHADO, M. A.; VERDEJO, R. In situ Foaming Evolution of Flexible Polyurethane Foam Nanocomposites. **Macromolecular Chemistry and Physics**, [*s. l.*], v. 212, n. 9, p. 971–979, 2011.

BHATTACHARYA, S. *et al.* Occurrence and transport of SARS-CoV-2 in wastewater streams and its detection and remediation by chemical-biological methods. **Journal of Hazardous Materials Advances**, [*s. l.*], v. 9, p. 100221, 2023.

BISWAS, S. *et al.* Preparation and Characterization of Raw and Inorganic Acid-Activated Pine Cone Biochar and Its Application in the Removal of Aqueous-Phase Pb2+ Metal Ions by Adsorption. **Water, Air, & Soil Pollution**, [*s. l.*], v. 231, n. 1, p. 3, 2020.

BOLISETTY, S.; PEYDAYESH, M.; MEZZENGA, R. Sustainable technologies for water purification from heavy metals: review and analysis. **Chemical Society Reviews**, [*s. l.*], v. 48, n. 2, p. 463–487, 2019.

BOSCH, D. *et al.* Alternative feedstock for the production of activated carbon with ZnCl2: Forestry residue biomass and waste wood. **Carbon Resources Conversion**, [*s. l.*], v. 5, n. 4, p. 299–309, 2022.

BRASIL. **Lei ° 9.433 – Resolução CONAMA 357/2005**, de 18 de março de 2005. Disponível em: www.mma.gov.br/port/Conama/res/res05/res35705.pdf. Acesso em: 10 janeiro 2020

CABULIS, U.; IVDRE, A. Recent developments in the sustainability of the production of polyurethane foams from polyols based on the first- to the fourth-generation of biomass feedstock. **Current Opinion in Green and Sustainable Chemistry**, [*s. l.*], v. 44, p. 100866, 2023.

CHAKRABORTY, R. *et al.* Adsorption of heavy metal ions by various low-cost adsorbents: a review. **International Journal of Environmental Analytical Chemistry**, [*s. l.*], v. 102, n. 2, p. 342–379, 2022.

CHAN, J. F.-W. *et al.* Genomic characterization of the 2019 novel human-pathogenic coronavirus isolated from a patient with atypical pneumonia after visiting Wuhan. **Emerging Microbes & Infections**, [*s. l.*], v. 9, n. 1, p. 221–236, 2020.

CHEN, X. *et al.* Isotherm models for adsorption of heavy metals from water - A review. **Chemosphere**, [*s. l.*], v. 307, p. 135545, 2022.

CHI, T. **Introduction to Adsorption: Basics, Analysis, and Applications**. [*S. l.*]: Elsevier, 2019.

CHOI, B.-J. *et al.* Estimating the prevalence of COVID-19 cases through the analysis of SARS-CoV-2 RNA copies derived from wastewater samples from North Dakota. **Global Epidemiology**, [*s. l.*], v. 6, p. 100124, 2023.

CRINI, G.; LICHTFOUSE, E. Advantages and disadvantages of techniques used for wastewater treatment. **Environmental Chemistry Letters**, [*s. l.*], v. 17, n. 1, p. 145–155, 2019.

DA ROSA SCHIO, R. *et al.* Synthesis of a bio–based polyurethane/chitosan composite foam using ricinoleic acid for the adsorption of Food Red 17 dye. **International Journal of Biological Macromolecules**, [*s. l.*], v. 121, p. 373–380, 2019.

DĄBROWSKI, A. Adsorption — from theory to practice. **Advances in Colloid and Interface Science**, [*s. l.*], v. 93, n. 1–3, p. 135–224, 2001.
DAS, A. *et al.* Advancements in adsorption based carbon dioxide capture technologies-A comprehensive review. **Heliyon**, [*s. l.*], v. 9, n. 12, p. e22341, 2023.

DAS, S. *et al.* Porous Organic Materials: Strategic Design and Structure–Function Correlation. **Chemical Reviews**, [*s. l.*], v. 117, n. 3, p. 1515–1563, 2017.

DAS, N. Recovery of precious metals through biosorption — A review. **Hydrometallurgy**, [*s. l.*], v. 103, n. 1–4, p. 180–189, 2010.

DASH, B.; JENA, S. K.; RATH, S. S. Adsorption of Cr (III) and Cr (VI) ions on muscovite mica: Experimental and molecular modeling studies. **Journal of Molecular Liquids**, [*s. l.*], v. 357, p. 119116, 2022.

DE AGUIAR LINHARES, F.; ROMEU MARCÍLIO, N.; JUAREZ MELO, P. Estudo da produção de carvão ativado a partir do resíduo de casca da acácia negra com e sem ativação química. **Scientia cum Industria**, [*s. l.*], v. 4, n. 2, p. 74–79, 2016.

DE AVILA DELUCIS, R. *et al.* Forest-based resources as fillers in biobased polyurethane foams. **Journal of Applied Polymer Science**, [*s. l.*], v. 135, n. 3, p. 45684, 2018.

DEMARCO, C. F. *et al.* Resistance mechanisms of Hydrocotyle ranunculoides to Cr(VI): A biolfilter plant. **Journal of Cleaner Production**, [*s. l.*], v. 405, p. 136721, 2023.

DERGHAM, J. *et al.* Isolation of Viable SARS-CoV-2 Virus from Feces of an Immunocompromised Patient Suggesting a Possible Fecal Mode of Transmission. **Journal of Clinical Medicine**, [*s. l.*], v. 10, n. 12, p. 2696, 2021.

DÖNMEZ, G.; AKSU, Z. Removal of chromium(VI) from saline wastewaters by Dunaliella species. **Process Biochemistry**, [*s. l.*], v. 38, n. 5, p. 751–762, 2002.

DURANOĞLU, D.; TROCHIMCZUK, A. W.; BEKER, Ü. A comparison study of peach stone and acrylonitrile-divinylbenzene copolymer based activated carbons as chromium(VI) sorbents. **Chemical Engineering Journal**, [*s. l.*], v. 165, n. 1, p. 56–63, 2010.

EBADOLLAHZADEH, H.; ZABIHI, M. Competitive adsorption of methylene blue and Pb (II) ions on the nano-magnetic activated carbon and alumina. **Materials Chemistry and Physics**, [*s. l.*], v. 248, p. 122893, 2020.

FAOSTAT. **Production of peaches and nectarines in 2016; Crops/Regions/World/Production Quantity (from pick lists)**. [*S. l.*], 2018.

FIOL, N. *et al.* Sorption of Pb(II), Ni(II), Cu(II) and Cd(II) from aqueous solution by olive stone waste. **Separation and Purification Technology**, [*s. l.*], v. 50, n. 1, p. 132–140, 2006.

FOLADORI, P. *et al.* SARS-CoV-2 from faeces to wastewater treatment: What do we know? A review. **Science of The Total Environment**, [*s. l.*], v. 743, p. 140444, 2020. Disponível em: https://www.sciencedirect.com/science/article/pii/S0048969720339668.

FUSCHI, C. *et al.* Wastewater-Based Epidemiology for Managing the COVID-19 Pandemic. **ACS ES&T Water**, [*s. l.*], v. 1, n. 6, p. 1352–1362, 2021.

GAMA, N. V. **Espumas de poliuretano funcionais derivadas de subprodutos industriais**. 2017. 1–139 f. - Universidade de Aveiro, Aveiro, 2017.

GAMA, N.; FERREIRA, A.; BARROS-TIMMONS, A. Polyurethane Foams: Past, Present, and Future. **Materials**, [*s. l.*], v. 11, n. 10, p. 1841, 2018.

GAO, X. *et al.* Behaviors and influencing factors of the heavy metals adsorption onto microplastics: A review. **Journal of Cleaner Production**, [*s. l.*], v. 319, p. 128777, 2021.

GAO, D. *et al.* Interaction of micro(nano)plastics and bisphenols in the environment: A recent perspective on adsorption mechanisms, influencing factors and ecotoxic impacts. **TrAC Trends in Analytical Chemistry**, [*s. l.*], v. 165, p. 117132, 2023.

GEORGAKI, M.-N. *et al.* Chromium in Water and Carcinogenic Human Health Risk. **Environments**, [*s. l.*], v. 10, n. 2, p. 33, 2023.

GUERRERO-LATORRE, L. *et al.* SARS-CoV-2 in river water: Implications in low sanitation countries. **Science of The Total Environment**, [*s. l.*], v. 743, p. 140832, 2020. Disponível em: https://www.sciencedirect.com/science/article/pii/S0048969720343564.

HEIDARINEJAD, Z. *et al.* Methods for preparation and activation of activated carbon: a review. **Environmental Chemistry Letters**, [*s. l.*], v. 18, n. 2, p. 393–415, 2020.

HEJNA, A. *et al.* Management of ground tire rubber waste by incorporation into polyurethane-based composite foams. **Environmental Science and Pollution Research**, [*s. l.*], 2023. Disponível em: https://doi.org/10.1007/s11356-023-25387-w.

HONG, J. *et al.* Metal (Cd, Cr, Ni, Pb) removal from environmentally relevant waters using polyvinylpyrrolidone-coated magnetite nanoparticles. **RSC Advances**, [*s. l.*], v. 10, n. 6, p. 3266–3276, 2020.

HU, C. *et al.* Comparative study on adsorption and immobilization of Cd(II) by rape component biomass. **Environmental Science and Pollution Research**, [*s. l.*], v. 27, n. 8, p. 8028–8033, 2020.

HUANG, J. *et al.* A novel polyfunctional polyurethane acrylate prepolymer derived from bio-based polyols for UV-curable coatings applications. **Polymer Testing**, [*s. l.*], v. 106, p. 107439, 2022.

JOSEPH, L. *et al.* Removal of heavy metals from water sources in the developing world using low-cost materials: A review. **Chemosphere**, [*s. l.*], v. 229, p. 142–159, 2019.

KANWAR, V. S. *et al.* Phytoremediation of toxic metals present in soil and water environment: a critical review. **Environmental Science and Pollution Research**, [*s. l.*], v. 27, n. 36, p. 44835–44860, 2020.

KARIMI, S.; TAVAKKOLI YARAKI, M.; KARRI, R. R. A comprehensive review of the adsorption mechanisms and factors influencing the adsorption process from the perspective of bioethanol dehydration. **Renewable and Sustainable Energy Reviews**, [*s. l.*], v. 107, p. 535–553, 2019.

KARRI, R. R.; SAHU, J. N.; MEIKAP, B. C. Improving efficacy of Cr (VI) adsorption process on sustainable adsorbent derived from waste biomass (sugarcane bagasse) with help of ant colony optimization. **Industrial Crops and Products**, [*s. l.*], v. 143, p. 111927, 2020.

KHAMIS, F. *et al.* Comprehensive review on pH and temperature-responsive polymeric adsorbents: Mechanisms, equilibrium, kinetics, and thermodynamics of adsorption processes for heavy metals and organic dyes. **Chemosphere**, [*s. l.*], p. 140801, 2023.

KIM, J.-M. *et al.* Detection and Isolation of SARS-CoV-2 in Serum, Urine, and Stool Specimens of COVID-19 Patients from the Republic of Korea. **Osong Public Health and Research Perspectives**, [*s. l.*], v. 11, n. 3, p. 112–117, 2020.

KURANCHIE, C.; YAYA, A.; BENSAH, Y. D. The effect of natural fibre reinforcement on polyurethane composite foams – A review. **Scientific African**, [*s. l.*], v. 11, p. e00722, 2021.

KUYUCAK, N.; VOLESKY, B. Biosorbents for recovery of metals from industrial solutions. **Biotechnology Letters**, [*s. l.*], v. 10, n. 2, p. 137–142, 1988.

LI, X. *et al.* SARS-CoV-2 shedding sources in wastewater and implications for wastewater-based epidemiology. **Journal of Hazardous Materials**, [*s. l.*], v. 432, p. 128667, 2022.

LIMA, E. C. *et al.* A critical review of the estimation of the thermodynamic parameters on adsorption equilibria. Wrong use of equilibrium constant in the Van't Hoof equation for calculation of thermodynamic parameters of adsorption. **Journal of Molecular Liquids**, [*s. l.*], v. 273, p. 425–434, 2019.

LIMA, É. C. *et al.* Adsorption: Fundamental aspects and applications of adsorption for effluent treatment. *Em*: GREEN TECHNOLOGIES FOR THE DEFLUORIDATION OF WATER. [*S. l.*]: Elsevier, 2021. p. 41–88.

LIU, T. *et al.* Efficient activation of peroxymonosulfate by copper supported on polyurethane foam for contaminant degradation: Synergistic effect and mechanism. **Chemical Engineering Journal**, [*s. l.*], v. 427, p. 131741, 2022. Disponível em: https://www.sciencedirect.com/science/article/pii/S1385894721033222.

LIU, L. Emerging study on the transmission of the Novel Coronavirus (COVID-19) from urban perspective: Evidence from China. **Cities**, [*s. l.*], v. 103, p. 102759, 2020. Disponível em: https://www.sciencedirect.com/science/article/pii/S026427512030531X.

LIU, Y. Is the Free Energy Change of Adsorption Correctly Calculated?. **Journal of Chemical & Engineering Data**, [*s. l.*], v. 54, n. 7, p. 1981–1985, 2009. Disponível em: https://doi.org/10.1021/je800661q.

LIU, G. *et al.* Visible light-induced hydrogels towards reversible adsorption and desorption based on trivalent chromium in aqueous solution. **Reactive and Functional Polymers**, [*s. l.*], v. 163, p. 104886, 2021.

MALIK, A. *et al.* Sources, distribution, associated health risks and remedial technologies for inorganic contamination in groundwater: A review in specific context of the state of Haryana, India. **Environmental Research**, [*s. l.*], v. 236, p. 116696, 2023.

MARONEZI, V. *et al.* Mecanismos de remoção de Cromo(VI) do solo pela interação entre matéria orgânica e Ferro(III). **Revista do Instituto Geológico**, [*s. l.*], v. 40, n. 2, p. 17–33, 2019.

MARTIN-MARTINEZ, M. *et al.* Exploring the activity of chemical-activated carbons synthesized from peach stones as metal-free catalysts for wet peroxide oxidation. **Catalysis Today**, [*s. l.*], v. 313, p. 20–25, 2018.

MEDEMA, G. *et al.* Presence of SARS-Coronavirus-2 RNA in Sewage and Correlation with Reported COVID-19 Prevalence in the Early Stage of the Epidemic in The Netherlands. **Environmental Science & Technology Letters**, [*s. l.*], v. 7, n. 7, p. 511–516, 2020. Disponível em: https://doi.org/10.1021/acs.estlett.0c00357.

MISHRA, S. *et al.* Heavy Metal Contamination: An Alarming Threat to Environment and Human Health. *Em*: ENVIRONMENTAL BIOTECHNOLOGY: FOR SUSTAINABLE FUTURE. Singapore: Springer Singapore, 2019. p. 103–125.

MOHAMMAD, S. G.; EL-SAYED, M. M. H. Removal of imidacloprid pesticide using nanoporous activated carbons produced via pyrolysis of peach stone agricultural wastes. **Chemical Engineering Communications**, [*s. l.*], v. 208, n. 8, p. 1069–1080, 2021.

MOHAMMADPOUR, R.; MIR MOHAMAD SADEGHI, G. Effect of Liquefied Lignin Content on Synthesis of Bio-based Polyurethane Foam for Oil Adsorption Application. **Journal of Polymers and the Environment**, [*s. l.*], v. 28, n. 3, p. 892–905, 2020.

NÚÑEZ-DECAP, M.; WECHSLER-PIZARRO, A.; VIDAL-VEGA, M. Mechanical, physical, thermal and morphological properties of polypropylene composite materials developed with particles of peach and cherry stones. **Sustainable Materials and Technologies**, [*s. l.*], v. 29, p. e00300, 2021.

ORIBAYO, O. *et al.* Synthesis of lignin-based polyurethane/graphene oxide foam and its application as an absorbent for oil spill clean-ups and recovery. **Chemical Engineering Journal**, [*s. l.*], v. 323, p. 191–202, 2017.

OSSMAN, M. E.; ABDELFATTAH, M. Polyurethane Composites for Dye and Heavy Metal Removal: (Adsorption Kinetics and Isotherms Studies). *Em*: , 2018. **ICASET-**

18,ACBES-1,EEHIS-18 June 20-21, 2018 Paris (France). [*S. l.*]: Universal Researchers, 2018.

PANHWAR, A. *et al.* Water resources contamination and health hazards by textile industry effluent and glance at treatment techniques: A review. **Waste Management Bulletin**, [*s. l.*], v. 1, n. 4, p. 158–163, 2024.

PARCHETA, P.; GŁOWIŃSKA, E.; DATTA, J. Effect of bio-based components on the chemical structure, thermal stability and mechanical properties of green thermoplastic polyurethane elastomers. **European Polymer Journal**, [*s. l.*], v. 123, p. 109422, 2020.

PARLAYICI, Ş. Modified peach stone shell powder for the removal of Cr (VI) from aqueous solution: synthesis, kinetic, thermodynamic, and modeling study. **International Journal of Phytoremediation**, [*s. l.*], v. 21, n. 6, p. 590–599, 2019. Disponível em: https://doi.org/10.1080/15226514.2018.1540541.

PRASAD, P Supriya *et al.* Biosilica/Silk Fibroin/Polyurethane biocomposite for toxic heavy metals removal from aqueous streams. **Environmental Technology & Innovation**, [*s. l.*], v. 28, p. 102741, 2022. Disponível em: https://www.sciencedirect.com/science/article/pii/S2352186422002449.

QIAO, L. *et al.* Fabrication of superporous cellulose beads via enhanced inner cross-linked linkages for high efficient adsorption of heavy metal ions. **Journal of Cleaner Production**, [*s. l.*], v. 253, p. 120017, 2020.

RAJASULOCHANA, P.; PREETHY, V. Comparison on efficiency of various techniques in treatment of waste and sewage water – A comprehensive review. **Resource-Efficient Technologies**, [*s. l.*], v. 2, n. 4, p. 175–184, 2016.

REN, L. *et al.* Recyclable polyurethane foam loaded with carboxymethyl chitosan for adsorption of methylene blue. **Journal of Hazardous Materials**, [*s. l.*], v. 417, p. 126130, 2021. Disponível em: https://www.sciencedirect.com/science/article/pii/S0304389421010943.

REN, S. *et al.* Simultaneous robustness, reprocessing and self-healing of castor oil-based polyurethane vitrimers enabled by supramolecular nitrogen-coordinated dynamic covalent boronic ester. **Industrial Crops and Products**, [*s. l.*], v. 206, p. 117738, 2023.

SANTOS, O. S. H. *et al.* Polyurethane foam impregnated with lignin as a filler for the removal of crude oil from contaminated water. **Journal of Hazardous Materials**, [*s. l.*], v. 324, p. 406–413, 2017.

SATHTHASIVAM, J. *et al.* COVID-19 (SARS-CoV-2) outbreak monitoring using wastewater-based epidemiology in Qatar. **Science of The Total Environment**, [*s. l.*], v. 774, p. 145608, 2021.

SCHOELER, G. P. *et al.* SARS-CoV-2 removal with a polyurethane foam composite. **Environmental Science and Pollution Research**, [*s. l.*], 2022.

SEKULIĆ, Z. *et al.* Application of artificial neural networks for estimating Cd, Zn, Pb removal efficiency from wastewater using complexation-microfiltration process. **International Journal of Environmental Science and Technology**, [*s. l.*], v. 14, n. 7, p. 1383–1396, 2017.

SEKULIĆ, Z. *et al.* The Prediction of Heavy Metal Permeate Flux in Complexation-Microfiltration Process: Polynomial Neural Network Approach. **Water, Air, & Soil Pollution**, [*s. l.*], v. 230, n. 1, p. 23, 2019.

SHAIKHIEV, I. G.; KRAYSMAN, N. V; SVERGUZOVA, S. V. Review of Peach (Prúnus pérsica) Shell Use to Remove Pollutants from Aquatic Environments. **Biointerface Research in Applied Chemistry**, [*s. l.*], v. 13, n. 5, p. 1–14, 2023.

SHARMA, K.; DALAI, A. K.; VYAS, R. K. Removal of synthetic dyes from multicomponent industrial wastewaters. **Reviews in Chemical Engineering**, [*s. l.*], v. 34, n. 1, p. 107–134, 2017.

SHIN, D. Y. *et al.* Adverse Human Health Effects of Chromium by Exposure Route: A Comprehensive Review Based on Toxicogenomic Approach. **International Journal of Molecular Sciences**, [*s. l.*], v. 24, n. 4, p. 3410, 2023.

SILVA, P. A. P.; ORÉFICE, R. L. Bio-sorbent from castor oil polyurethane foam containing cellulose-halloysite nanocomposite for removal of manganese, nickel and cobalt ions from water. **Journal of Hazardous Materials**, [*s. l.*], v. 454, p. 131433, 2023.

SINGH, S.N. **Blowing Agents for Polyurethane Foams**. Shrewsbury: ISmithers Rapra Teechnology: Shawbury, U.K, 2002. p. 142.

SINGH, V. P.; VAISH, R. Candle soot coated polyurethane foam as an adsorbent for removal of organic pollutants from water. **The European Physical Journal Plus**, [*s. l.*], v. 134, n. 9, p. 419, 2019.

SOLIS-CEBALLOS, A. *et al.* Selective adsorption of Cr(III) over Cr(VI) by starch-graft-itaconic acid hydrogels. **Journal of Hazardous Materials Advances**, [*s. l.*], v. 10, p. 100255, 2023.

SUWALSKY, M. *et al.* Cr(III) exerts stronger structural effects than Cr(VI) on the human erythrocyte membrane and molecular models. **Journal of Inorganic Biochemistry**, [*s. l.*], v. 102, n. 4, p. 842–849, 2008.

TANGAROMSUK, J. *et al.* Cadmium biosorption by Sphingomonas paucimobilis biomass. **Bioresource Technology**, [*s. l.*], v. 85, n. 1, p. 103–105, 2002.

TOKAY, B.; AKPINAR, I. A comparative study of heavy metals removal using agricultural waste biosorbents. **Bioresource Technology Reports**, [*s. l.*], v. 15, p. 100719, 2021.

TORRELLAS, S. Á. *et al.* Chemical-activated carbons from peach stones for the adsorption of emerging contaminants in aqueous solutions. **Chemical Engineering Journal**, [*s. l.*], v. 279, p. 788–798, 2015.

TSONCHEVA, T. *et al.* Activated carbon from Bulgarian peach stones as a support of catalysts for methanol decomposition. **Biomass and Bioenergy**, [*s. l.*], v. 109, p. 135–146, 2018. Disponível em: https://www.sciencedirect.com/science/article/pii/S0961953417304439.

UKHUREBOR, K. E. *et al.* Effect of hexavalent chromium on the environment and removal techniques: A review. **Journal of Environmental Management**, [*s. l.*], v. 280, p. 111809, 2021.

UYSAL, T. *et al.* Production of activated carbon and fungicidal oil from peach stone by two-stage process. **Journal of Analytical and Applied Pyrolysis**, [*s. l.*], v. 108, p. 47–55, 2014. Disponível em: https://www.sciencedirect.com/science/article/pii/S0165237014001235.

VAKILI, A. *et al.* The impact of activation temperature and time on the characteristics and performance of agricultural waste-based activated carbons for removing dye and residual COD from wastewater. **Journal of Cleaner Production**, [*s. l.*], v. 382, p. 134899, 2023.

VINCENT, J. B. New Evidence against Chromium as an Essential Trace Element. **The Journal of Nutrition**, [*s. l.*], v. 147, n. 12, p. 2212–2219, 2017.

WARREN-VEGA, W. M. *et al.* A Current Review of Water Pollutants in American Continent: Trends and Perspectives in Detection, Health Risks, and Treatment Technologies. **International Journal of Environmental Research and Public Health**, [*s. l.*], v. 20, n. 5, p. 4499, 2023.

XUE, X. *et al.* Review: Phytate modification serves as a novel adsorption strategy for the removal of heavy metal pollution in aqueous environments. **Journal of Environmental Chemical Engineering**, [*s. l.*], v. 11, n. 6, p. 111440, 2023.

WHO, World Health Organization. **Guidelines for Drinking-Water Quality: Fourth Edition Incorporating the First Addendum World Health Organization**. Geneva 2017a.

WHO, World Health Organization. **Progress on Drinking Water, Sanitation and Hygiene: 2017 Update and SDG Baselines**. UNICEF, United Nations Children's Fund 2017b.

WHO, World Health Organization. **World Health Statistics 2018: monitoring health for the SDGs sustainable development Goals**. Geneva, 2018.

YAHYA, M. A.; AL-QODAH, Z.; NGAH, C. W. Z. Agricultural bio-waste materials as potential sustainable precursors used for activated carbon production: A review. **Renewable and Sustainable Energy Reviews**, [*s. l.*], v. 46, p. 218–235, 2015.

YAN, J. *et al.* Adsorption of heavy metals and methylene blue from aqueous solution with citric acid modified peach stone. **Separation Science and Technology**, [*s. l.*], v. 53, n. 11, p. 1678–1688, 2018.

ZAIMEE, M. Z. A.; SARJADI, M. S.; RAHMAN, M. L. Heavy Metals Removal from Water by Efficient Adsorbents. **Water**, [*s. l.*], v. 13, n. 19, p. 2659, 2021.

ZAMHURI, S. A. *et al.* A review on the contamination of SARS-CoV-2 in water bodies: Transmission route, virus recovery and recent biosensor detection techniques. **Sensing and Bio-Sensing Research**, [*s. l.*], v. 36, p. 100482, 2022.

ZHANG, M. *et al.* High and fast adsorption of Cd(II) and Pb(II) ions from aqueous solutions by a waste biomass based hydrogel. **Scientific Reports**, [*s. l.*], v. 10, n. 1, p. 3285, 2020.

ZHANG, R.; TIAN, Y. Characteristics of natural biopolymers and their derivative as sorbents for chromium adsorption: a review. **Journal of Leather Science and Engineering**, [*s. l.*], v. 2, n. 1, p. 24, 2020.

ZHOU, X. *et al.* Dispersion and reinforcing effect of carrot nanofibers on biopolyurethane foams. **Materials & Design**, [*s. l.*], v. 110, p. 526–531, 2016.

ZHU, N. *et al.* A Novel Coronavirus from Patients with Pneumonia in China, 2019. **New England Journal of Medicine**, [*s. l.*], v. 382, n. 8, p. 727–733, 2020.

ZHU, R. *et al.* Analysis of factors influencing pore structure development of agricultural and forestry waste-derived activated carbon for adsorption application in gas and liquid phases: A review. **Journal of Environmental Chemical Engineering**, [*s. l.*], v. 9, n. 5, p. 105905, 2021.

ZOGHLAMI, A.; PAËS, G. Lignocellulosic Biomass: Understanding Recalcitrance and Predicting Hydrolysis. **Frontiers in Chemistry**, [*s. l.*], v. 7, 2019.